UNIVERSITÀ DEGLI STUDI DI CAGLIARI

PhD DEGREE
Scuola di Dottorato in Fisica
XXXI cycle

Aspects of the relation between the black hole entropy and the entanglement entropy

Scientific Disciplinary Sector: FIS/02

PhD Student:
Parul Jain

Coordinator: Prof. Paolo Ruggerone
Università degli Studi di Cagliari, Italy

Supervisor: Prof. Mariano Cadoni
Università degli Studi di Cagliari, Italy

Co-Supervisor: Prof. Gautam Sengupta
Indian Institute of Technology-Kanpur, India

Final exam. Academic Year 2017 – 2018
Thesis defence: January-February 2019 Session

Abstract

The relationship between Bekenstein-Hawking and entanglement entropy is one of the most intriguing problems of black hole and theoretical physics. Although both entropies have the same geometric characterization (they scale as an area), they have a different origin. The Bekenstein-Hawking entropy has it's roots in the thermal correlations whereas the entanglement entropy describes the quantum correlations. In this thesis we address this problem from a holographic perspective, making large use of the AdS/CFT correspondence.

We first look at the BTZ black hole in which case the black hole horizon and the conical singularity are related to each other. Using the modular transformations of the dual 2D CFT, we first obtain an expression of the holographic entanglement entropy for the Euclidean BTZ black hole, AdS_3 vacua and conical singularity and then analyse the behaviour of the leading terms in the expansions of the holographic entanglement entropy for the BTZ black hole and the conical singularity. From these calculations, we have extracted the "signatures" through which entanglement entropy differentiates between the horizon and the conical singularity. When we deal with CFT at a finite temperature then it is well known that, entanglement entropy fails as a measure and hence it is replaced by entanglement negativity which is able to separate the thermal/classical correlations from the quantum correlations thereby capturing "distillable" entanglement. We address the problem of finding a suitable holographic prescription to calculate the entanglement negativity for two adjacent intervals when the CFT is at a finite temperature and in turn dual to a black hole in the bulk. We first propose a conjecture for the holographic entanglement negativity for two adjacent intervals in the AdS_3/CFT_2 setup and perform calculations in the various cases to support this conjecture. We further push forward the validity of this conjecture by calculating the holographic entanglement negativity for two adjacent subsystems when we have RN-AdS black holes in the bulk which in turn are dual to CFT with a conserved charge.

Acknowledgements

First and foremost I would like to express my sincere gratitude to my supervisor Prof. Mariano Cadoni and my co-supervisor Prof. Gautam Sengupta for their continuous help and support. Both of them are excellent mentors whose immense knowledge and beautiful intuitive insights in physics has helpled me a lot during my thesis and has further motivated me towards research in physics. I am extremely thankful to them for showing faith in my ideas, stimulating discussions on physics which has in turn boosted my confidence as a researcher in physics. I am grateful to them for their patience and encouragement. For me, it has been a wonderful journey of physics under their guidance.

I am also extremely thankful to my collaborators Vinay Malvimat and Sayid Mondal for their help. I really enjoyed working with them. I would like to thank staff members at IIT - Kanpur, India for their help and hospitality. Also, I would like to thank my friends at IIT - Kanpur for their help. It is because of their warm friendship that I had a great time at the IIT campus.

I am grateful to the members of the Department of Physics, University of Cagliari for their help. A special vote of thanks for all my friends at this department as because of their help and wonderful discussions on physics and other topics I had an enjoyable stay at the department.

I am also grateful to the staff members of the Euraxess office, University of Cagliari for their extensive help and guidance.

I am grateful to the University of Cagliari and INFN, Cagliari for the financial support.

Last but not the least I am grateful to my teachers, family and friends in India without whose help and support this journey wouldn't have been possible.

Contents

Preface

The research work presented through this thesis was carried out at the Department of Physics, University of Cagliari,Italy and also at the Department of Physics, Indian Institute of Technology - Kanpur, India.

I declare that the research work presented in this thesis is original and it has not been submitted for any other degree or professional qualification.

List of publications included in this thesis are :-

1. Chapter 6 is based on the paper:
How is the Presence of Horizons and Localized Matter Encoded in the Entanglement Entropy?
Mariano Cadoni, Parul Jain
arXiv:1703.02505 [hep-th]
Published in Int.J.Mod.Phys. A32 (2017) no.15, 1750083

2. Chapter 7 is based on the paper:
Holographic entanglement negativity conjecture for adjacent intervals in $\mathbf{AdS_3/CFT_2}$
Parul Jain, Vinay Malvimat, Sayid Mondal, Gautam Sengupta
arXiv:1707.08293 [hep-th]

3. Chapter 8 is based on the paper:
Holographic Entanglement Negativity for Conformal Field Theories with a Conserved Charge
Parul Jain, Vinay Malvimat, Sayid Mondal, Gautam Sengupta
arXiv:1804.09078 [hep-th]

Introduction

In recent years the issue of quantum entanglement has attracted intense interest leading to exciting insights in an expansive list of phenomena from quantum gravity to quantum computers. Generally, quantum entanglement is described by entanglement entropy which is expressed as the the von Neumann entropy of the reduced density matrix for a given bipartite quantum system. Recently, research dealing with the connection between entanglement and gravity has received considerable attention for example one of the ideas is that the spacetime geometry and gravity emerge as a result of an entanglement process present in an underlying microscopic theory [1–9]. Most of these calculations involve the setup of AdS/CFT duality as it permits the well defined calculation of the entanglement entropy connecting both the gravitational and field theoretic backgrounds and opening new ways for the emergent gravity/spacetime scenario. Holographic entanglement entropy seems closely related with the Bekenstein-Hawking entropy [10, 11]. The fact that even the entanglement entropy scales as an area has given birth to the idea of spacetime being a network of tensors [1]. Further, it has been noted that the emergence of bulk locality and quantum error correction can be seen related in the AdS/CFT setup [12, 13]. Also, it has been shown that the spacetime connectivity can be related to entanglement [2]. The development of this concept has lead to a better understanding of aspects of quantum gravity [14, 15] and of the information puzzle in the black hole evaporation process [16–18]. In a parallel devellopment, connections between entanglement and Einstein's equations have also been explored in [4, 9, 19]. Recently in [7] it was shown that the emergent nature of space time, entanglement, dark energy and aspects of dark matter, in de Sitter space can be correlated.

This research activity which involves the exploration of the connection between entanglement and the spacetime structure and dynamics was stimulated by the ideas like interplay between thermodynamics and black hole physics [20–22], microscopic origin of the Bekenstein-Hawking entropy [23], AdS/CFT correspondence [24], holographic entanglement entropy [25, 26], black hole information problems [15, 16, 27].

A related area where we can explore the connection between entanglement and gravity and which has received considerable attention is the relation between the black hole entropy and the entanglement entropy. This thesis is devoted to the investigation of relationship between the black hole entropy and the entanglement entropy from a holographic perspective. In fact we will make large use of the AdS/CFT correspondence and of the Ryu-Takayanagi proposal, which allows us to compute the entanglement entropy in a dual QFT in terms of geometric quantities in the bulk gravity theory. Research into the area of the black hole entropy and entanglement entropy led to the indications of the connection

between these two types of entropies for example when people studied entanglement entropy in quantum field theories and found it proportional to area of the boundary separating accessible from inaccessible regions [28]. Calculation of the entanglement entropy for a quantum field in the background of the black hole was performed in [29] and it was found to be proportional to the area of the black hole horizon. Also it was shown in [30, 31] that quantum corrections to the black hole entropy can be seen as entanglement entropy. A further step towards a better understanding of this relation under the holographic setting was done in [25, 32] where the duality between the thermal entropy obtained from the high temperature limit of the entanglement entropy for a thermal CFT was shown to be dual to the black hole entropy. The issue of the relation between the Bekenstein-Hawking and entanglement entropy in the simplified context on 3D AdS gravity has been addressed in [33]. In the 3D case the AdS/CFT correspondence is well understood. Moreover, one can make use of the modular transformations of the dual 2D CFT, which will allow us to relate the 3D AdS, BTZ black hole to conical singularities of the 3D AdS spacetime. These calculations stimulates the question about the links between the entanglement entropy associated to conical singularities and black holes. This issue will be discussed in Chapter 6. Essentially, in this chapter we study how the entanglement entropy differentiates between black hole horizon and conical singularity as both of these are related to each other for the case of 3D AdS gravity.

Entanglement entropy in conformal field theories is computed using the replica method [34, 35]. It was also shown that the entanglement entropy for a given two-dimensional conformal field theory has a logarithmic behaviour [34–37]. Entanglement entropy has also been shown to be related to the quantum phase transitions [38–40], c-theorem [41]. Further, using the AdS/CFT correspondence a holographic method to calculate the entanglement entropy was proposed by Ryu-Takayanagi [25, 26, 42] which involved the computation of the area of the bulk co-dimension two static minimal surfaces. Later, this method was further generalized for time dependent scenario in [43]. The holographic entanglement entropy led to a considerable research in the holographic aspect of entanglement entropy [42, 44–49]. Also, the proof for the Ryu-Takayanagi conjecture has received considerable attention [10, 11, 50–53].

When we deal with the holographic entanglement entropy for a black hole then the dual CFT is at a finite temperature and the computation of the holographic entanglement entropy in the high temperature limit shows presence of thermal entropy which indicates that we have "Mixed State". Since the entanglement entropy fails to differentiate between classical and quantum correlations, it can no longer be considered as a measure of entanglement for mixed state. The solution to this problem was given by Vidal and Werner [54] who proposed "Entanglement Negativity" as a measure of "distillable" quantum entanglement as it essentially captures only the quantum correlations in a mixed state and removes the thermal contributions. The non-convex and monotone nature of the entanglement negativity was shown in [55]. Using a modified version of the replica technique entanglement negativity has also been calculated for conformal field theories [56–58]. As entanglement entropy can be calculated holographically, in [59, 60] attempts were made to extract entanglement negativity holographically. Recently, a clear solution was put forth in [61, 62] where the entanglement negativity has been computed in a holographic fashion for a single interval on the boundary CFT. The authors in [61, 62] have calculated the

holographic entanglement negativity for a single interval first in the AdS_3/CFT_2 setup and then also for a generalized AdS_{d+1}/CFT_d scenario. A covariant calculation for the holographic entanglement negativity for a single interval was given in [63]. These calculations for the holographic entanglement negativity involved an algebraic combination of the areas of the bulk co-dimension two extremal surfaces and the holographic results were able to reproduce the corresponding CFT results in the large central charge limit, thus giving a strong support to the conjecture. This conjecture for a single interval was further strengthened in [64].

Entanglement Negativity for two adjacent intervals has been calculated for conformal field theories [56]. Since entanglement entropy and entanglement negativity for a single interval has a holographic counterpart, in this thesis we will addrress the question about the possibility to express entanglement negativity for two adjacent intervals in a holographic manner. The issue of the holographic entanglement negativity for two adjacent intervals will be discussed in Chapter 7. Essentially, in this chapter we use the holographic setup of AdS_3/CFT_2 to formulate the conjecture for the holographic entanglement negativity for the mixed states of two adjacent intervals lying on the 2D boundary CFT.

The calculations for the holographic entanglement negativity for two adjacent subsystems in the generalized AdS_{d+1}/CFT_d scenario was done in [65]. The calculations were done for the finite temperature case which is dual to the AdS_{d+1}-Schwarzschild black hole. It was noticed that in the high temperature limit, the volume terms representing thermal correlations were completely eliminated and as a result the holographic entanglement negativity scales as area. This area dependence for the entanglement negativity has also been seen in [66, 67]. A covariant calculation for the holographic entanglement negativity for two adjacent subsystems was given in [68].

Apart from the BTZ and AdS_{d+1}-Schwarzschild black hole, another class of black holes that are very intersesting from the entanglement entropy point of view are the charged AdS black holes [69–72]. In [70] the authors have studied the holographic entanglement entropy for the RN-AdS_{d+1} black hole. Aspects of entanglement thermodynamics for a boundary field theory at a finite temperature and charge were studied in [46, 73, 74]. In [49] the authors have used the setup of [47] to analyse the temperature and charge dependence of the holographic entanglement entropy for the RN-AdS_4/CFT_3 scenario where the boundary subsystem has a strip like geometry and also studied the entanglement thermodynamics for the same. Motivated by these investigations, we will address in this thesis the question about the holographic entanglement negativity in case of the charged AdS black holes. In chapter 8, we will further apply the conjecture for the holographic entanglement negativity for two adjacent subsystems when the dual CFT carries a conserved charge. In this case, the bulk configuration is the RN-AdS black hole. We consider both the extremal and the non-extremal cases. We will first deal with the RN-AdS_4/CFT_3 setup followed by RN-AdS_{d+1}/CFT_d case.

This thesis is structured as follows. We begin the thesis with essential ingredients of the background material, from chapter 1 to 5 as required to understand the results in the chapters 6,7 and 8. In chapter 1, we talk about the essentials about AdS space followed by basics of conformal field theory in chapter 2. In chapter 3, we give a brief review of the AdS/CFT correspondence followed by basics of entanglement entropy in chapter 4 and entanglement negativity

in chapter 5. We begin with the research work presented through this thesis with chapter 6, where we investigate how entanglement entropy differentiates between black holes and conical singularities. In chapter 7, we study the holographic entanglement negativity conjecture for two adjacent intervals for the AdS_3/CFT_2 case and subsequently for the RN-AdS black holes in chapter 8. Towards the end we summarize and dicuss the results in the conclusion section.

Chapter 1

AdS space

In this chapter, we will review some aspects of AdS spacetime which are relevant for the chapters ahead.

The geometrical properties of AdS space time plays an important role in the AdS/CFT correspondence. Here, we will review some features of AdS space time relevant to this correspondence. Einstein's equations with a negative cosmological constant

$$R_{\mu\nu} - \frac{1}{2}Rg_{\mu\nu} + \Lambda g_{\mu\nu} = 0, \tag{1.1}$$

where $R_{\mu\nu}$ is the Ricci tensor, R is the scalar curvature, Λ is the cosmological constant and $g_{\mu\nu}$ is the metric of the spacetime.
Hyperboloid space is the maximally symmetric solution for the above equation. A d-dimensional hyperboloid space is given as

$$-X_{-1}^2 + X_1^2 + ... + X_d^2 = -R^2. \tag{1.2}$$

When we turn to the Minkowski space, we get the d- dimensional Anti de Sitter space (AdS).

$$-X_{-1}^2 - X_0^2 + X_1^2 + ... + X_{d-1}^2 = -R^2. \tag{1.3}$$

We can see clearly now that it has d(d+1)/2 Killing vectors and so AdS_d is invariant under the group SO(d-1,2) which is isomorphic to the conformal group in d-1 dimensions SO(d-1,2). This AdS_d is embedded in the $d+1$ dimensional flat space with the metric

$$ds^2 = -dX_{-1}^2 - dX_0^2 + dX_1^2 + ... + dX_{d-1}^2. \tag{1.4}$$

1.1 COORDINATES FOR AdS

If we take the following parametrization for the AdS_d coordinates :-

$$\begin{aligned} &X_{-1} = R\cosh\rho\cos\tau, \\ &X_0 = R\cosh\rho\sin\tau, \\ &X_i = R\sinh\rho\ \Omega_i\ , \qquad \sum_{i=1}^{d-1}\Omega_i^2 = 1, \end{aligned} \tag{1.5}$$

where Ω_i can be expressed in terms of the $d-2$ angular coordinates of the $d-2$ sphere S_{d-2}, we obtain the metric for AdS_d

$$ds^2 = R^2(-\cosh^2\rho d\tau^2 + d\rho^2 + \sinh^2\rho\ d\Omega_{d-2}^2), \tag{1.6}$$

where $d\Omega_{d-2}^2$ is the metric on S_{d-2}. These coordinates cover the entire AdS with $(\rho \geq 0, 0 \leq \tau \leq 2\pi)$ and are called as global coordinates. When we unroll the periodic coordinate τ such that $\tau \in (-\infty, \infty)$ we get the universal cover for the AdS.
We can also parametrize AdS in terms of Poincaré coordinates which are given as

$$\begin{array}{l} X_{-1} = \frac{1}{2z}(z^2 + R^2 + x^2 - t^2), \\ X_0 = \frac{Rt}{z}, \\ X_i = \frac{Rx^i}{z}, \quad i = 1, ..., d-2, \\ X_{d-1} = \frac{1}{2z}(z^2 - R^2 + x^2 - t^2). \end{array} \tag{1.7}$$

In terms of the Poincaré coordinates the AdS metric is

$$ds^2 = \frac{R^2}{z^2}(-dt^2 + dz^2 + \sum_{i=1}^{d-2} dx_i^2). \tag{1.8}$$

Here, both t, x lie in the interval $-\infty < t, x < \infty$. The coordinate z behaves as a radial coordinate lying in the interval $0 \leq z < \infty$ and dividing the entire AdS into two regions corresponding to $z > 0$ and $z < 0$. Poincaré coordinates cover, therefore, only a part of the entire AdS.
Another important coordinate system for AdS is the conformal coordinates which we get by taking $\sinh\rho = \tan\theta$ in eq. (1.6). We then get the following metric

$$ds^2 = \frac{R^2}{\cos^2\theta}(-d\tau^2 + d\theta^2 + \sin^2\theta\ d\Omega_{d-2}^2). \tag{1.9}$$

Here , θ lies between $-\frac{\pi}{2} \leq \theta \leq \frac{\pi}{2}$. In this case, the AdS has a boundary at $\theta = \pm\frac{\pi}{2}$.

1.2 CONFORMAL COMPACTIFICATION OF AdS

It so happens that sometimes in order to understand a particular phenomenon, we need to know it's asymptotic behaviour. In our case, we are interested in in the global, causal, structure of the spacetime, in particular of AdS. In order to describe globally the spacetime we need, in particular, to have under control the asymptotical properties of the spacetime. Owing to the non-compactness of AdS, it is not easy to understand what is going on "asymptotically" but fortunately Penrose invented a technique called conformal compactification of spacetime which essentially defines an equivalence class of metrics $g_{ab} = \Omega^2(x)g_{ab}$ where $\Omega(x)$ is a positive scalar function of spacetime that modifies the distance scale but leaves invariant the causal structure of the spacetime making the

asymptotics of the physical metric accessible to study so that one can describe the global, causal, structure of the spacetime. Often in this procedure, it will be useful to employ the Penrose diagrams also called as Conformal Diagrams which are 2 dimensional representations of spacetime which preserve the causal nature of space-time. In this case, infinity in its three different, causal, versions (timelike, spacelike and null) is represented as part of the boundary of the diagram.
We need to understand the conformal structure of AdS as it is one of it's important aspects [75] which shows causal and geometric relation with the conformal structure of the flat space.
The AdS/CFT correspondence employs the idea of the holographic principle, which states that a (d + 1)-dimensional gravitational theory can be described by a dual d-dimensional boundary field theory. To better understand this connection between the gravity and conformal field theories, we need to understand how AdS behaves both in the bulk and at the boundary, where the conformal field theory lives.
Thus the asymptotic/boundary behaviour of AdS spacetime is important to understand the boundary on which the CFT lives.

1.2.1 Conformal structure of 2D Minkowski space

So, let us begin by looking at the conformal structure of flat space. We start with the 2 dimensional Minkowski space $\mathbb{R}^{1,1}$ whose metric is given as

$$ds^2 = -dt^2 + dx^2, \tag{1.10}$$

where $-\infty < t, x < \infty$.
Using lightcone coordinates $u_\pm = t \pm x$ we get the metric as

$$ds^2 = -du_+ du_-. \tag{1.11}$$

We use the following transformations to make them finite

$$u_\pm = \tan \tilde{u}_\pm, \tag{1.12}$$

where $\tilde{u}_\pm = \frac{\tau \pm \theta}{2}$.
As a result of these new coordinates, the metric is

$$ds^2 = \frac{1}{4 \cos^2 \tilde{u}_+ \cos^2 \tilde{u}_-}(-d\tau^2 + d\theta^2). \tag{1.13}$$

Taking hints from eq. (1.13) using a conformal transformation (Weyl rescaling) of the metric, which preserves the causal structure of the spacetime if we drop the conformal factor, then we have a flat 2 dimensional space which is finite in nature as $|\tilde{u}_\pm| \leq \pi/2$ because $|\tau \pm \theta| \leq \pi$ and this results in a diamond shaped penrose diagram [75] as depicted in Fig. 1.

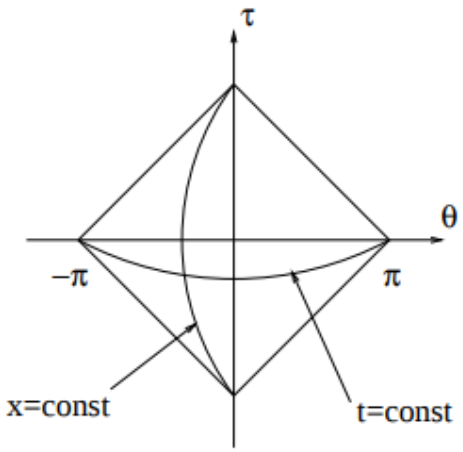

Figure 1: Penrose diagram of 2D Minkowski space. $(\tau, \theta) = (0, \pm\pi)$ correspond to the spatial infinities $x = \pm\infty$.

Since, after conformal compactification the boundary nature is that of flat space, hence this space-time is called as asymptotically flat.

1.2.2 Conformal structure of higher dimensional Minkowski space

We will now try to analyse the conformal structure for a higher dimensional Minkowski space $\mathbb{R}^{1,d-1}$ whose metric is given as

$$ds^2 = -dt^2 + dr^2 + r^2 d\Omega_{d-2}^2, \tag{1.14}$$

where $d\Omega_{d-2}^2$ is the metric on the unit sphere S^{d-2}. We also see that there is an additional radial coordinate r which is defined in the range $r \geq 0$. Using the same transformations, as we had used for 2D Minkowski space, we arrive at the following form of the metric

$$ds^2 = \frac{1}{4\cos^2\tilde{u}_+ \cos^2\tilde{u}_-}(-d\tau^2 + d\theta^2 + \sin^2\theta d\Omega_{d-2}^2). \tag{1.15}$$

From the above eq. (1.15) if we drop the conformal factor, we get a space-time whose geometry is $\mathbb{R} \times S^{d-1}$ which is also the geometry of the Einstein Static Universe.

1.2.3 Conformal structure of AdS_{d+1}

To look at the conformal structure of AdS_{d+1} we start with eq. (1.9)

$$ds^2 = \frac{R^2}{\cos^2\theta}(-d\tau^2 + d\theta^2 + \sin^2\theta\ d\Omega_{d-1}^2). \tag{1.16}$$

After a conformal rescaling, the above metric can be written as

$$ds^2 = -d\tau^2 + d\theta^2 + \sin^2\theta\ d\Omega_{d-1}^2. \tag{1.17}$$

The penrose diagram in this case is a solid cylinder as shown in Fig. 2 with r being the radial coordinate and τ, Ω on the surface [76]. The penrose diagram for the Poincaré patch of AdS is a triangle as shown in Fig. 3 [77]. The boundary is timelike and it so happens that the massless particles can reach the boundary in finite time whereas the massive particles never reach the boundary. We see here that the above metric dictates a space-time whose geometry is $\mathbb{R} \times S^{d-1}$ which is again that of Einstein Static Universe with $0 \leq \theta < \pi/2$. Therefore, we can say that the conformal compactification of AdS_{d+1} results in the boundary structure which resembles half of Einstein static Universe. Now, if a space-time can be conformally compactified in such a way that the boundary structure corresponds to half of Einstein Static Universe then such a space-time is called asymptotically AdS. So we see here that after conformal compactification the boundary of AdS_{d+1} is $\mathbb{R} \times S^{d-1}$ which is same as that of conformally compactified Minkowski space on $\mathbb{R}^{1,d-1}$.
Also, it can be shown that the Euclidean AdS_{d+1} can be conformally compactified into a d+1 dimensional disk.

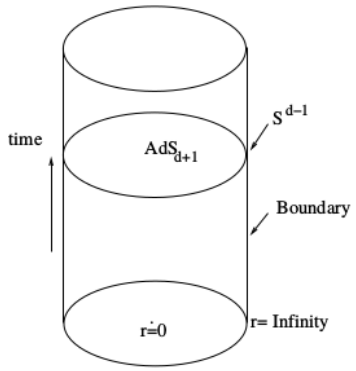

Figure 2 : Penrose diagram for AdS_{d+1} which is a cylinder.

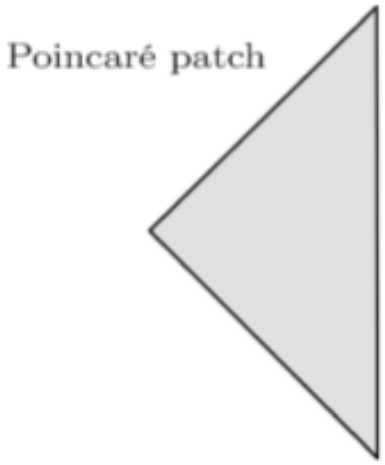

Figure 3 : Penrose diagram for Poincaré patch of AdS which is a triangle.

1.3 Conformal Group

As we have already seen that the boundary of conformally compactified AdS_{d+1} space coincides with the boundary of conformally compactified Minkwoski space on $\mathbb{R}^{1,d-1}$, it becomes interesting to see if the isometry group of AdS_{d+1} is isomorphic to that of the boundary of AdS_{d+1} and how is it related to the group structure of the Minkowskian space. To begin our analysis, we will start by looking at the group structure of conformally compactified d- dimensional Minkowskian space and then the group structure of conformally compactified AdS_{d+1} space.

1.3.1 Group structure for Minkowskian space and it's boundary

We begin with the metric of the d-dimensional Minkowskian space

$$ds^2 = -dt^2 + dr^2 + r^2 d\Omega_{d-2}^2. \tag{1.18}$$

For a d-dimensional Minkowski space, there is a d-dimensional conformal group [78, 79]. Conformal transformations are those transformations which preserve the angle between the two lines. In the context of general relativity they preserve the metric upto a scale factor as they preserve the causal structure of space-time and are given as $g_{ab} = \Omega^2(x) g_{ab}$ where $\Omega(x)$ is a positive function which is smooth everywhere. By conformal group we also have the following set of transformations [80]

$$\begin{aligned}
&Translations : x'^{\mu} = x^{\mu} + a^{\mu}, \\
&Rotations : x'^{\mu} = M^{\mu}_{\nu} x^{\nu}, \\
&Dilations : x'^{\mu} = \alpha x^{\mu}, \\
&Special\ conformal\ transformations : x'^{\mu} = \tfrac{x^{\mu} - (x.x) b^{\mu}}{1 - 2(b.x) + (b.b)(x.x)}.
\end{aligned} \tag{1.19}$$

This statement implies that the metric is invariant under Poincaré transformations. Apart from the Poincaré transformations, the metric is rescaled by a conformal factor under the action of dilations and special conformal transformations which acts on it's conformal boundary. This follows simply from the fact that the conformal boundary is defined up to a conformal rescaling of the metric. Thus, conformal transformations acting on the boundary do not change the bulk metric. The boundary of conformally compactified d-dimensional Minkowski space is invariant under the action of the Lie algebra for infinitesimal - Poincaré transformations, scaling and special conformal transformations. Hence, we see that the boundary of conformally compactified d-dimensional Minkowski space is invariant under the action of the Lie algebra of SO(d,2) and because of this, we say that the boundary of conformally compactified d-dimensional Minkowski space is invariant under the conformal group SO(d,2).

1.3.2 Group structure for AdS and it's boundary

We begin with the metric for AdS_{d+1} space which is embedded in (2,d)-dimensional Minkowski space [78]

$$ds^2 = -dX_0^2 - dX_{d+1}^2 + \sum_{i=1}^{d} dX_i^2. \tag{1.20}$$

Since, in the bulk AdS_{d+1} is a maximally symmetric space and has therefore (d+1)(d+2)/2 Killing vectors. Its isometry group is inherited by the embedding in (2,d)-dimensional Minkowski space and is therefore SO(d,2). Next, we look at the invariance group of the conformal boundary. After conformal compactification one can find out the killing vectors acting on the boundary and it so happens that this group includes dilations and special conformal transformations apart from the Poincaré transformations. Thus at the conformal boundary, we have the same invariance group given by the conformal group SO(d,2).

So, we see that the conformal group SO(d,2) is the symmetry group of both the bulk and at the boundary of AdS_{d+1} This result also dictates that the the conformal boundary of AdS_{d+1} has the same conformal group i.e. SO(d,2), just like the conformal boundary of d-dimensional Minkowski space.
Hence, the conformal symmetries of the boundary of AdS permits a conformal field theory living on the AdS boundary and as a result there is a correspondence between the bulk and the boundary as the symmetries of the group structure is same.

1.4 BTZ black hole

We will now briefly review an important part of 3D AdS space which is the BTZ black hole. Einstein's equations in 3 dimensions with negative cosmological constant has the BTZ black hole solution which is given by [81–83]

$$ds^2 = -N^2 dt^2 + N^{-2} dr^2 + r^2 (N^\phi dt + d\phi)^2, \tag{1.21}$$

where $N^2(r) = -8GM + \frac{r^2}{l^2} + \frac{16G^2J^2}{r^2}$ and $N^\phi(r) = \frac{-4GJ}{r^2}$. J is the angular momentum and M is the mass of the BTZ black hole. The horizons are given by the condition $N^2(r) = 0$,

$$r_\pm^2 = 4GMl^2 \left\{ 1 \pm \left[1 - \left(\frac{J}{Ml} \right)^2 \right]^{1/2} \right\}, \tag{1.22}$$

where $M = \frac{r_+^2 + r_-^2}{8Gl^2}$ and $J = \frac{r_+ r_-}{4Gl}$. From the above expression, we have the conditions $M > 0$, $|J| \leq Ml$ for the existence of the horizon. It showcases the property of a true black hole having an event horizon at r_+ and in the rotating case, a Cauchy horizon at r_-.

The BTZ black hole is asymptotically anti-de Sitter, having no curvature singularity but rather possessing a conical singularity. Because of the constant curvature, the BTZ black hole is locally isometric to anti-de Sitter space but globally they are inequivalent. In the global case, BTZ black hole can be identified in AdS_3 by a discrete subgroup of its isometry group. Also it has been shown that it can occur as the final state of collapsing matter and can have thermodynamic properties having a Hawking Temperature $T = \frac{\hbar(r_+^2 - r_-^2)}{2\pi l^2 r_+}$ and entropy $S = \frac{2\pi r_+}{4\hbar G}$.

Chapter 2

Conformal Field Theory

When we work with quantum field theories, symmetry plays an important role [75, 84]. Apart from the usual Poincaré invariance, sometimes it is also useful to hunt for scale invariance to understand physics pertaining to quantum field theories at different scales. This typically happens when the physical system has no intrinsic scale, like e.g a mass or a coupling constant with length dimensions. Examples are free-field theories of massless fields and thermodynamical systems at the critical point.

Often the scale invariance is broken at the quantum level even though it might be present at the classical level because of generation of the renormalization scale for instance as a result from a conformal anomaly. Renormalization involves a cutoff ϵ, bare coupling constant λ_0, bare mass m_0, renormalization scale μ and from these quatities we calculate the renormalized coupling $\lambda = \lambda(\lambda_0, m_0, \epsilon, \mu)$. The β function which furnishes information about the running of the coupling constant is given as

$$\beta(\lambda, \epsilon) = \mu \frac{d\lambda}{d\mu}|_{\lambda_0, m_0, \epsilon}. \tag{2.1}$$

If we say a quantum field theory is scale invariant it means λ in the eq. (2.1) is μ independent which in turn would lead to vanishing of the β function. This means that scale invariance is related at the quantum level with the appearance of fixed points, i.e to points in which the renormalized couplings do not flow.

The breaking of scale invariance in a theory can lead to renormalization group flows. Research in quantum field theories has lead to the fact that there may exist field theories which have renormalization group flows from a UV fixed point to an IR fixed point. To have scale invariance in the context of renormalization i.e. $\beta = 0$, we have two possible scenarios :-

• To have $\beta = 0$ everywhere implies a trivial QFT, i.e a theory for which there is no renormalization group flow.

OR

• If β is not identically zero and hence the QFT is nontrivial, then it needs to have a zero(fixed point) away from $\lambda = 0$ where a nontrivial theory will emerge i.e. - non-trivial CONFORMAL FIELD THEORY.

As stated earlier even though scale invariance is broken at the quantum mechanical level, conformal invariance can be still respected as a local symmetry

near to a fixed point and therefore we also tend to seek for conformal invariant theories at the quantum scale. It is also been shown that unitary scale-invariant theories are also conformally invariant i.e the space–time symmetry group enlarges from the Poincaré to the conformal group of symmetries. So, we see that study of conformal field theories can be fruitful in various physical situations and the leading reason for us is the AdS/CFT correspondence as we need to understand how the conformal field theory on the "boundary" of AdS is related to the quantities inside the "bulk" of AdS.

2.1 Conformal Group and Algebra

Conformal group transformations are those transformations which preserve the form of the metric upto a scale factor $g_{ab} = \Omega^2(x) g_{ab}$ where $\Omega(x)$ is a positive function [75]. The conformal group is an extension of Poincaré group which involves the following transfromations [80]:-

$$
\begin{aligned}
&Translations : x'^{\mu} = x^{\mu} + a^{\mu}, \\
&Rotations : x'^{\mu} = M^{\mu}_{\nu} x^{\nu}, \\
&Dilations : x'^{\mu} = \alpha x^{\mu}, \\
&Special\ conformal\ transformations : x'^{\mu} = \tfrac{x^{\mu} - (x.x) b^{\mu}}{1 - 2(b.x) + (b.b)(x.x)}.
\end{aligned}
$$

and the corresponding generators are

$$
\begin{aligned}
&Translations : P_{\mu} = -i\partial_{\mu}, \\
&Rotations : L_{\mu\nu} = i(x_{\mu}\partial_{\nu} - x_{\nu}\partial_{\mu}), \\
&Dilations : D = -ix^{\mu}\partial_{\mu}, \\
&Special\ conformal\ transformations : K_{\mu} = -i(2x_{\mu}x^{\nu}\partial_{\nu} - (x.x)\partial_{\mu}).
\end{aligned}
$$

These generators obey the conformal algebra [75]

$$
\begin{aligned}
&[M_{\mu\nu}, P_{\rho}] = -i(\eta_{\mu\rho}P_{\nu} - \eta_{\nu\rho}P_{\mu}), \\
&[M_{\mu\nu}, K_{\rho}] = -i(\eta_{\mu\rho}K_{\nu} - \eta_{\nu\rho}K_{\mu}), \\
&[M_{\mu\nu}, M_{\rho\sigma}] = -i\eta_{\mu\rho}M_{\nu\sigma} \pm permutations, \\
&[M_{\mu\nu}, D] = 0, \\
&[D, K_{\mu}] = iK_{\mu}, \\
&[D, P_{\mu}] = -iP_{\mu}, \\
&[P_{\mu}, K_{\nu}] = 2iM_{\mu\nu} - 2i\eta_{\mu\nu}D.
\end{aligned}
$$

The rest of the commutators vanish.
This algebra can be shown to be ismorphic to SO(d,2) when we use the signature (-, +, +, $\cdots$, +,-) with generators $J_{\mu\nu} = (\mu, \nu = -1, 0, 1, \cdots, d-1)$ and obtaining the following [80]

$$
\begin{aligned}
&J_{\mu\nu} = M_{\mu\nu}, \\
&J_{-1,0} = D, \\
&J_{-1,\mu} = \frac{1}{2}(P_{\mu} - K_{\mu}), \\
&J_{0,\mu} = \frac{1}{2}(P_{\mu} + K_{\mu}).
\end{aligned}
$$

It is worth noting here that for d=2, the conformal group becomes the two-dimensional diffeorphim group it has therefore infinite generators which closes in two copies of the Virasoro algebra, hence it is infinite dimensional.

2.2 Primary Operators

The representations of the conformal group have operators ϕ which are eigenfunctions of the scaling operator D with eigenvalue -iΔ where Δ is called the scaling dimension of the operator [75]. This implies that under a scaling transformation they transform as $\phi(x) \to \phi'(x) = \lambda^{\Delta}\phi(\lambda x)$. Now, from the commutation relation [77]

$$[D, P_\mu] = -iP_\mu \Rightarrow D(P_\mu\phi) = P_\mu(D\phi) - iP_\mu\phi = -i(\Delta+1)(P_\mu\phi), \tag{2.2}$$

we can see that P_μ raises the scaling dimension of the operator by 1 whereas K_μ lowers it by 1 as we have

$$[D, K_\mu] = iK_\mu. \tag{2.3}$$

So we see that P_μ acts as a creation operator whereas K_μ acts as an annihilation operator with respect to the eigenstates of D.

Unitarity conditions puts a lower bound on the dimensions of the operators, particularly in the case of scalar fields it is $\Delta \geq (d-2)/2$ where the equality is for free fields. Because of such a lower bound, the representation of the conformal group has an operator of the lowest dimension and which is annihilated by K_μ at the origin i.e. at $x = 0$ and such an operator is called as the primary operator. They have the following commutation relations :-

$$\begin{aligned}
&[P_\mu, \phi(x)] = i\partial_\mu\phi(x),\\
&[M_{\mu\nu}, \phi(x)] = [i(x_\mu\partial_\nu - x_\nu\partial_\mu) + \Sigma_{\mu\nu}]\phi(x),\\
&[D, \phi(x)] = i(-\Delta + x^\mu\partial_\mu)\phi(x),\\
&[K_\mu, \phi(x)] = [i(x^2\partial_\mu - 2x_\mu x^\nu\partial_\nu + 2x_\mu\Delta) - 2x^\nu\Sigma_{\mu\nu}]\phi(x).
\end{aligned}$$

Here, $\Sigma_{\mu\nu}$ are matrices for the representations of the Lorentz group. The representation for the conformal group in case of the primary operator is characterized by the Lorentz group and the scaling dimension Δ. Apart from the primary operator, the descendant operators are generated by acting on the primary operator with P_μ. In case of conformal group, we use the eigenfunctions of D and not the eigenfunctions of the Hamiltonian P_0 or $M^2 = -P^\mu P_\mu$.
An important characterization of the conformal group SO(d,2) is in terms of the maximally compact subgroup SO(d)×SO(2). Here, the generator for SO(2) is $J_{0(d+1)} = \frac{1}{2}(K_0 + P_0)$. This subsgroup is important when we do the radial quantization of the conformal field theory on $S^{d-1} \times \mathbb{R}$ which is related to the AdS space when the metric is written in terms of global coordinates.
When we do radial quantization [84] in Euclidean space then the spin of the field is given in terms of the SO(d) subgroup whereas the charge in the SO(2) subgroup is the scaling dimension Δ of the field. In case of radial quantization, the Euclidean $\mathbb{R}^d$ is foliated by (d-1) spheres, S^{d-1}, concentric at the origin and this configuration defines the Hilbert space for the CFT states at a radial slice. The operator D is the evolution generator of the states from one radial slice to

another. This is how we see that there is a state-operator correspondence in the Hilbert space.
Now, if we define $|0\rangle$ as the conformal vacuum, then each operator $\phi(x)$ can define a state at the origin by $\phi(0)|0\rangle$. In the context of radial quantization, by virtue of scale invariance this will also represent a state of any size S^{d-1} around the origin. On the other hand, using the same scale invariance we can also move a state at a given radius to the origin by contracting the sphere.
To shed more light on this state-operator correspondence, we see that [75] time acts as a radial direction in $\mathbb{R}$ and the origin corresponds to the past infinity, using the operator $J_{-1,0}$ as the Hamiltonian we can map the opeartor $\mathcal{O}$ to the state as $|\mathcal{O}\rangle = \lim_{x\to 0}\mathcal{O}(x)|0\rangle$. So, when we insert the operator at the origin then the state cooresponding to it is a functional integral on a ball around the origin. On the other hand, when we want to map state to an operator then we take the state as a functional of values of field on a ball around the origin, next shrink this ball to size zero using conformal invariance, this act is equivalent to insertion of some local operator.

2.3 Correlation Functions

The symmetries of the conformal group puts restrictions on the correlation functions of primary fields [75, 84] in terms of their scaling dimensions and spin. It has been shown that the Euclidean correlation functions are also valid for Minkowski space-time. Correlation functions of descendant fields can be obtained by taking the derivative of the primary fields.
For a scalar field, where both the operators have the same scaling dimension $\Delta_1 = \Delta_2 = \Delta$, we have the following form of a two point function:-

$$\langle \mathcal{O}(x_1)\mathcal{O}(x_2)\rangle = \frac{c_{12}}{|x_1 - x_2|^{2\Delta}}, \tag{2.4}$$

where c_{12} is the structure constant.
The three point function is given as

$$\langle \mathcal{O}(x_1)\mathcal{O}(x_2)\mathcal{O}(x_3)\rangle = \frac{C_{123}}{|x_1 - x_2|^{\Delta_1+\Delta_2-\Delta_3}|x_1 - x_3|^{\Delta_1+\Delta_3-\Delta_2}|x_2 - x_3|^{\Delta_2+\Delta_3-\Delta_1}}, \tag{2.5}$$

where C_{123} is the structure constant.
The four point function is given as

$$\langle \mathcal{O}(x_1)\mathcal{O}(x_2)\mathcal{O}(x_3)\mathcal{O}(x_4)\rangle = c_{1234}(u,v)\prod_{i<j}^{4}|x_{ij}|^{\frac{1}{3}\Delta-\Delta_i-\Delta_j}, \tag{2.6}$$

where $c_{1234}(u,v)$ is now a function of the 2 independent cross-ratios u, v which are conformally invariant and are given as

$$u = \frac{|x_{12}||x_{34}|}{|x_{13}||x_{24}|}\ ,\ v = \frac{|x_{14}||x_{23}|}{|x_{13}||x_{24}|}. \tag{2.7}$$

Now, these conformal invariants increase with the increment in the insertion points, so the higher n-point functions will have more of these independent invariants as the constraints imposed by conformal symmetry will be less.

In the case of conformal algebra, the scaling dimension of only two operators are determined by the conformal group, the first is the energy-momentum tensor $T_{\mu\nu}$ which is an operator of dimension $\Delta = d$ and the second is the conserved current J_μ which is an operator of dimension $\Delta = d - 1$.

2.4 Operator Product Expansion

One of the aspects of field theory is the operator product expansion which says that as we bring two operators $\mathcal{O}_1(x)$ and $\mathcal{O}_2(y)$ close enough to each other such that $x \to y$ i.e. they start acting at the same point, then this act results in a generation of a local disturbance at that point which in turn can be written as the sum of local operators whose action is on that same point.
Generally, OPE are written as $\mathcal{O}_1(x)\mathcal{O}_2(y) \to \sum_n C_{12}^n(x-y)\mathcal{O}_n(y)$. When it comes to conformal field theory [84], for two scalar primaries we have the following form

$$\mathcal{O}_{\Delta_i}(x)\mathcal{O}_{\Delta_j}(0) = \sum_k c_{ijk}|x|^{-\Delta_i-\Delta_j+\Delta_k}(\mathcal{O}_{\Delta_k}(0) + descendants), \tag{2.8}$$

where the sum extends over all primaries and their descendants. The coefficients for the decendants for each primary is determined by the conformal invariance. It is also interesting to see that the coefficients c_{ijk} in front of the primaries are similar to the coefficients for the case of three point functions.
So we see that in general any n point correlation can be extracted by using operator product expansion. Using OPE for any two adjacent points we can subsitute n point correlators by an infinite sum of $n-1$ point function.
Generally using the information related to primary fields like scaling dimension Δ, coefficients c_{ijk} etc we can extract a lot of details about the CFT but then we have non-trivial relations arising out of unitarity and crossing symmetry of OPE's which will serve as a hindrance to a proper understanding of the CFT as these conditions are very difficult to tackle. Because of this problem, we look for alternative approaches for CFT and one such way is AdS/CFT correspondence in which the correlation function is expressed in terms of the partition function of the bulk gravity theory in the following manner

$$Z[\phi_{\Delta_i}] \equiv \Big\langle \exp\Big(\int d^dx\ \phi_{\Delta_i}(x)\mathcal{O}_{\Delta_i}(x) \Big) \Big\rangle_{CFT}. \tag{2.9}$$

Here, $\phi_{\Delta_i}(x)$ are classical sources associated with each operator and when we take derivative of Z w.r.t these sources we get the correlation functions as follows

$$\langle \mathcal{O}_{\Delta_1}(x_1)\mathcal{O}_{\Delta_2}(x_2).....\rangle = \frac{\partial^n Z[\phi_{\Delta_i}]}{\partial\phi_{\Delta_1}(x_1)\partial\phi_{\Delta_2}(x_2)....}|_{\phi_{\Delta_i}=0}. \tag{2.10}$$

When the correlators are conformally invariant, the partion function is also conformally invariant. For example under the scaling transformation we have

$$\int d^dx\ \phi_\Delta(x)\mathcal{O}_\Delta(x) = \int d^d(\lambda x)\ \phi_\Delta(\lambda x)\mathcal{O}_\Delta(\lambda x) = \lambda^{d-\Delta}\int d^d(x)\ \phi_\Delta(\lambda x)\mathcal{O}_\Delta(x), \tag{2.11}$$

which implies invariance of Z when the source undergoes a scaling transformation as follows

$$\phi_\Delta(x) \to \lambda^{d-\Delta}\phi_\Delta(\lambda x). \tag{2.12}$$

So we see that even when the source undergoes a transformation of the conformal group, Z still remains an invariant of the conformal group.

Chapter 3

AdS/CFT Correspondence

One of the intriguing aspects of theoretical physics are dualities which have revolutionized perspectives of physics at the fundamental level. Dualities relate two different facets and thus they leads to an enhanced understanding of physics. Implication of this duality is that the mathematical structure of the two theories maybe identical but there may be differences from a physical standpoint. One of the interesting dualities that we will talk about in this chapter is the AdS/CFT correspondence which connects conformal field theory on a flat space-time to string theory. This is interesting because string theory, is a theoretical setup for quantum gravity whereas quantum field theory is not. Now, even though these two theories are different, AdS/CFT correspondence assumes the existence of a correspondence between the two theories and this is one of the most attractive features of this duality, which pushes research for it's deeper understanding and possible applications.

Another interesting feature of AdS/CFT correspondence is the fact that it is a realization of the holographic principle. The holographic principle says that for a gravitational theory the number of degrees of freedom for a given volume V scales as the surface area ∂V of that volume. This holographic principle has it's roots in the Bekenstein bound which states that the maximum entropy for a given volume V is given by $S \leq \frac{2\pi ER}{\hbar c}$ where E is the mass-energy of the system, R is the radius of the sphere inside which the system fits [85]. In case of AdS/CFT correspondence the quantum gravity theory/string theory is defined on a manifold, which has the form $AdS \times X$, where AdS is the Anti-de Sitter space which holds the gravitational theory and X is a compact space and the "holographically dual" field theory exists on the conformal boundary this Anti-de Sitter space.

A further rich aspect of AdS/CFT correspondence is that in a certain limit of string theory it exhibits features of strong-weak coupling duality which means that when the boundary field theory is strongly coupled, the dual bulk gravitational theory is weakly curved, thus classical gravitational tools become valid here. The validity of the classical gravity theory further prompts research into the area of understanding of strongly coupled boundary field theory using classical gravitational setup.

3.1 Aspects related to the AdS/CFT correspondence

Before proceeding with the AdS/CFT correspondence, it is worthy to look at few concepts of physics which are closely related to it and which will be helpful in understanding the correspondence itself.

3.1.1 Holography

The first important idea that is closely related to the above mentioned correspondence is that of Holography. The idea of holography was motivated by the result that the entropy of a black hole is propotional to area of the horizon. Before we go ahead, it is important to go through few notions related to entropy itself. We will essentially talk about Thermodynamic entropy and Shannon Entropy.

Thermodynamic Entropy, S, in its statistical mechanics interpretation tells us how many possible microstates are there for a given macrostate and it is formally given as

$$dS = \frac{\Delta Q}{T}, \tag{3.1}$$

where Q is heat and T is the temperature. In some sense, it measures the amount of disorder in a system. On the other hand Shannon Entropy was proposed by a mathematician as a measure of information content and it essentially gives a measure of no. of bits required for a particular process or a configuration. It uses bits as it's unit which are dimensionless.

Generally, it so happens that the thermodynamic entropy is much greater than Shannon entropy as because the degrees of freedom in both cases are different. In the first case we deal with atoms, electrons etc, in the later case we simply deal with electronic stuff. But, for same degrees of freedom they will be same , so now, we raise 2 questions :-
First- What are the elementary degrees of freedom?
Second - How much information can be there per unit of the elementary degree of freedom so as to calculate total information/entropy for a given configuration?

The answers to the above two questions are closely related to the idea of holography. In 1970's it was proposed that the area of the event horizon never decreases and using this as a clue Bekenstein proposed that even black holes have entropy to solve the entropy problem related to the black holes at that time. Before Bekenstein's proposal it was believed that black holes have no entropy and if one throws some matter inside the black hole then it disappears as because we dont't know what happens inside a blackhole. As a result, violation of second law of thermodynamics takes place. Bekenstein's idea was that the increase in the black hole entropy compensates more or in same amount for the loss of matter entropy and this preserves then the 2nd law of thermodynamics. In generalised fashion, this statement would mean that the black hole entropy along with the entropy of material outside the black hole never decreases and this statement is called Generalised Second Law of Thermodynamics. This law is preserved when Hawking predicted that black holes need to radiated if they carry entropy and in this case the entropy of thermal radiation more than compensates for the loss due to black hole entropy.

Next step was taken by Sorkin who related black hole entropy with the area of the horizon. But, there came another problem-that of black hole information paradox - loss of information of the material going inside the black hole and in order to resolve this issue the idea of Holography was proposed which said that the information content of the infalling material is encoded in fluctuations of the horizon. Hence, effectively one can say that information/entropy of a given region of space time depends on its surface area.

We now return to the previous two questions, the answer to the first is maybe that the elementary degrees of freedom are strings as it was in the context of string theory that a proposal for solving this paradox has been elaborated and the maximum information can be known from what is called as Bousso Bound. Thus we see how Holography nicely explains two very important aspects of physics finally leading to the idea that quantum gravity in a given d dimensional spacetime can be described by a theory on it's d-1 dimensional boundary having less than one degree of freedom per planck area.

3.1.2 Large N expansion

The large N expansion is the domain where physicists saw initial glimpses of relation between string theory and gauge theory [86].

String Theory was originally developed to explain strong interactions but later on it was realised that it was QCD that could describe the strong interactions. However, QCD is not helpful enough to study strong interactions in the low energy limit and it is here that the concept of "Duality" becomes important, in particular to study the strongly coupled low energy regime of gauge theory one can expect a dual description of QCD which will be weakly coupled. There are indications that this weakly coupled candidate might be string theory and 't Hooft's large N expansion was one these indications. At low energies, QCD is a confining theory, in the sense, there are only bound states, i.e mesons and baryons and no free quarks or gluons and there exists a linear potential between quark and an antiquark at large distance between them and the flux lines are confined to a flux tube or string.

It is difficult to explain the low energy regime, as the QCD coupling constant is not a good expansion parameter, so in a hope to simplify the theory, it was proposed by 't Hooft to generalize SU(3) to SU(N) so that we have N colours instead of 3 and then do perturbation in terms of parameter 1/N. Introducing the 't Hooft coupling which is $\lambda = g^2_{YM}N$ in which λ is held fixed as N is taken to infinity (This limit is called 'Hooft limit) and scaling the fields we see that the entire Lagrangian is

$$\mathcal{L} = \frac{1}{g^2_{YM}}\mathrm{Tr}(F^2_{\mu\nu} + ...) = \frac{N}{\lambda}\mathrm{Tr}(F^2_{\mu\nu} + ...). \tag{3.2}$$

As a result each vertex will carry a factor propotional to $\frac{N}{\lambda}$ and for each propagator $\frac{\lambda}{N}$.

One can use the pictorial representation of Feynman graphs in what is called as the "Double Line Notation" . In this, the fields in the fundamental representation of the SU(N) group are represented by q_i and fields in the antifundamental representation of the SU(N) group are represented $q_{\bar{i}}$ where the bar is used as the distinguishing factor and $i, \bar{i} = 1...N$. The fields in the adjoint representation of the SU(N) group are writen using branching rules as hermitian matrices,

as a direct product of fundamental and antifundamental fields. Using the Feynman graph notation, the oriented lines are represented using indices $i, \bar{j}$ and this enables us to write the propagators as a double line. So, Feynamn diagrams for adjoint fields can be represented in terms of Double Lines. On analysing such diagrams one can think of them in the following manner:-

The Propagators as the edges of some polyhedron(E)

The vertices as the vertices of this polyhedron(V)

The region bounded by the polyhedron (or closed loops) as the face of the polyhedron(F)
As a result each Feynman diagram will carry a factor given as

$$N^{V-E+F}\lambda^{E-V} = N^{\chi}\lambda^{E-V}, \tag{3.3}$$

where $\chi = 2 - 2g$ is Euler characteristic for the surface corresponding to the diagram, g being the genus of the surface. Thus we see that the 't Hooft expansion organizes graphs according to their topology and the perturbative expansion of the free energy is of the form

$$F = \sum_{0}^{\infty} N^{2-2g} f_g(\lambda). \tag{3.4}$$

In the large N limit , it will turn out that only planar diagrams will give a contribution of order N^2 while all other diagrams gets suppressed by a factor $\frac{1}{N^2}$.

This expansion turns out to be similar to the closed string perturbative expansion in string theory which is [87]

$$Z = \sum_{g \geq 0} g_s^{2g-2} Z_g, \tag{3.5}$$

if we identify g_s with 1/N.

Thus, we see how string theory might be related to gauge theory.

3.1.3 D-brane

In this section we will look at D-branes which are one of the important ingredients of the AdS/CFT correspondence. They play a role in both open string and closed string scenario.

D - branes in open string setup

In string theory, open strings are allowed for two kinds of boundary conditions - Neumann and Dirichlet. [77, 88]. Neumann boundary conditions imply the endpoints of the string is free where as the Dirichlet boundary conditions imply that the endpoints are fixed. Now, we can have p+1 Neumann boundary conditions where there are p spatial dimensions or d-p-1 Dirichlet boundary conditions which imply that the endpoints are fixed on p+1 dimensional membrane called as D-p-brane where p denotes the spatial dimensional extension. So accordingly we have, p=0 called as a point like object, p=1 as string and p=2 as a membrane. These D-p brane or D-brane (D stands for Dirichlet) are dynamical

in nature, having degrees of freedom on it. Now, in the regime of small string coupling constant that is $g_s \ll 1$ when we consider low energy spectrum that is neglecting massive string excitations, then the open string spectrum corresponds to a supersymmetric gauge theory living on the D-Brane. Open string excitations which are parallel to the D-brane correspond to the gauge field while the transverse are related to the scalar fields. Now, if we have N coincident D-branes then the gauge group is $U(N)$ and the coupling constant is now g_sN. Hence this N D-brane setup is valid for $g_sN \ll 1$.

D - branes in closed string setup

When we generalize black hole solutions in higher dimensions allowing for some flat directions, we call them as p - branes [77, 89, 90]. If there exists a p-brane solution without charge then it is a Schwarzschild black hole extended on a flat torus. If they carry charge (extremal/non-extremal) then they extend in p spatial dimensions and they carry charge due to p + 1-form antisymmetric tensor field and the metric is dictated by harmonic functions. As these black branes can live in various dimensions, there can be various names for them depending on the horizon topology. So for example, p = 0 corresponding to a horizon is a black hole, p = 1 is called a black string and p = 2 is called a black membrane.

Now, when we study these p - brane solutions in supergravity setup, then these solutions turned out to be the alternative description of what is called as D - Branes. In closed string perspective, D-branes are looked upon as solitonic solutions in the low energy limit of SUGRA. They are then considered as sources of gravitational field, bending the spacetime around them. This scenario works when there is a weak curvature implying the characteristic length scale of AdS space L to be large. Since in this case we have $\frac{L^4}{\alpha'^2} \propto g_sN$, where $\alpha' = l_s^2$, l_s being the string length we have the validity condition for a stack of N D-Branes as $g_sN \gg 1$.

3.1.4 Greybody factor

Another important aspect that is closely related to AdS/CFT is the calculation of the greybody factors for black holes in the setup of D-branes [75]. Now, generally when one calculates the differential rate of spontaneous emission of particles from black holes, it so turns out that the absorption cross section for a particle which is coming in form infinity does not remains constant but rather varies. Hence, this variational nature of absorption cross section has lead to it's name as the greybody factor.

It was observed that the Hawking radiation can also be explained as two open strings colliding on a D-brane and then forming a closed string which then propagates in the bulk and that the D-Brane setup can explain the microscopic aspects of the black hole thermodynamics which can explain these greybody factor calculations in a neat manner.

This cross section was calculated at the tree level using D3 branes on which lives the gauge theory and also in the supergravity context. In the both these setups, the calculations were in agreement with each other. This beautiful result - that green's functions for a gauge theory can be calculated using tools

of supergravity further boosted the research arena to better understand the connections between gauge theory and string theory.

3.2 AdS_5/CFT_4 correspondence

The bouquet of ideas presented in the above section were put together beautifully by Maldacena in what is now known as AdS/CFT Correspondence [75].

We consider D3 branes in 10 dimensional spacetime on which open strings end. We consider two types of perturbative excitations in this case. The first one is that of closed string excitations corresponding to that of excitations of empty space and in the low energy limit, only the massless states are excited hence the associated action would be that of supergravity.

Next, there will be open string excitations on the D brane which again in the low energy limit would correspond to excitations of D brane itself and the associated action in this case would be that of $\mathcal{N} = 4$ $U(N)$ supersymmteric Yang-Mills Theory.

There would be another action term which would correspond to interaction between the brane and bulk. Therefore the complete effective action of the massless modes (only massless modes, as we are considering low energy,energies lower than the string scale $1/l_s$) is

$$S = S_{bulk} + S_{brane} + S_{int}, \tag{3.6}$$

where S_{bulk} corresponds to the action related to supergravity, S_{brane} corresponds to $\mathcal{N} = 4$ SYM on D3 brane and S_{int} corresponds to the interaction between the bulk modes and the brane modes. Now, the S_{int} has terms proportional to κ which goes as $g_s\alpha'^2 \to 0$ as we take the low energy limit by keeping energy fixed and taking $l_s \to 0$ or $\alpha' \to 0$. So we see that in the low energy limit S_{int} goes to zero and we are left with two decoupled systems - supergravity in the bulk and SYM theory on the D3 brane.

Now, another aspect D3-branes is that they also behave like solitons in string theory as mentioned above and it has been shown that they satisfy extremal solution of supergravity, in the strong string coupling regime. Looking at the metric of black brane which is

$$\begin{aligned} ds^2 &= f^{-1/2}(-dt^2 + dx_1^2 + dx_2^2 + dx_3^2) + f^{1/2}(dr^2 + r^2 d\Omega_5^2), \\ F_5 &= (1 + *)dt dx_1 dx_2 dx_3 df^{-1}, \\ f &= 1 + \tfrac{R^4}{r^4}, \quad R^4 = 4\pi g_s N \alpha'^2. \end{aligned} \tag{3.7}$$

Here, again we have two types of excitations in the low energy regime (from the perpective of an observer at infinity), massless particles in the bulk and excitations near $r = 0$. But in the low energy regime, because the absorption cross section goes as ω^3, these two types of excitations decouple from each other. This decoupling can be understood as a result of the fact the wavelength of the particle in the bulk becomes greater than that of brane and excitations near $r = 0$ find it difficlut to cross the gravitational barrier and escape to the asymptotic region. Hence, we have two decoupled regions - supergravity in the bulk and the near horizon geometry region.

In the near horizon case when $r \ll R$ we get,

$$ds^2 = \frac{r^2}{R^2}(-dt^2 + dx_1^2 + dx_2^2 + dx_3^2) + R^2\frac{dr^2}{r^2} + r^2 d\Omega_5^2. \tag{3.8}$$

From the above metric we see that the first two terms are that of AdS_5 metric while the last term is that of S^5. Therefore the near horizon geometry turns out to be that of $AdS_5 \times S^5$ while asmptotically it is flat.

Now when we compare these two forms of decoupled systems and noticing that there are free closed strings propagating in the bulk in both cases (or supergravity), we are led to the conclusion that the $\mathcal{N} = 4$ $U(N)$ SYM field theory in 3+1 dimensions is dual to type IIB superstring on $AdS_5 \times S^5$.

Matching of Symmetries

Another piece of supporting evidence for this duality comes from matching the symmetries from both the sides.

Now, looking at the metric for AdS_5, we can see that the isometry group for AdS_5 is $SO(4,2)$ whereas the isometry group for S^5 is $SO(6)$. Therefore the full symmetry group for $AdS_5 \times S^5$ is $SO(4,2) \times SO(6)$. On the field theory side we have the conformal group in 4 dimensions. Also, the global internal symmetry for $\mathcal{N} = 4$ SYM is $SU(4)$ is related to the $SO(6)$ R symmetry, so the full symmetry group on the field theory side is $SO(4,2) \times SO(6)$ which coincides with the symmetry group of the string theory on $AdS_5 \times S^5$.

Limits and Validity

Now we will analyze the validity of the above correspondence.

A perturbative analysis for Yang-Mills theory is valid when

$$g_{YM}^2 N \sim g_s N \sim \frac{R^4}{l_s^4} \ll 1. \tag{3.9}$$

On the other side, the supergravity regime is valid when the AdS radius R is large compared to the string length and this implies

$$\frac{R^4}{l_s^4} \sim g_s N \sim g_{YM}^2 N \gg 1. \tag{3.10}$$

We also require N to be large in the supergravity regime.

So, we see that the correspondence is valid in both the cases for different strenghths of coupling. It relates the weakly coupled field theory to the strongly coupled gravity or vice-versa. Hence, we have "duality" here.

There are also various forms of this correspondence, which are :-

• Weak form: Correspondence is valid for large $g_s N$, thus it is valid in the supergravity regime but the full string theory might not be mapped to the field theory.

• Mid-way form: Correspondence is valid for finite $g_s N$, we can take the 't Hooft limit here, by keeping $\lambda = g_s N$ fixed and taking $N \to \infty$ limit.

• Strong form: Correspondence is valid for all values of g_s and N.

The Field-Operator Correspondence

This duality, which has been described above, becomes useful if we know how to setup a map between String Theory or in the large N limit AdS gravity and Field Theory.

In the bulk, in the large N limit we have the SUGRA fields and their dynamics is dictated by the action $\mathcal{S}_{sugra}[\phi]$. Solving their equation of motions require the boundary value of fields ϕ_i. The classical on-shell action for SUGRA is then given as a functional of ϕ_i. Another way to look at these ϕ_i will be as external sources for operators $\mathcal{O}_i$ of the CFT. So, we see that there is a one to one correspondence between the bulk SUGRA fields ϕ_i and the boundary CFT operators $\mathcal{O}_i$. In the general case we will see that the,
String theory partition function

$$Z_{string}(\phi_i) = \int\limits_{\Phi_i|_{boundary}=\phi_i} D\Phi_i \; e^{-S_{string}(\phi_i)}, \tag{3.11}$$

and CFT partition function

$$\Big\langle \exp(\int d^4x \; \phi_i \mathcal{O}_i) \Big\rangle_{CFT} = e^{-W(\phi_i)} = Z_{CFT}(\phi_i), \tag{3.12}$$

are related as

$$\int\limits_{\Phi_i|_{boundary}=\phi_i} D\Phi_i \; e^{-S_{string}(\phi_i)} = \Big\langle \exp(\int d^4x \; \phi_i \mathcal{O}_i) \Big\rangle_{CFT}. \tag{3.13}$$

When the SUGRA approximation holds we have

$$e^{-S_{sugra}(\phi_i)}\Big|_{\delta S_{sugra}=0, \Phi_i|_{boundary}=\phi_i} = Z_{CFT}(\phi_i). \tag{3.14}$$

It is to be noted that on the r.h.s, the required limit for CFT is $N \to \infty$ and $\lambda \to \infty$.

Using this relation between boundary and bulk, we can calculate correlation functions for the field theory.

UV-IR relation

Another interesting feature of this correspondence is the scale/radius relation also known as the UV/IR duality. Now, by analyzing the conformal transformations on the Poincaré coordinates, we can see that the radial direction in the bulk corresponds to an energy scale in the boundary field theory. This implies that high energy(short distance/UV) on the boundary will correspond to large radius(IR) in the bulk, further, if we have a UV cutoff for the boundary field theory, then it will map to an IR cutoff in the bulk. This can be seen as follows.

Now, in the case of $\mathcal{N} = 4$ SYM on a unit radius S^3, the number of degrees of freedom scales as

$$S \sim N^2 \delta^{-3}, \tag{3.15}$$

where δ is the UV cutoff.

In case of gravity, when we measure the area in terms of planck units, then we have

$$\frac{Area}{4G_N} = \frac{V_{S^5} R^3 \delta^{-3}}{4G_N} \sim N^2 \delta^{-3}, \tag{3.16}$$

here, δ is related to the radial coordinate r as $r = 1 - \delta$ and since the area is given for $\delta \ll 1$, it means large radius cutoff/IR cutoff in the bulk.

The above physics relating UV parameter of the field theory to the IR of the bulk, also showcased the underlying holographic nature of the AdS_5/CFT_4 correspondence explicitly.

Chapter 4

Entanglement Entropy

In this chapter, we will look at the entanglement entropy starting from its basic, quantum mechanical, meaning and then extending it to various setups like QFT,CFT and also in the AdS/CFT context.

4.1 Basic concepts

We will start with the review of basic concepts of the entanglement entropy and it's related relevant properties [26].

4.1.1 Definition

We consider a quantum mechanical system at zero temperature and divide it into two parts A and B such that the total Hilbert space can be written as the direct product of the two subspaces as $\mathcal{H}_{tot} = \mathcal{H}_A \otimes \mathcal{H}_B$ where $\mathcal{H}_A$ corresponds to the subsystem A and $\mathcal{H}_B$ corresponds to the subsystem B. Next, we consider an observer, who has access through measurement only to the subsystem A, such a quantum system is described by the reduced density matrix ρ_A as

$$\rho_A = \mathrm{Tr}_B \rho_{tot}, \tag{4.1}$$

where $\rho_{tot} = |\Psi\rangle\langle\Psi|$ is the density matrix for the ground state and the trace is only over $\mathcal{H}_B$.

Next, we use the von Neumann entropy of the reduced density matrix ρ_A to define the the entanglement entropy of the subsystem A with respect to the subsystem B where the DOF have been traced out, as follows

$$S_A = -\mathrm{Tr}_A \rho_A \log \rho_A. \tag{4.2}$$

The above equation called as the "Entanglement Entropy" , which is an aspect of the "Quantum" world, gives us a measure of the "entanglement" between the two subsystems A and B.

Also, closely related to the von Neumann entropy is the Rényi entropy given as

$$S_A^{(n)} = \frac{1}{1-n} \ln \mathrm{Tr} \rho_A^n. \tag{4.3}$$

The two above stated entropies are related as follows

$$S_A = \lim_{n \to 1} S_A^{(n)}. \tag{4.4}$$

Renyi entropy is very useful for calculating the entanglement entropy.

If we want to define entanglement entropy for a system at finite temperature where $T = \beta^{-1}$ then we need to use the thermal density matrix $\rho_{thermal} = e^{-\beta H}$, H being the total Hamiltonian of the system. It is important to stress that for systems at finite temperature entanglement entropy contains contributions both from quantum correlations ("quantum entanglement") and thermal correlations. An important point, which we will discuss in this thesis is the possibility to distill quantum correlations out of the entanglement entropy for thermal states.

4.1.2 Properties

Some of the useful and important properties of the entanglement entropy are :-

1. When we consider the density matrix at zero temperature and bipartition of the system is such that B is the complement of A then we have the following condition

$$S_A = S_B. \tag{4.5}$$

The above condition holds true for Rényi entropy also as we have $S_A^{(n)} = S_B^{(n)}$. This condition showcases the fact the entanglement entropy is "not" an extensive quantity hence this condition is violated at the finite temperature when the entanglement entropy contains extensive thermal contributions.

2. If we divide the system A into two subsystems A_1 and A_2, which do not intersect each other then we have the following subadditivity relation

$$S_{A_1} + S_{A_2} \geq S_A. \tag{4.6}$$

The above relation can be used to define mutual information $I(A_1, A_2)$ as

$$I(A_1, A_2) = S_{A_1} + S_{A_2} - S_A \geq 0. \tag{4.7}$$

This mutual information can also be written in terms of Rényi entropy as follows

$$I^{(n)}(A_1, A_2) = S_{A_1}^{(n)} + S_{A_2}^{(n)} - S_A^{(n)} \geq 0. \tag{4.8}$$

In case, they do intersect, then we have

$$S_{A_1} + S_{A_2} \ \geq \ S_{A_1 \cup A_2} + S_{A_1 \cap A_2}. \tag{4.9}$$

3. If we have three subsystems A, B, C which do not intersect each other, then we have the following strong subadditivity inequality

$$S_{A+B+C} + S_B \ \leq \ S_{A+B} + S_{B+C}. \tag{4.10}$$

$$S_A + S_C \ \leq \ S_{A+B} + S_{B+C}. \tag{4.11}$$

4.2 Entanglement Entropy in QFT

The features discussed in the previous section holds for a generic quantum system. In this section we consider the specific case of a quantum field theory (QFT). We consider a quantum field theory on a manifold which has d+1 dimensions and has the form $\mathbb{R} \times N$ where $\mathbb{R}$ corresponds to the time direction and N corresponds to the d-dimensional space-like manifold. We then define the subsystem A, at a fixed time $t = t_0$, as a d-dimensional submanifold of N, i.e $A \subset N$ and next we define submanifold B as the complement of A. So, effectively we have the boundary of A, denoted by ∂A, dividing the manifold N into two submanifolds A and B. Now, using eq.(4.2) we define, S_A, the entanglement entropy for the subsystem A. As this entanglement entropy has divergent contributions in the UV, due to the short distance correlations, we introduce an UV cutoff a. In the expression for the S_A, it was found that the leading term is proportional to the area of the boundary of A, that is ∂A [28,29]

$$S_A = \gamma . \frac{\text{Area}(\partial A)}{a^{d-1}} + \text{subleading terms}, \tag{4.12}$$

where γ is a constant, depending on the system in consideration. This expression for S_A is better known as the "Area Law" and it can be interpreted by arguing that the area between the region A and B give a measure of the correlations which have been traced out. Since, this expression for S_A is dependent on the geometry of the submanifold A, it is also called as the geometric entropy.

It is worthy to note here that the area law has a strong resemblance to the Bekenstein-Hawking thermodynamical entropy or the Black Hole entropy denoted as S_{BH}. The area law, has it's motivational roots in the Bekenstein-Hawking entropy which in turn is proportional to the area of the event horizon and is given as

$$S_{BH} = \frac{\text{Area of horizon}}{4G_N}, \tag{4.13}$$

where G_N is the Newton constant.

The analogy between eqs. (4.12) and (4.13) has inspired several attempts to give an interpretation of the Bekenstein Hawking entropy in terms of entanglement of quantum fields in the black hole geometry [28, 29]. For instance, if we say that let the subsystem B correspond to the region inside the black hole horizon and A outside the horizon, then S_{BH} can be looked upon as the entanglement entropy for an observer who has access only to the region A and traces over the DOF localized in the region B as it is inside the horizon.

However, there are differences between the Bekenstein-Hawking entropy and the entanglement entropy. The main difference is that differently from the entanglement entropy black hole entropy is universal. The entanglement entropy is proportional to the number of matter fields which is not the case for the black hole entropy. Also, the entanglement entropy includes the UV divergences which is again not the case for the black hole entropy. One promising direction for trying to understand the relationship between Bekenstein-Hawking entropy and entanglement entropy is to consider entanglement entropy as originated not from matter fields but from gravitational DOF, like e.g in the framework of induced gravity. [30, 31, 91–94].

4.3 Entanglement Entropy in two dimensional CFT

In the previous section we saw the area law for entanglement entropy in a quantum field theory, in d+1 dimensions. An important particular case of that we obtain for $d = 1$. In this case the boundary between the region A and B are two isolated points for which one cannot define an area. One can show that in the particular case of 2D CFT's the entanglement entropy scales logarithmically as the length l of the subsystem A and is given as $S_A = \frac{c}{3} \log \frac{l}{a}$, where c is the central charge for the corresponding CFT. In order to better understand the entanglement entropy for 2D CFT's, it is also required to properly comprehend the calculational mechanism for entanglement entropy in conformal field theories. So, we now move to the calculational tools for entanglement entropy in two-dimensional CFT.

4.3.1 Replica trick

In case of two-dimensional CFT's, entanglement entropy is calculated using the replica trick [35].

The replica method starts by considering a lattice quantum field theory in 1 space and 1 time dimension. The lattice sites are denoted by x, which is a discrete variable and a denotes the lattice spacing. Observables are given by $\hat{\phi}(x)$, eigenstates are given by $|\phi(x)\rangle$ which spans the basis of the Hilbert space and the corresponding eigenvalues are given by $\phi(x)$. H being the Hamiltonian of the theory, the partition function at an inverse temperature β is described by $Z(\beta) = \text{Tr } e^{-\beta H}$. Next, we work in the Euclidean space and write the thermal density matrix elements as a path integral on the imaginary time interval $(0, \beta)$ as follows

$$\rho(\phi_x|\phi'_{x'}) = Z^{-1} \int [d\phi(y,\tau)] \prod_{x'} \delta(\phi(y,0) - \phi'_{x'}) \prod_{x} \delta(\phi(y,\beta) - \phi_x) e^{-S_E}, \quad (4.14)$$

where S_E is the euclidean action.

When we normalize the above equation, in path integral framework it means we are joining the two edges along $\tau = 0$ and $\tau = \beta$ and this results in a cylinder whose circumference is β.

We now consider a subsystem A whose points x lies in the disjoint interval $(u_1, v_1)....(u_N, v_N)$. We obtain the reduced density matrix ρ_A by joining points which do lie in A. As a result of this action, we will end up with an open cut for each interval on the cylinder. Next, we take n copies of this cylinder and join all these cylinders along the open cuts in a cyclic fashion, this entire exercise now gives us $\text{Tr}\rho_A^n$ which can be written as

$$\text{Tr}\rho_A^n = \frac{Z_n(A)}{Z^n}, \quad (4.15)$$

where $Z_n(A)$ is the partition function on this n copies of cylinder. We now move from the lattice setup to a continuum setup by letting $a \to 0$. When we move to the continuum limit, we end up with fields $\phi(x, \tau)$, the points can now take real values and the cuts u_i, v_i now represent branch points and these n cylinders are

now n sheeted Riemann surface. This n sheeted Riemann surface is denoted by $\mathcal{R}_{n,N}$ where there are $2N$ branch points.

It so turns out, that calculating partition functions on this n sheeted Riemann surfaces is not easy, hence we move the calculations to the complex plane $\mathbf{C}$ as follows

$$Z_{\mathcal{R}} = \int_{\mathcal{C}_{u_1,v_1}} [d\varphi_1.....d\varphi_n] \exp\Bigg[- \int_{\mathbf{C}} dx d\tau \Big(\mathcal{L}[\varphi_1](x,\tau) + ... + \mathcal{L}[\varphi_n](x,\tau) \Big) \Bigg], \tag{4.16}$$

where $\int_{\mathcal{C}_{u_1,v_1}}$ means "restricted" path integral having conditions

$$\varphi_i(x,0^+) = \varphi_{i+1}(x,0^-),\ x \in [u_1,v_1],\ i = 1....n, \tag{4.17}$$

where we have $n + i \equiv i$.
The lagrangian density of the multi-copy model on the complex plane $\mathcal{L}^{(n)}[\varphi_1....\varphi_n](x,\tau)$ is now expressed as a sum of lagrangian's of the individual n copies and is written as

$$\mathcal{L}^{(n)}[\varphi_1....\varphi_n](x,\tau) = \mathcal{L}[\varphi_1](x,\tau) + ... + \mathcal{L}[\varphi_n](x,\tau). \tag{4.18}$$

As a result of eq.(4.16) we have local fields at $(u_i,0),(v_i,0)$ which are called as "Twist" fields $\mathcal{T}_n$ / "Anti-twist" fields $\tilde{\mathcal{T}}_n$. The twist field is associated with permutation symmetry $i \mapsto i+1$ whereas the anti-twist field $\tilde{\mathcal{T}}_n$ is associated with $i+1 \mapsto i$. These fields reflect the symmetry under the exchange of the individual copies.
So finally, we can write the partition function in terms of these fields as

$$Z_{\mathcal{R}_{n,N}} \propto \langle \mathcal{T}_n(u_1,0)\tilde{\mathcal{T}}_n(v_1,0)...\mathcal{T}_n(u_N,0)\tilde{\mathcal{T}}_n(v_N,0)\rangle_{\mathcal{L}^{(n)},\mathbf{C}}. \tag{4.19}$$

More importantly, we have for correlation functions on $\mathcal{R}_{n,1}$

$$\langle \mathrm{O}(x,\tau;\text{sheet } i).....\rangle_{\mathcal{L},\mathcal{R}_{n,1}} = \frac{\langle \mathcal{T}_n(u_1,0)\tilde{\mathcal{T}}_n(v_1,0)\mathrm{O}(x,\tau)...\rangle_{\mathcal{L}^{(n)},\mathbf{C}}}{\langle \mathcal{T}_n(u_1,0)\tilde{\mathcal{T}}_n(v_1,0)\rangle_{\mathcal{L}^{(n)},\mathbf{C}}}, \tag{4.20}$$

where O is a field in the multi-copy model $\mathcal{L}^{(n)}$, representing $\mathcal{L}$ on the i^{th} sheet. The above expression takes care of the proportionality constants and the same will be valid in the case of $\mathcal{R}_{n,N}$, with added products of twist/anti-twist fields.

Going ahead further, we can define $\tilde{\varphi}_k = \sum_{j=1}^{n} e^{2\pi i \frac{k}{n} j}\varphi_j,\ k = 0,1,..,n-1$ which diagonalize the twist/anti-twist operator as follows

$$\mathcal{T}_n\tilde{\varphi}_k = e^{2\pi i \frac{k}{n}}\tilde{\varphi}_k, \tag{4.21}$$

$$\tilde{\mathcal{T}}_n\tilde{\varphi}_k = e^{-2\pi i \frac{k}{n}}\tilde{\varphi}_k. \tag{4.22}$$

When the various values of k decouple, then the total partition function can be written as a product of partition function of individual k

$$Z_{\mathcal{R}} = \prod_{k=0}^{n-1} \langle \mathcal{T}_{k,n}(u_1,0)\tilde{\mathcal{T}}_{k,n}(v_1,0)....\rangle_{\mathcal{L}^{(n)},\mathbf{C}}, \tag{4.23}$$

where we now have $\mathcal{T}_{k,n}\tilde{\varphi}_k = e^{2\pi i\frac{k}{n}}\tilde{\varphi}_k$, $\tilde{\mathcal{T}}_{k,n}\tilde{\varphi}_k = e^{-2\pi i\frac{k}{n}}\tilde{\varphi}_k$ and

$$\mathcal{T}_n = \prod_{k=0}^{n-1}\mathcal{T}_{k,n}, \qquad \tilde{\mathcal{T}}_n = \prod_{k=0}^{n-1}\tilde{\mathcal{T}}_{k,n}. \tag{4.24}$$

After calculating $\mathrm{Tr}\rho_A^n$ for positive integral n, using twist/anti-twist operators, the final step to calculate the entanglement entropy S_A, now involves taking the derivative of $\mathrm{Tr}\rho_A^n$ w.r.t n and then take the limit $n \to 1$ and is given as follows

$$S_A = -\lim_{n\to 1}\frac{\partial}{\partial n}\mathrm{Tr}\rho_A^n = \lim_{n\to 1} S_A^{(n)}, \tag{4.25}$$

where $S_A^{(n)}$ is the Rényi entropy.

4.3.2 Entanglement entropy for a single interval

We first consider $N = 1$ and a two dimensional euclidean space with a planar topology implying that there is a single interval $[u, v]$ of length $l \equiv |u - v|$ [35]. This interval lies on an infinitely long one dimensional quantum system at zero temperature and one can use $w, \bar{w}$ as the complex coordinate on this system in the following manner : $w = x + i\tau$, $\bar{w} = x - i\tau$. So, this system is the n-sheeted Riemann surface $\mathcal{R}_{n,1}$ and next, we will map this system on the complex plane $\mathbf{C}$ where the coordinates are $z, \bar{z}$.

We start this mapping by considering the holomorphic component of the stress tensor and the relation is

$$T(w) = \Big(\frac{dz}{dw}\Big)^2 T(z) + \frac{c}{12}\{z, w\}, \tag{4.26}$$

where $\{z, w\}$ is the Schwarzian derivative.
Next, we proceed with the expectation value of this stress tensor and using the above relation we get

$$\langle T(w)\rangle_{\mathcal{R}_{n,1}} = \frac{c}{12}\{z, w\} = \frac{c(n^2-1)}{24n^2}\frac{(v-u)^2}{(w-u)^2(w-v)^2}, \tag{4.27}$$

as $\langle T(z)\rangle_{\mathbf{C}} = 0$ because of translation and rotation invariance.
Now, using eq. (4.20), the expectation value of the stress tensor is mapped to the z-plane $\mathbf{C}$ where we have n copies of $\langle T(w)\rangle$ and we get

$$\frac{\langle \mathcal{T}_n(u,0)\tilde{\mathcal{T}}_n(v,0)T^{(n)}(w)\rangle_{\mathcal{L}^{(n)},\mathbf{C}}}{\langle \mathcal{T}_n(u,0)\tilde{\mathcal{T}}_n(v,0)\rangle_{\mathcal{L}^{(n)},\mathbf{C}}} = \frac{c(n^2-1)}{24n}\frac{(v-u)^2}{(w-u)^2(w-v)^2}, \tag{4.28}$$

where we have multiplied the r.h.s of the above equation by n.
Next, on comparing eq. (4.28) with the conformal Ward identity, we will see that the correlation function of twist/anti-twist fields $\langle \mathcal{T}_n(u,0)\tilde{\mathcal{T}}_n(v,0)\rangle_{\mathcal{L}^{(n)},\mathbf{C}}$ behaves like a two point function of the primary operators

$$\langle \mathcal{T}_n(u,0)\tilde{\mathcal{T}}_n(v,0)\rangle_{\mathcal{L}^{(n)},\mathbf{C}} = |u-v|^{-2d_n}, \tag{4.29}$$

where d_n is the scaling dimension and is given as $d_n = \frac{c}{12}\Big(n - \frac{1}{n}\Big)$.
Now, using eqs. (4.15),(4.19) and the above stated behaviour, we get

$$\mathrm{Tr}\rho_A^n = c_n\left(\frac{v-u}{a}\right)^{-c(n-1/n)/6}, \tag{4.30}$$

where a has been used to make the results dimensionless and c_n are constants. We use eq. (4.3) along with (4.30) to compute the Rényi entropy which is as follows

$$S_A^{(n)} = \frac{c}{6}\left(1+\frac{1}{n}\right)\log\frac{l}{a} + c'_n, \tag{4.31}$$

where $c'_n \equiv \frac{\log c_n}{1-n}$.
Finally, taking the limit $n \to 1$, as given in eq. (4.4), we get the entanglement entropy

$$S_A = \frac{c}{3}\log\frac{l}{a} + c'_1 \tag{4.32}$$

Finite temperature

We can go ahead further and extend this result obtained in the zero temperature case for a single interval to the case of finite temperature [35]. To do so, we will now consider a 2D Euclidean space having the toplogy of an infinite cylinder, with compact euclidean time dimension of circumference β and take the single interval along the axis of this infinite cylinder of circumference β, which means the system has periodic boundary conditions for the temporal axis. Here, β also stands for the inverse temperature. To map coordinates from the cylindrical geometry to the complex plane, we will use the conformal map

$$w = (\beta/2\pi)\log z, \tag{4.33}$$

where w lies on the cylinder and z on the plane. This will map the interval "along the axis" of the cylinder.
To map the two point function we will use the following relation

$$\langle \mathcal{T}_n(z_1,\bar{z}_1)\tilde{\mathcal{T}}_n(z_2,\bar{z}_2)\rangle = |w'(z_1)w'(z_2)|^{d_n}\langle \mathcal{T}_n(w_1,\bar{w}_1)\tilde{\mathcal{T}}_n(w_2,\bar{w}_2)\rangle. \tag{4.34}$$

Using eqs. (4.33),(4.34) we can extract $\mathrm{Tr}\rho_A^n$ in a thermal mixed state existing at a finite temperature β^{-1} and consequently S_A as

$$S_A = \frac{c}{3}\log\left(\frac{\beta}{\pi a}\sinh\frac{\pi l}{\beta}\right) + c'_1. \tag{4.35}$$

For low temperature regime, when $l \ll \beta$ eq. (4.35) can be approximated and we have

$$S_A = \frac{c}{3}\log\frac{l}{a} + c'_1. \tag{4.36}$$

On the other hand, for large temperature regime, when $l \gg \beta$, from eq. (4.35), we have

$$S_A = \frac{\pi c l}{3\beta} + c'_1. \tag{4.37}$$

So, we see that at high temperatures thermal correlations dominates over quantum correlations and von Neumann entropy converts into the expected (extensive) form of Gibbs thermal entropy for a 2D QFT.

Finite size

Let us now consider the case in which the 2D euclidean space has cylindric toplogy but with a compact "space" dimension and the single interval lies along the circumference of this infinite cylinder. In this case, the circumference is denoted by L_{cir} and β is now aligned along the axis of the cylinder. So, now we have an interval of length l on a finite 1D system whose length is L_{cir} and this system has periodic boundary conditions for the spatial axis. Physically, this means that the subsystem A is at zero temperature and has a finite size since the interval lies along the circumference.
In this case we have to use the following conformal map

$$w = (iL_{cir}/2\pi)\log z, \tag{4.38}$$

where w lies on the cylinder and z on the plane.
Using eq. (4.34) and (4.38), we get S_A as

$$S_A = \frac{c}{3}\log\left(\frac{L_{cir}}{\pi a}\sin\frac{\pi l}{L_{cir}}\right) + c_1'. \tag{4.39}$$

Notice, that eq. (4.39) is symmetric under the exchange of $l \to L_{cir} - l$, which is expected, as this is a pure state and must respect $S_A = S_B$ where B in this case would be the system with length $L_{cir} - l$. We also see from (4.39) that the entanglement entropy is maximal when $l = \frac{L_{cir}}{2}$ and reduces to eq. (4.32) when we take $L_{cir} \to \infty$.

Finite temperature and Finite size

Let us now consider the case in which we have a 2D CFT at a finite temperature and size. If, we want the underlying geometry of the total system to be finite in extent and also at finite temperature, then we need to have periodic boundary conditions for both spatial and temporal axis. This action of imposing periodic boundary conditions on both space and time means we have the topology of the torus. Now, differently from the cylinder case correlation function on torus are not universal, as they depend on the full operator content of the conformal field theory. Moreover, we don't have any maps to move from plane to torus so calculation of correlation function on torus is of non-trivial nature. The computation has therefore to be performed case by case.

In [32], the authors have calculated the entanglement entropy on a torus for the case of massless Dirac fermion where β is the periodicity for the compact temporal direction and the total/finite length for the non-compact spatial direction is taken to be 1. The single interval of length L lies along the non-compact spatial direction. For their calculations, the authors have used the following relation

$$\mathrm{Tr}\rho_A^n = \prod_{k=0}^{n-1}\langle \mathcal{T}_{n,k}(z,\bar{z})\tilde{\mathcal{T}}_{n,k}(0,0)\rangle. \tag{4.40}$$

This is the representation of the partition function that we had initially seen in (4.23).

The form of the two point function is

$$\langle \mathcal{T}_{n,k}(l)\tilde{\mathcal{T}}_{n,k}(0)\rangle = \left|\frac{2\pi\eta(\tau)^3}{\theta_1(L|\tau)}\right|^{\frac{2k^2}{n^2}} \frac{|\theta_\nu(\frac{kL}{n}|\tau)|^2}{|\theta_\nu(0|\tau)|^2}, \tag{4.41}$$

where θ is the Jacobi theta function and η is the Dedekind eta function. This relation is valid for $\nu = 2, 3, 4$ fermionic sector. We see that as k enters in the argument of the theta function, the analytic continuation is difficult and so we can obtain closed expressions in high and low temperature expansions only. In case of high temperature expansion for $\nu = 3$ we have

$$\begin{aligned} S_A = \tfrac{1}{3}\log\left[\frac{\beta}{\pi a}\sinh\frac{\pi L}{\beta}\right] + \tfrac{1}{3}\sum_{m=1}^{\infty}\log\frac{(1-e^{2\pi L/\beta}e^{-2\pi m/\beta})(1-e^{-2\pi L/\beta}e^{-2\pi m/\beta})}{(1-e^{-2\pi m/\beta})^2} \\ +2\sum_{l=1}^{\infty}\frac{(-1)^l}{l}\frac{\frac{\pi Ll}{\beta}\coth\left(\frac{\pi Ll}{\beta}\right)-1}{\sinh\left(\frac{\pi l}{\beta}\right)}. \end{aligned} \tag{4.42}$$

If we take an infinite spatial extent, then we move from torus to an infinite cylinder and accordingly from eq. (4.42) we will get the leading term for S_A as

$$S_A = \frac{1}{3}\log\left[\frac{\beta}{\pi a}\sinh\frac{\pi L}{\beta}\right]. \tag{4.43}$$

which as expected coincides with the result (4.35). When we try to extract the finite piece for S_A then as expected, the leading term turns out to be the thermal entropy $\frac{\pi}{3\beta}$.

In case of low temperature expansion for $\nu = 3$ we have

$$\begin{aligned} S_A = \tfrac{1}{3}\log\left[\tfrac{1}{\pi a}\sin(\pi L)\right] + \tfrac{1}{3}\sum_{m=1}^{\infty}\log\frac{(1-e^{2\pi iL}e^{-2\pi\beta m})(1-e^{-2\pi iL}e^{-2\pi\beta m})}{(1-e^{-2\pi\beta m})^2} \\ +2\sum_{l=1}^{\infty}\frac{(-1)^{l-1}}{l}\frac{1-\pi lL\cot\pi lL}{\sinh(\pi l\beta)}. \end{aligned} \tag{4.44}$$

and at zero temperature, eq. (4.44) reduces to

$$S_A = \frac{1}{3}\log\left[\frac{1}{\pi a}\sin(\pi L)\right]. \tag{4.45}$$

which as expected coincides with the result (4.39).

4.4 Holographic Entanglement Entropy

In the previous sections, we came across entanglement entropy in QFT's and also in the context of CFT's, we now move on to understand entanglement entropy in the the context of the AdS/CFT correspondence. The holographic setup for calculations of the entanglement entropy is very useful from two different perspectives. First, one can use the bulk gravitational theory to calculate the entanglement entropy of the dual QFT living in the boundary. As we will see

this is a very powerful tool, which allows entanglement entropy computations in terms of bulk geometric quantities. Second, one can use the holographic correspondence in the other direction. One can try to understand quantum entanglement in the bulk gravitational background by using the dual QFT. This approach is particularly useful for tackling difficult problems suach as the above-mentioned problem of the realtionship between entanglement entropy and Bekenstein-Hawking entropy for black holes.

Using the AdS/CFT duality, the idea to calculate entanglement entropy for a given CFT using gravitational tools was originally proposed by Ryu-Takayanagi [25]. According to their proposal, the entanglement entropy S_A for a subsystem A on $d+1$ dimensional CFT is given as

$$S_A = \frac{\text{Area}(\gamma_\text{A})}{4G_N^{(d+2)}}, \tag{4.46}$$

where γ_A is a d dimensional spacelike surface having minimal surface area in the bulk AdS_{d+2} and γ_A is constructed in such a way that, if it's boundary is denoted by $\partial\gamma_A$ then we have $\partial\gamma_A = \partial A$, where ∂A is the $d-1$ dimensional boundary of subsystem A lying on the boundary CFT and $G_N^{(d+2)}$ is the $d+2$ dimensional Newton constant.

As an explanation of eq. (4.46) we note that on the CFT_{d+1}, we divide the system into two parts A, B. S_A then stands for the entanglement entropy relative to the observer in A for whom the region B is inaccessible as it's degrees of freedom have been traced over. The boundary ∂A is then extended inside the bulk such that we have a manifold γ_A satisfying $\partial\gamma_A = \partial A$ and whose surface area picks up the minimal value. On the bulk gravity side, γ_A serves as a holographic screen which covers the region B, inside the AdS space. The idea of saturation of the entropy bound is reflected in the fact that the eq. (4.46) picks the surface which has the minimal area [26].

4.4.1 Holographic Entanglement Entropy in $\text{AdS}_3/\text{CFT}_2$

We consider $\text{AdS}_3/\text{CFT}_2$ as it is one of the simple and well-understood setups for calculating the holographic entanglement entropy [25,26,42]. Also, $\text{AdS}_3/\text{CFT}_2$ has the advantage that the holographic results can be cross-checked against the 2D CFT results which we have discussed in the previous section. Going by the AdS/CFT correspondence, the central charge of the 2D CFT is related to R, the radius of AdS_3 [95] as

$$c = \frac{3R}{2G_N^{(3)}}, \tag{4.47}$$

where $G_N^{(3)}$ is the three dimensional Newton constant.

At the AdS_3 boundary, the metric is divergent, so we need to introduce a cutoff ρ_0 for regularization purpose. This means that our physical space is now restricted as we have $\rho \leq \rho_0$. According to the IR/UV relation discussed in the previous section, this procedure of introducing cutoff in the bulk corresponds to having a UV cutoff for the dual CFT [96,97]. If L is the total length of the system and a is the UV cutoff in the dual CFT then we have

$$e^{\rho_0} \sim L/a. \tag{4.48}$$

We have seen in chapter **1.** that 3D gravity with a negative cosmological constant allows for three different classes of solutions namely pure AdS_3 in Poincaré and global coordinates and the BTZ black hole. To these different bulk solutions there will correspond a dual 2D CFT living on different boundaries. The use of the Ryu-Takayanagi formula (4.46) will therefore produce a different result for the three cases. In case of pure AdS_3, the dual 2D CFT lives on an infinite cylinder with compact dimension along the spacelike direction. Infinite plane corresponds to a 2D CFT at zero temperature with infinite spacelike direction. In the case of the AdS_3 black hole, the dual CFT lives on an infinite cylinder with compact dimension along the time-like direction. This corresponds to a 2D CFT at a finite temperature with infinite spacelike direction. In all of these cases the minimal surface γ_A turns out to be one dimensional spacelike geodesic connecting the two points on the boundary. So, in order to calculate S_A we simply need to calculate the length of this spacelike geodesic and use this length as the Area(γ_A) in eq. (4.46) and later make use of eqs. (4.47),(4.48) to match it against the CFT results. We will discuss the three cases separately.

Zero Temperature - Poincaré Coordinates

We now proceed to calculate the holographic entanglement entropy at zero temperature when the dual boundary CFT lies on a plane, hence we use the Poincaré metric for AdS_3

$$ds^2 = \frac{R^2}{z^2}(-dt^2 + dz^2 + dx^2). \tag{4.49}$$

Here, the space is spanned by (t, x) and x lies in the range $-\infty < x < \infty$. The subsystem A has length l and it's endpoints are $(x_1, z) = (-l/2, a)$ and $(x_2, z) = (l/2, a)$. The geodesic between these two points is given by the half circle

$$(x, z) = \frac{l}{2}(\cos s, \sin s), \quad (\epsilon \leq s \leq \pi - \epsilon), \tag{4.50}$$

where $\epsilon = \frac{2a}{l}$ and the length of the geodesic is given as

$$\text{Length}(\gamma_\text{A}) = 2R \int_\epsilon^{\pi/2} \frac{ds}{\sin s} = -2R \log(\epsilon/2) = 2R \log \frac{l}{a}. \tag{4.51}$$

The holographic entanglement entropy is given as

$$S_A = \frac{\text{Length}(\gamma_\text{A})}{4G_N^{(3)}} = \frac{c}{3} \log \frac{l}{a} \tag{4.52}$$

We see that the above eq. (4.52) matches with the CFT result as obtained in (4.32).

Zero Temperature - Global Coordinates

Moving on, we will now calculate the holographic entanglement entropy at zero temperature when the dual boundary CFT lies on an infinite cylinder with compact space-like direction, hence we use the AdS_3 metric in global coordinates

$$ds^2 = R^2(-\cosh \rho^2 dt^2 + d\rho^2 + \sinh \rho^2 d\theta^2). \tag{4.53}$$

Here, cylinder is spanned by (t, θ) at the boundary $\rho = \rho_0$. The subsystem A has length l and the total length of the system is L. The endpoints of A are $\theta = 0$ and $\theta = \frac{2\pi l}{L}$. The length of the geodesic L_{γ_A} is given as

$$\cosh\left(\frac{L_{\gamma_A}}{R}\right) = 1 + 2\sinh\rho_0^2 \ \sin^2\left(\frac{\pi l}{L}\right). \tag{4.54}$$

Considering large UV cutoff, we have $e^{\rho_0} \gg 1$ and consequently, the holographic entanglement entropy is given as

$$S_A \simeq \frac{R}{4G_N^{(3)}} \ \log\left(e^{2\rho_0}\sin^2\left(\frac{\pi l}{L}\right)\right) = \frac{c}{3}\log\left(e^{\rho_0}\sin\left(\frac{\pi l}{L}\right)\right). \tag{4.55}$$

Next, using eq. (4.48), finally we can have

$$S_A = \frac{c}{3}\log\left(\frac{L}{\pi a}\sin\left(\frac{\pi l}{L}\right)\right). \tag{4.56}$$

We see that the above eq. (4.56) matches with the CFT results as obtained in (4.39).

Finite Temperature - Global Coordinates

We now move on to calculate holographic entanglement entropy at finite temperature when the dual boundary CFT lies on a cylinder of circumference β and the length of the total system L is infinite such that $\beta/L \ll 1$. At such high temperature, the bulk configuration corresponds to the Euclidean BTZ black hole [81] as discussed in chapter 1, whose metric is

$$ds^2 = (r^2 - r_+^2)d\tau^2 + \frac{R^2}{(r^2 - r_+^2)}dr^2 + r^2 d\varphi^2, \tag{4.57}$$

where φ has the periodicity $\varphi \sim \varphi + 2\pi$ and to obtain a smooth geometry, the Euclidean time is compactified as $\tau \sim \tau + \frac{2\pi R}{r_+}$. When we take the boundary limit $r \to \infty$, we get the relation between the boundary CFT and the bulk BTZ black hole

$$\frac{\beta}{L} = \frac{R}{r_+} \ll 1. \tag{4.58}$$

The subsystem A has endpoints $\varphi = 0$ and $\varphi = \frac{2\pi l}{L}$. Now, to find the geodesic distance we notice that the Euclidean BTZ black hole at a temperature T is dual to a thermal AdS_3 at a temperature $1/T$, this duality can be achieved through a modular transformation on the CFT side [98]. Next, we define new coordinates

$$r = r_+\cosh\rho, \quad r_+\tau = R\theta, \quad r_+\varphi = Rt, \tag{4.59}$$

such that eq. (4.57) becomes the Euclidean version of the AdS_3 metric (4.53). Using this Euclidean version of AdS_3 metric, the geodesic length L_{γ_A} is given as

$$\cosh\left(\frac{L_{\gamma_A}}{R}\right) = 1 + 2\cosh\rho_0^2 \ \sinh^2\left(\frac{\pi l}{\beta}\right), \tag{4.60}$$

where we have $e^{\rho_0} \sim \beta/a$.
Using (4.46), the holographic entanglement entropy is now given as

$$S_A(\beta) = \frac{c}{3} \log \left(\frac{\beta}{\pi a} \sinh \left(\frac{\pi l}{\beta} \right) \right). \tag{4.61}$$

We see that the above eq. (4.61) matches with the CFT results as obtained in (4.35). The geodesic for various lengths of A takes shape [42] as shown in Fig. 4(a) when it coincides with that of normal AdS_3. If the subsystem length becomes very large, then eventually the geodesic will cover a part of the horizon. When this happens, we start seeing a thermal extensive behaviour because now $l/\beta \gg 1$. So, we see that under AdS/CFT duality the thermal entropy for a boundary CFT is dual to the black hole entropy in the bulk gravity. When there is a horizon, then geodesics corresponding to S_A and S_B (B is the complement of A) cover different parts of the horizon, so then, S_A is no longer equal to S_B as shown in Fig. 4(b). This violation of $S_A = S_B$ is expected as the system is now composed of mixed states. Also, when the length of A becomes large enough, such that it equals the total system length then γ_A will break into two pieces, one will wrap the horizon completely and the other will be hinged at the boundary as shown in Fig. 4(c).

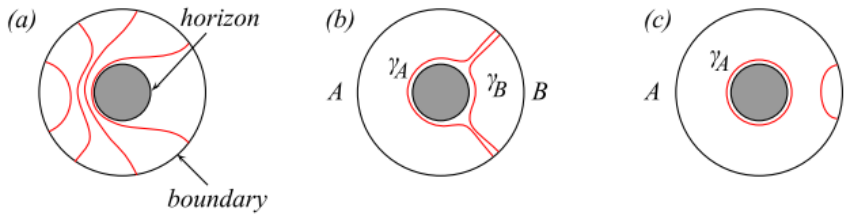

Figure 4 : Geodesic nature for various lengths of A.

Chapter 5

Entanglement Negativity

When we consider entanglement for a quantum system which is in pure state then the von Neumann entropy or the entanglement entropy serves as a good measure to capture entanglement. But when we consider mixed state, then the entanglement entropy contains an extensive thermal entropy term and fails to give an appropriate measure of quantum correlations [56, 59]. Also, it has been shown by Werner in [99] that mixed states do no always violate Bell's inequality. Because of these issues, there is the need to define a new measure to characterize entanglement for mixed states and this new measure called as *negativity* was provided by Vidal and Werner [54]. We will discuss entanglement negativity in various setups in this chapter.

5.1 Basic concepts

The starting point for entanglement negativity is the identification of a parameter analogous to the Bell's inequality through which we can characterize quantum entanglement in mixed states. To detect whether a given state is entangled or not, we need a separability criterion and for mixed states we use positive partial transpose criterion also known as PPT.

For PPT, we consider a bipartite system whose Hilbert space is written as a tensor product $\mathcal{H}_L \otimes \mathcal{H}_R$ [59]. The basis for $\mathcal{H}_R$ is $|\tau_a\rangle$ where $a \in \{1, 2.., \dim(\mathcal{H}_\mathcal{R})\}$ and basis for for $\mathcal{H}_L$ is $|e_\alpha\rangle$ where $\alpha \in \{1, 2.., \dim(\mathcal{H}_\mathcal{L})\}$. The matrix elements for a density matrix ρ, in this basis can be written as

$$\rho_{a\alpha,b\beta} = \langle \tau_a e_\alpha | \rho | \tau_b e_\beta \rangle. \tag{5.1}$$

We define the partial transpose of the density matrix, ρ^Γ, with respect to the left subsystem as

$$\rho^\Gamma_{a\alpha,b\beta} = \rho_{a\beta,b\alpha} = \langle \tau_a e_\beta | \rho | \tau_b e_\alpha \rangle. \tag{5.2}$$

If ρ^Γ has non-negative eigenvalues, then ρ has positive partial transpose (PPT). Then, as put forth by Peres [100] we have that when ρ has PPT, then ρ is separable.

To understand the Peres criterion better, we start with the fact that the density matrix ρ and it's transpose will have the same non-negative eigenvalues.

Let us now write a two particle state, which is separable, as a tensor product of two single particles

$$\rho_{12} = \sum_n p_n \ \rho_{1n} \otimes \rho_{2n}. \tag{5.3}$$

Now, as the single particle states have non-negative eigenvalues, we expect that the two particle state density matrix ρ_{12} must also have all non-negative eigenvalues.

We now consider another density matrix σ which is built by taking partial transpose of only a single particle state in the two particle state density matrix ρ_{12}

$$\sigma_{12} = \sum_n p_n \ (\rho_{1n})^T \otimes \rho_{2n}. \tag{5.4}$$

Recalling, now that the $(\rho_{1n})^T$ has the same non-negative eigenvalues as ρ_{1n}, we expect that σ_{12} will also possess all non-negative eigenvalues and in case it has a *negative* eigenvalue then σ_{12} is not separable. Thus, we see that if ρ has PPT then it is considered separable.

Another property associated with the PPT criterion is that ρ is undistillable if ρ has PPT [101]. "Undistillable" here means that it is not possible to extract any pure entanglement, in case we are able to extract, then we have "distillable" entanglement and the measure of this "distillable" entanglement is called as *negativity*. So, *entanglement negativity* can be seen a measure of the amount of violation of the PPT criterion and it is defined as

$$\mathcal{N}(\rho) = \frac{\|\rho^\Gamma\| - 1}{2}, \tag{5.5}$$

where $\|\rho^\Gamma\|$ is the trace norm and represents sum of the absolute values of the eigenvalues of $\|\rho^\Gamma\|$ i.e. $\|\rho^\Gamma\| = \mathrm{Tr}|\rho^\Gamma|$. So, if we have

$$\mathrm{Tr}(\rho^\Gamma) = \sum_i \lambda_i^{(+)} + \sum_j \lambda_j^{(-)} \equiv 1 = \mathrm{Tr}(\rho), \tag{5.6}$$

then going by the definition of negativity we have,

$$\mathcal{N}(\rho) = \frac{1}{2}\left(\sum_i |\lambda_i^{(+)}| + \sum_j |\lambda_j^{(-)}| - 1 \right) = \sum_j |\lambda_j^{(-)}|, \tag{5.7}$$

implying negativity is the sum of the absolute values of the negative eigenvalues of ρ.

We also have *logarithmic negativity* which is defined as

$$\mathcal{E}(\rho) = \log \|\rho^\Gamma\|, \tag{5.8}$$

which gives an upper bound of the distillable entanglement. Further, we have

$$\mathcal{E}(\psi_{max}) = S(\rho_{max}^{R,L}), \tag{5.9}$$

implying that for a maximally entangled state ψ_{max} present in a bipartite system, the logarithmic negativity is equal to the entanglement entropy of the reduced density matrix $\rho_{max}^{R,L}$ of one of the subsystems.

5.2 Entanglement Negativity in CFT

In the previous chapter, we have described the replica trick which is used to calculate the entanglement entropy in CFT's. In this section we will see how to compute the entanglement negativity using a modified version of this replica trick as in the case of entanglement negativity we have the notion of partial transpose which is absent for entanglement entropy [56].

5.2.1 $\mathcal{E}$ and parity of n

To begin with, we consider a density matrix ρ for a bipartite system whose Hilbert space is written as $\mathcal{H} = \mathcal{H}_1 \otimes \mathcal{H}_2$ and $|e_i^{(1)}\rangle$ and $|e_j^{(2)}\rangle$ are the corresponding bases for each of the Hilbert space. We next define the partial transpose of ρ with respect to the second Hilbert space as follows

$$\langle e_i^{(1)} e_j^{(2)} | \rho^{T_2} | e_k^{(1)} e_l^{(2)} \rangle = \langle e_i^{(1)} e_l^{(2)} | \rho | e_k^{(1)} e_j^{(2)} \rangle. \tag{5.10}$$

Let us consider the trace of $(\rho^{T_2})^n$ in terms of the parity of n, as follows

$$\begin{aligned} \mathrm{Tr}(\rho^{T_2})^{n_e} &= \sum_i \lambda_i^{n_e} = \sum_{\lambda_i>0} |\lambda_i|^{n_e} + \sum_{\lambda_i<0} |\lambda_i|^{n_e}, \\ \mathrm{Tr}(\rho^{T_2})^{n_o} &= \sum_i \lambda_i^{n_o} = \sum_{\lambda_i>0} |\lambda_i|^{n_o} - \sum_{\lambda_i<0} |\lambda_i|^{n_o}, \end{aligned} \tag{5.11}$$

where n_e stands for even n and n_o stands for odd n. If we put $n_o = 1$ in the above equation, we get the normalization $\mathrm{Tr}(\rho^{T_2}) = 1$ and we put $n_e = 1$, then we have

$$\mathrm{Tr}(\rho^{T_2}) = \sum_{\lambda_i>0} |\lambda_i| + \sum_{\lambda_i<0} |\lambda_i| = \sum_i |\lambda_i| = \mathrm{Tr}|\rho^{T_2}|. \tag{5.12}$$

Using the analytic continuation for even n i.e $n_e \to 1$, we can get

$$\mathcal{E} = \lim_{n_e \to 1} \ln \mathrm{Tr}(\rho^{T_2})^{n_e}. \tag{5.13}$$

The above equation tells us that only even n needs to be considered for calculating $\mathcal{E}$.

Moving on, we consider the case of a pure state $|\psi\rangle$, which in terms of the bases is given as

$$|\psi\rangle = \sum_j c_j |e_j^{(1)} e_j^{(2)}\rangle, \tag{5.14}$$

where the coefficient $c_j \in [0, 1]$. The density matrix $\rho = |\psi\rangle\langle\psi|$ is given as

$$\rho = \sum_{i,j} c_i c_j |e_j^{(1)} e_j^{(2)}\rangle\langle e_i^{(1)} e_i^{(2)}|, \tag{5.15}$$

and it's partial transpose with respect to the second space is

$$\rho^{T_2} = \sum_{i,j} c_i c_j |e_j^{(1)} e_i^{(2)}\rangle\langle e_i^{(1)} e_j^{(2)}|. \tag{5.16}$$

The n-th power of ρ^{T_2} is

$$(\rho^{T_2})^n = \begin{cases} \sum_{i_1,j_1} c_{i_1}^{n_o} c_{j_1}^{n_o} |e_{i_1}^{(2)} e_{j_1}^{(1)}\rangle\langle e_{j_1}^{(2)} e_{i_1}^{(1)}|, & n = n_o \ odd, \\ \\ \sum_{i_1,j_1} c_{i_1}^{n_e} c_{j_1}^{n_e} |e_{i_1}^{(2)} e_{j_1}^{(1)}\rangle\langle e_{i_1}^{(2)} e_{j_1}^{(1)}|, & n = n_e \ even, \end{cases} \tag{5.17}$$

and the resulting trace is

$$\mathrm{Tr}(\rho^{T_2})^n = \begin{cases} \sum_r c_r^{2n_o} = \mathrm{Tr}\rho_2^{n_o}, & n = n_o \ odd, \\ \\ \Big[\sum_r c_r^{n_e}\Big]^2 = \Big(\mathrm{Tr}\rho_2^{n_e/2}\Big)^2, & n = n_e \ even, \end{cases} \tag{5.18}$$

where $\rho_2 = \mathrm{Tr}_1(\rho) = \sum_j c_i^2 |e_i^{(2)}\rangle\langle e_i^{(2)}|$.
If, we now do the analytic continuation for odd n i.e $n_o \to 1$, we have the normalization $\mathrm{Tr}(\rho^{T_2}) = \mathrm{Tr}\rho_2 = 1$.
For $n_e \to 1$, we have the following result for the pure state

$$\mathcal{E} = 2 \ln \mathrm{Tr}\rho_2^{1/2} = S_{A_2}^{(1/2)}. \tag{5.19}$$

The above equation says that for a pure state the entanglement negativity is equal to the Rényi entropy of order 1/2 and thus we see a confirmation of the statement conveyed through eq. (5.9).

5.2.2 Partial Transpose

We move on with the calculation of entanglement negativity for a ground state in a one dimensional system when we have the tripartition of the system into A_1, A_2 and B as shown in Fig. 5 below [56].

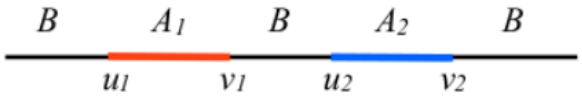

Figure 5 : Tripartition of the system into A_1, A_2 and B.

We consider the entanglement between A_1 and A_2 whose union is A i.e. $A_1 \cup A_2 = [u_1, v_1] \cup [u_2, v_2] = A$ and the complementary is B. We have the following reduced density matrix

$$\begin{aligned} \rho_1 \equiv \rho_{A_1} &= \mathrm{Tr}_{A_2}(\rho_A) = \mathrm{Tr}_{B\cup A_2}(\rho), \\ \rho_2 \equiv \rho_{A_2} &= \mathrm{Tr}_{A_1}(\rho_A) = \mathrm{Tr}_{B\cup A_1}(\rho). \end{aligned} \tag{5.20}$$

We denote the form of the reduced denisty matrix after partial transpose with respect to A_1 degree of freedom as

$$\rho_A^{T_{A_1}} = \rho_A^{T_1}, \tag{5.21}$$

and with respect to A_2 degree of freedom as

$$\rho_A^{T_{A_2}} = \rho_A^{T_2}. \tag{5.22}$$

If we use the replica trick as mentioned previously for calculating entanglement entropy, for two disjoint intervals we have

$$\mathrm{Tr}\rho_A^n = \langle \mathcal{T}_n(u_1)\overline{\mathcal{T}}_n(v_1)\mathcal{T}_n(u_2)\overline{\mathcal{T}}_n(v_2)\rangle_{\mathbb{C}}. \tag{5.23}$$

In order to obtain partial transpose we need to interchange the upper edge with the lower edge of the second cut as shown in the middle of Fig. 6 [56]. If we now join cyclically n copies of such interchanged edges, i.e $\rho_A^{T_2}$, we will have an n sheeted Riemann surface which will have reversed order of row and column indices as compared to the initial one, this problem is solved by again reversing the order of row and column indices in A_2 as shown in the bottom of Fig. 6. This is now called as *reversed partial transpose* $\rho_A^{C_2}$ and it's relation with the partial transpose is $\rho_A^{C_2} = C\rho_A^{T_2}C$ where C will reverse the order of indices either on the upper or on the lower edge and $C^2 = 1$.

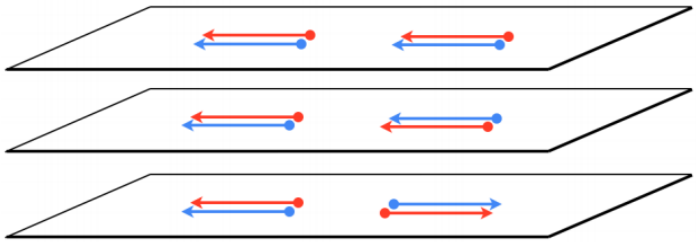

Figure 6: Top: The reduced density matrix ρ_A for 2 disjoint intervals. Middle: The partial transpose with respect to the second interval $\rho_A^{T_2}$. Bottom: The reversed partial transpose $\rho_A^{C_2}$.

As $\mathrm{Tr}(\rho_A^{T_2})^n = \mathrm{Tr}(\rho_A^{C_2})^n$, we can join cyclically n of $\rho_A^{C_2}$, to get $\mathrm{Tr}(\rho_A^{T_2})^n$ as the partition function on this n sheeted Riemann surface as shown in Fig. 7 [56].

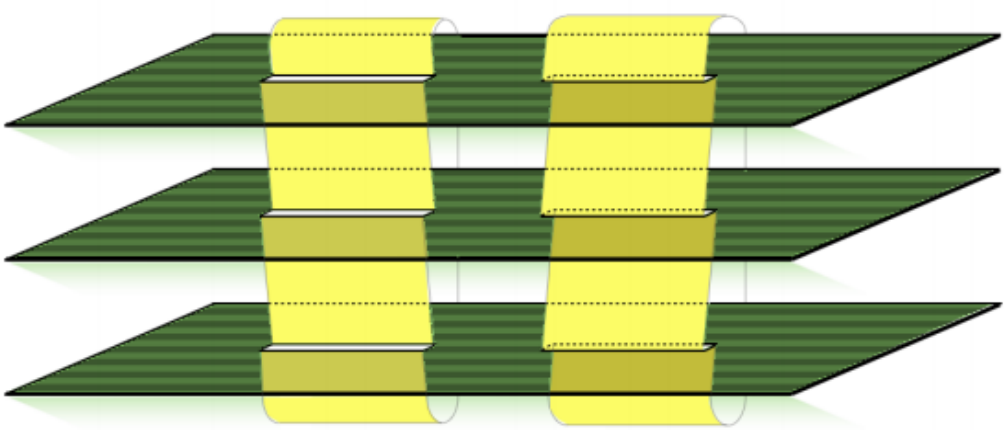

Figure 7: $\mathrm{Tr}(\rho_A^{T_2})^n = \mathrm{Tr}(\rho_A^{C_2})^n$ for $n = 3$.

Finally, the four point function of the twist/anti-twist fields can now be written as

$$\mathrm{Tr}(\rho_A^{T_2})^n = \mathrm{Tr}(\rho_A^{C_2})^n = \langle \mathcal{T}_n(u_1)\overline{\mathcal{T}}_n(v_1)\overline{\mathcal{T}}_n(u_2)\mathcal{T}_n(v_2)\rangle_{\mathbb{C}}. \tag{5.24}$$

We see that as compared to eq. (5.23), the act of partial transpose exchanges the twist with the anti-twist field for the second interval. For $n = 2$, we have $\mathcal{T}_2 = \overline{\mathcal{T}}_2$, hence $\mathrm{Tr}\rho_A^2 = \mathrm{Tr}(\rho_A^{T_2})^2$.

5.2.3 Single Interval - Pure state

To move from two disjoint intervals to a single interval for a pure state we let $B \to \emptyset$ as we consider $u_2 \to v_1$ and $v_2 \to u_1$ which results in

$$\mathrm{Tr}(\rho_A^{T_2})^n = \langle \mathcal{T}_n^2(u_2)\overline{\mathcal{T}}_n^2(v_2)\rangle. \tag{5.25}$$

The above equation is dependent on the parity on n as $\mathcal{T}_n^2$ connects the (i)-th sheet with $(i+2)$-th one. So for the even case i.e $n = n_e$, the n_e sheeted Riemann surface decouples into two independent $n_e/2$ sheeted Riemann surface while for the odd case, finally, we have n_o sheeted Riemann surface as shown in Fig. 8 [56].

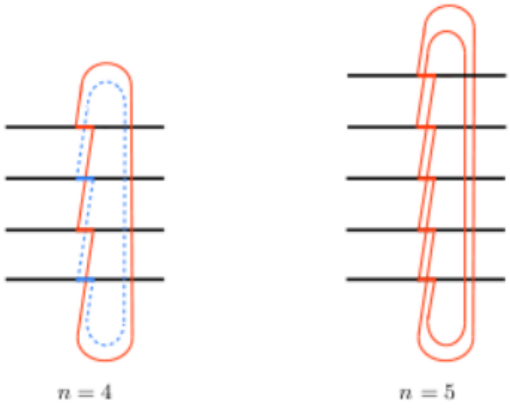

Figure 8 : Left is for even, where we see decoupling. Right is for odd, where we see reshuffling.

As a result of this parity dependence, we have

$$\begin{aligned}
&\mathrm{Tr}(\rho_A^{T_2})^{n_e} = (\langle \mathcal{T}_{n_e/2}(u_2)\overline{\mathcal{T}}_{n_e/2}(v_2)\rangle)^2 = (\mathrm{Tr}\rho_{A_2}^{n_e/2})^2, \\
&\mathrm{Tr}(\rho_A^{T_2})^{n_o} = \langle \mathcal{T}_{n_o}(u_2)\overline{\mathcal{T}}_{n_o}(v_2)\rangle = \mathrm{Tr}\rho_{A_2}^{n_o},
\end{aligned} \tag{5.26}$$

which matches with the results in eq. (5.18). It is worthy to note here that the above result was obtained in a field theoretic context, showing the relation between the Riemann surface and the parity of n.
Next, we put $l = v_2 - u_2$ and use

$$\mathrm{Tr}\rho_A^n = \langle \mathcal{T}_n(u)\overline{\mathcal{T}}_n(v)\rangle = c_n\Big(\frac{l}{a}\Big)^{-c/6(n-1/n)}, \tag{5.27}$$

where c_n are constants to have

$$\begin{aligned}
&\mathrm{Tr}(\rho_A^{T_2})^{n_e} = (\langle \mathcal{T}_{n_e/2}(u_2)\overline{\mathcal{T}}_{n_e/2}(v_2)\rangle)^2 = (\mathrm{Tr}\rho_{A_2}^{n_e/2})^2 = c_{n_e/2}^2\big(\tfrac{l}{a}\big)^{-\frac{c}{3}(n_e/2-2/n_e)}, \\
&\mathrm{Tr}(\rho_A^{T_2})^{n_o} = \langle \mathcal{T}_{n_o}(u_2)\overline{\mathcal{T}}_{n_o}(v_2)\rangle = \mathrm{Tr}\rho_{A_2}^{n_o} = c_{n_o}\big(\tfrac{l}{a}\big)^{-\frac{c}{6}(n_o-1/n_o)},
\end{aligned} \tag{5.28}$$

where we have used the fact that the conformal dimensions have the following form

$$\begin{aligned}
&\text{For } n = n_e, \text{even, } \mathcal{T}_{n_e}^2 \text{ and } \overline{\mathcal{T}}_{n_e}^2 \text{have dimensions} \\
&\Delta_{\mathcal{T}_{n_e}^2} = \Delta_{\overline{\mathcal{T}}_{n_e}^2} = \tfrac{c}{6}\big(\tfrac{n_e}{2} - \tfrac{2}{n_e}\big), \\
&\text{For } n = n_o, \text{odd, } \mathcal{T}_{n_o} \text{ and } \overline{\mathcal{T}}_{n_o} \text{have dimensions} \\
&\Delta_{\mathcal{T}_{n_o}} = \Delta_{\overline{\mathcal{T}}_{n_o}} = \tfrac{c}{12}\big(n_o - \tfrac{1}{n_o}\big).
\end{aligned} \tag{5.29}$$

We do the analytic continuation for even n i.e. $n_e \to 1$ to have

$$\|\rho_A^{T_2}\| = \lim_{n_e\to 1}\mathrm{Tr}(\rho_A^{T_2})^{n_e} = c_{1/2}^2\Big(\frac{l}{a}\Big)^{\frac{c}{2}} \Rightarrow \mathcal{E} = \frac{c}{2}\ln\Big(\frac{l}{a}\Big) + 2\ln c_{1/2}. \tag{5.30}$$

The Rényi entropy is

$$\begin{aligned}
&\mathrm{Tr}\rho_{A_2}^n = c_n\Big(\frac{l}{a}\Big)^{-c/6(n-1/n)}\\
&\text{and for } n=1/2, \text{we have}\\
&\mathrm{Tr}\rho_{A_2}^{(1/2)} = c_{1/2}\Big(\frac{l}{a}\Big)^{-c/6(1/2-2)},\\
&\text{So, } 2\ln\mathrm{Tr}\rho_{A_2}^{(1/2)} = S_{A_2}^{(1/2)} = \tfrac{c}{2}\ln\Big(\tfrac{l}{a}\Big) + 2\ln c_{1/2}.
\end{aligned} \tag{5.31}$$

By looking at the eqs. (5.30),(5.31), we see that for the pure states the logarithmic negativity $\mathcal{E}$ matches with the Rényi entropy of order 1/2, which is the same result we had obtained earlier in eq. (5.19).

If we do the analytic continuation for odd n i.e. $n_o \to 1$, we get the normalization $\mathrm{Tr}\rho_A^{T_2} = 1$.

5.2.4 Single Interval - Mixed state

Let us now consider the case of a single interval for a CFT at finite temperature, we therefore consider the mixed state. We take a bipartite system, A having finite interval and B being rest of the system. We will evaluate the correlation function, $\langle\mathcal{T}_n(-L)\overline{\mathcal{T}}_n^2(-l)\mathcal{T}_n^2(0)\overline{\mathcal{T}}_n(L)\rangle$ on an infnite cylinder of circumference $\beta = 1/T$, along the imaginary time axis [58]. To move from the complex plane to the cylinder we use the map

$$z \to w = (\frac{\beta}{2\pi})\ln z, \tag{5.32}$$

where z is the coordinate on the complex plane and w is the coordinate on the cylinder. Under the map (5.32), the correlation function transform as

$$\langle\Phi_1(z_1,\bar{z}_1)\Phi_2(z_2,\bar{z}_2)...\rangle = \prod_j |w'(z_j)|^{\Delta_j}\langle\Phi_1(w_1,\bar{w}_1)\Phi_2(w_2,\bar{w}_2)...\rangle. \tag{5.33}$$

So, effectively our correlation function is

$$\begin{aligned}
&\langle\mathcal{T}_n(-L)\overline{\mathcal{T}}_n^2(-l)\mathcal{T}_n^2(0)\overline{\mathcal{T}}_n(L)\rangle_\beta\\
&= \Big(\frac{2\pi}{\beta}\Big)^{2\Delta_n+\Delta_n^{(2)}}\frac{\langle\mathcal{T}_n(e^{-2\pi L/\beta})\overline{\mathcal{T}}_n^2(e^{-2\pi l/\beta})\mathcal{T}_n^2(1)\overline{\mathcal{T}}_n(e^{2\pi L/\beta})\rangle_{\mathbb{C}}}{e^{2\pi\Delta_n^{(2)}l/\beta}}.
\end{aligned} \tag{5.34}$$

Now, using the properties of OPE's one can also have the following form for a four point function

$$\langle\mathcal{T}_n(z_1)\overline{\mathcal{T}}_n^2(z_2)\mathcal{T}_n^2(z_3)\overline{\mathcal{T}}_n(z_4)\rangle = \frac{c_n c_n^{(2)}}{z_{14}^{2\Delta_n}z_{23}^{2\Delta_n^{(2)}}}\frac{\mathcal{F}_n(x)}{x^{\Delta_n^{(2)}}}, \tag{5.35}$$

where $z_{ij} = |z_i - z_j|$ and x is the cross ratio, given as $x \equiv \frac{z_{12}z_{34}}{z_{13}z_{24}}$. Using eqs. (5.34) and (5.35), we have the following

$$\begin{aligned}
&\langle\mathcal{T}_n(e^{-2\pi L/\beta})\overline{\mathcal{T}}_n^2(e^{-2\pi l/\beta})\mathcal{T}_n^2(1)\overline{\mathcal{T}}_n(e^{2\pi L/\beta})\rangle_{\mathbb{C}}\\
&= \frac{c_n c_n^{(2)}}{(2\sinh(2\pi L/\beta))^{2\Delta_n}(1-e^{-2\pi l/\beta})^{2\Delta_n^{(2)}}}\frac{\mathcal{F}_n(x)}{x^{\Delta_n^{(2)}}}.
\end{aligned} \tag{5.36}$$

Finally, using eqs. (5.36) and (5.34), we have

$$\begin{aligned}&\langle\mathcal{T}_n(-L)\overline{\mathcal{T}}_n^2(-l)\mathcal{T}_n^2(0)\overline{\mathcal{T}}_n(L)\rangle_\beta\\&= c_n c_n^{(2)}\left[\frac{\beta}{\pi}\sinh\left(\frac{\pi l}{\beta}\right)\right]^{-2\Delta_n^{(2)}}\left[\frac{\beta}{\pi}\sinh\left(\frac{2\pi L}{\beta}\right)\right]^{-2\Delta_n}\frac{\mathcal{F}_n(x)}{x^{\Delta_n^{(2)}}}.\end{aligned}\tag{5.37}$$

We now take the replica limit

$$\begin{aligned}&\lim_{n_e\to 1}\ln[\langle\mathcal{T}_n(-L)\overline{\mathcal{T}}_n^2(-l)\mathcal{T}_n^2(0)\overline{\mathcal{T}}_n(L)\rangle_\beta]\\&= \frac{c}{2}\ln\left[\frac{\beta}{\pi a}\sinh\left(\frac{\pi l}{\beta}\right)\right]+\frac{c}{4}\ln(x)+f(x)+\text{constants},\end{aligned}\tag{5.38}$$

where we have introduced the UV cutoff a and $f(x)=\lim_{n_e\to 1}\ln[\mathcal{F}_{n_e}(x)]$. Also, for the above equation, we have used the fact that in the replica limit $n_e\to 1$, $\Delta_{n_e}\to 0$ and $\Delta_{n_e}^{(2)}\to -\frac{c}{4}$. If we now take the limit $L\to\infty$ for eq. (5.38), we have

$$\mathcal{E}=\frac{c}{2}\ln\left[\frac{\beta}{\pi a}\sinh\left(\frac{\pi l}{\beta}\right)\right]-\frac{\pi c l}{2\beta}+f(e^{-2\pi l/\beta})+\text{constants},\tag{5.39}$$

where we have $\lim_{L\to\infty} x=e^{-2\pi l/\beta}$. The above equation maybe rewritten as

$$\mathcal{E}=\frac{3}{2}\left[S_A-S_A^{th}\right]+f(e^{-2\pi l/\beta})+\text{constants},\tag{5.40}$$

where $S_A=\frac{c}{3}\ln\left[\frac{\beta}{\pi a}\sinh\left(\frac{\pi l}{\beta}\right)\right]$ is the entanglement entropy and $S_A^{th}=\frac{\pi c l}{3\beta}$ is the thermal entropy. So, we see that at finite temperature $\mathcal{E}$ separates out the quantum and the classical thermal correlations as expected. Also, at large temperature, as the first two terms cancel each other, we will be left with no quantum correlations, hence $\mathcal{E}=0$.

5.2.5 Holographic Entanglement Negativity for Single Interval - Mixed State

Recently, a holographic form for the single interval entanglement negativity in a 2D CFT at mixed state has been proposed in [61, 62]. Similarly to the Ryu-Takayanagi proposal this conjecture allows us to compute entanglement negativity for intervals in the dual CFT in terms of geodesic lenghts in the bulk gravity theory. In this section, we will describe their conjecture and review the holographic calculations for AdS_3/CFT_2 which reproduces the leading term in eq. (5.40) in the large central charge limit.

Conjecture

On the boundary CFT_2, we consider the partition of the system into spacelike slices A and $A^c=B$. We have B_1 and B_2, such that $B=B_1\cup B_2$. These are two finite intervals, present on the two sides of A as shown in Fig. 9 [61].

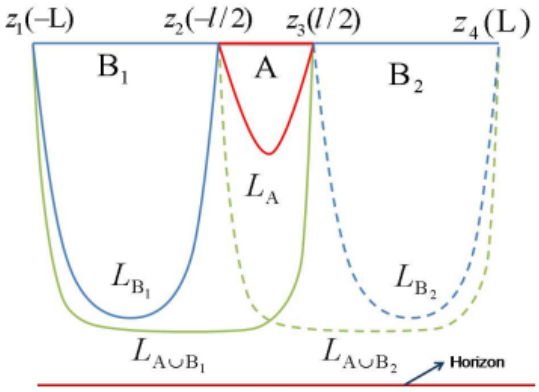

Figure 9 : Partitioning of the system alongwith the corresponding geodesics.

Now, the two point function in terms of twist fields can be expressed as

$$\langle \mathcal{T}_{n_e}(z_i)\overline{\mathcal{T}}_{n_e}(z_j)\rangle_{\mathbb{C}} = \frac{c_{n_e}}{z_{ij}^{\Delta_{n_e}}}. \tag{5.41}$$

Using the AdS/CFT correspondence, we can relate the two point function in the above equation with the length of the geodesic $\mathcal{L}_{ij}$ in the bulk AdS_3 whose endpoints are (z_i, z_j) on the boundary CFT as follows

$$\langle \mathcal{T}_{n_e}(z_i)\overline{\mathcal{T}}_{n_e}(z_j)\rangle_{\mathbb{C}} \sim e^{\frac{-\Delta_{n_e}\mathcal{L}_{ij}}{R}}. \tag{5.42}$$

Looking at Fig. 9, we have

$$\begin{aligned}
\mathcal{L}_{12} &= \mathcal{L}_{B_1},\\
\mathcal{L}_{23} &= \mathcal{L}_{A},\\
\mathcal{L}_{34} &= \mathcal{L}_{B_2},\\
\mathcal{L}_{13} &= \mathcal{L}_{A\cup B_1},\\
\mathcal{L}_{24} &= \mathcal{L}_{A\cup B_2},\\
\mathcal{L}_{14} &= \mathcal{L}_{A\cup B}.
\end{aligned} \tag{5.43}$$

Using eqs. (5.35),(5.42) and (5.43), we obtain

$$\langle \mathcal{T}_{n_e}(z_1)\overline{\mathcal{T}}^2_{n_e}(z_2)\mathcal{T}^2_{n_e}(z_3)\overline{\mathcal{T}}_{n_e}(z_4)\rangle_{\mathbb{C}} \sim e^{\frac{-\Delta_{n_e}\mathcal{L}_{A\cup B}}{R}} e^{\frac{-\Delta^{(2)}_{n_e}\mathcal{L}_A}{R}} \frac{1}{x^{\Delta^{(2)}_{n_e}}}, \tag{5.44}$$

where we have neglected in the large central charge limit, the subleading terms like the constants and $\mathcal{F}_{n_e}(x)$ and where $x^{\Delta^{(2)}_{n_e}}$ is

$$x^{\Delta^{(2)}_{n_e}} = e^{\frac{\Delta^{(2)}_{n_e}(\mathcal{L}_{B_1}+\mathcal{L}_{B_2}-\mathcal{L}_{A\cup B_1}-\mathcal{L}_{A\cup B_2})}{2R}}. \tag{5.45}$$

We now take the replica limit $n_e \to 1$ of eq. (5.44), to obtain

$$\lim_{n_e\to 1}\langle \mathcal{T}_{n_e}(z_1)\overline{\mathcal{T}}^2_{n_e}(z_2)\mathcal{T}^2_{n_e}(z_3)\overline{\mathcal{T}}_{n_e}(z_4)\rangle_{\mathbb{C}} \sim e^{\frac{c(2\mathcal{L}_A+\mathcal{L}_{B_1}+\mathcal{L}_{B_2}-\mathcal{L}_{A\cup B_1}-\mathcal{L}_{A\cup B_2})}{8R}}, \tag{5.46}$$

where we have used the fact, that when $n_e \to 1$, $\Delta_{n_e} \to 0$ and $\Delta^{(2)}_{n_e} \to \frac{-c}{4}$.
Using the Brown-Henneaux formula $c = \frac{3R}{2G^3_N}$ where G^3_N is the three dimensional gravitational constant [95] and taking the limit $B \to A^c$ ($L \to \infty$) implying $B_1, B_2 \to \infty$ for the eq. (5.46), we have $\mathcal{E}$ as

$$\mathcal{E} = \lim_{B\to A^c} \Big[\frac{3}{16G^3_N}(2\mathcal{L}_A + \mathcal{L}_{B_1} + \mathcal{L}_{B_2} - \mathcal{L}_{A\cup B_1} - \mathcal{L}_{A\cup B_2})\Big]. \tag{5.47}$$

Using the Ryu-Takayanagi formula (4.46), we can express the above equation as

$$\mathcal{E} = \lim_{B\to A^c} \left[\frac{3}{4}\Big(\mathcal{I}(A, B_1) + \mathcal{I}(A, B_2)\Big)\right], \tag{5.48}$$

where $\mathcal{I}$ is the holographic mutual information and is given as

$$\begin{aligned} \mathcal{I}(A, B_1) &= S_A + S_{B_1} - S_{A\cup B_1} = \tfrac{1}{4G^3_N}(\mathcal{L}_A + \mathcal{L}_{B_1} - \mathcal{L}_{A\cup B_1}), \\ \mathcal{I}(A, B_2) &= S_A + S_{B_2} - S_{A\cup B_2} = \tfrac{1}{4G^3_N}(\mathcal{L}_A + \mathcal{L}_{B_2} - \mathcal{L}_{A\cup B_2}). \end{aligned} \tag{5.49}$$

Eq. (5.48) gives a general expression for entanglement negativity of a 2D boundary CFT in the case of a tripartite system and single interval, in terms of geodesic lengths in the bulk .

Holographic Entanglement Negativity in $\mathrm{AdS}_3/\mathrm{CFT}_2$ for a Single Interval - Mixed State

We will now review the calculation of holographic entanglement negativity for a single interval at mixed state in the setup of $\mathrm{AdS}_3/\mathrm{CFT}_2$ as considered in [61,62]. According to the AdS/CFT duality, 2D CFT at a finite temperature ($T = \beta^{-1}$) is dual to an Euclidean BTZ black hole having the same Hawking temperature. The metric for the Euclidean BTZ black hole is

$$ds^2 = (r^2 - r_h^2)d\tau_E^2 + \frac{R^2}{(r^2 - r_h^2)}dr^2 + r^2 d\phi^2, \tag{5.50}$$

where the periodic Euclidean time τ_E satisfies $\tau_E \sim \tau_E + \frac{2\pi R}{r_h}$ and the coordinate ϕ is also periodic. The length of the geodesic for an interval of length l_γ on the boundary is $\mathcal{L}_\gamma$ and is given as

$$\mathcal{L}_\gamma = 2R \ln\Big[\frac{\beta}{\pi a}\sinh(\frac{\pi l_\gamma}{\beta})\Big], \tag{5.51}$$

where a is the UV cutoff and R is the AdS_3 radius.
Now, using eqs. (5.43),(5.47),(5.51), we have

$$\mathcal{E} = \lim_{L\to\infty}\left[\frac{3R}{4G}\ln\left[\frac{\beta}{\pi a}\frac{\sinh(\frac{\pi(\frac{L-l}{2})}{\beta})\sinh(\frac{\pi l}{\beta})}{\sinh(\frac{\pi(L+\frac{l}{2})}{\beta})}\right]\right]. \tag{5.52}$$

Finally, after taking the limit $L \to \infty$, for the above equation, we have

$$\mathcal{E} = \frac{c}{2}\ln\left[\frac{\beta}{\pi a}\sinh\Big(\frac{\pi l}{\beta}\Big)\right] - \frac{\pi c l}{2\beta}. \tag{5.53}$$

Comparing the above equation (5.53) with eq. (5.39), we see that the holographic entanglement negativity quite remarkably reproduces the leading terms in the large central charge limit. We can re-express the above equation as

$$\mathcal{E} = \frac{3}{2}\left[S_A - S_A^{th}\right], \tag{5.54}$$

where S_A, S_A^{th} is the same as expressed in eq. (5.40).
We see that even the holographic entanglement negativity separates out classical and quantum correlations as expected, capturing the distillable quantum entanglement.

Chapter 6

How is the Presence of Horizons and Localised Matter Encoded in the Entanglement Entropy?

Our theoretical knowledge of black holes is incomplete without understanding the various aspects of black hole entropy like the microscopic origin of the Bekenstein-Hawking entropy [23, 102], information puzzle aspects like firewalls and complementarity [15, 27]. In this context, one of the most intense areas of research, nowadays, is to explore the relation between entanglement entropy and black hole entropy as it has been found that both these two types of entropies might be connected [25, 33, 91, 103–107].

Research along this line is very promising because entanglement is a quantum phenomenon while black hole entropy has thermal nature.
So, it is important to understand in a deeper manner that how is entanglement related to the black hole entropy. To hunt answers, we begin with the question: How does entanglement entropy differentiates between black hole horizon and conical singularity? [108].

We will begin this chapter by reviewing some features of AdS_3 which are relevant for our purposes and then modular transformations of the dual 2D CFT. Next, we will see how to use the modular transformation on the torus to obtain entanglement entropy for various configurations of the boundary 2D CFT which lies on the cylinder and are dual to the bulk gravity configurations like black holes, AdS space and spacetimes with conical singularities. Moving on, we will discuss the holographic entanglement entropy for the same boundary 2D CFT configurations and the leading terms in this holographic entanglement entropy. We will then extend the discussion to the 3D gravity bulk configurations. Next, we will also see aspects of entanglement entropy in Minkowski spacetime and issues related to causality of holographic entanglement entropy. Finally, we will end this chapter trying to answer the question: How does entanglement entropy differentiates between black hole horizon and conical singularity? [108].

6.1 3D AdS gravity

3D AdS gravity is described by the action

$$A = \frac{1}{16\pi G_3} \int d^3x\sqrt{-g}\left(R + \frac{2}{L^2}\right), \tag{6.1}$$

where L is the radius of the anti-de Sitter space and G_3 is 3D Newton constant. All the solutions of this action are locally equivalent to 3d AdS spacetime (AdS_3).

As governed by the AdS_3/CFT_2 correspondence [24], in the large $\mathcal{N}$ limit, 3D AdS gravity is dual to the two dimensional conformal field theory on the boundary, so we have [95]

$$c = \bar{c} = \frac{3L}{2G_3} \gg 1, \tag{6.2}$$

where $c, \bar{c}$ are the central charges for the corresponding CFT_2.

3D AdS gravity has no propagating degrees of freedom and in the absence of matter sources, the spacetime appears locally equivalent to AdS_3. The global properties of the solutions of the action (6.1) are affected by the localized matter. For AdS_3, there are three types of geometries on the basis of the orbits (elliptic, hyperbolic, parabolic) of the $SL(2, R)$ group manifold [81–83]. The first of these three types of geometries is the BTZ black hole which gives the positive mass excitations. This geometry is asymptotically AdS having an event horizon, positive mass and is at finite temperature T. The second geometry pertains to the vacuum, having zero mass and in our case we consider the AdS_3 vacua in Poincaré coordinates as there two possible representations for the vacua, the other being in the global coordinates. The third geometry is that of conical singularity which separates these two vacuum solutions. This geometry has pointlike particles of positive mass as its source. In our case, we consider conical singularity in both space and time.
So, we will now have a look at all the four possible geometries.

- **AdS_3 vacua**
  AdS_3 has two vacua, one represented in global coordinates, the other in the Poincaré coordinates. In global coordinates it is given as

  $$ds^2 = -\left(1 + \frac{r^2}{L^2}\right)dt^2 + \left(1 + \frac{r^2}{L^2}\right)^{-1} dr^2 + \frac{r^2}{L^2}d\phi^2, \tag{6.3}$$

  where the coordinates range are $t \in [-\infty, \infty], \phi \in [0, 2\pi L], r \in [0, \infty)$.

  When we restrict $t \in [0, \beta]$ we have AdS_3 at finite temperature $T = 1/\beta$. This bulk configuration is dual to a CFT having the same temperature. This boundary CFT lives on the torus $\mathcal{T}(\beta, 2\pi L)$, where β and $2\pi L$ are periodicities for the time and space direction respectively.

  If we take the limit $r \to \infty$ in eq. (6.3), then we the AdS_3 vacua in the Poincaré coordinates.

  $$ds^2 = -\left(\frac{r^2}{L^2}\right)dt^2 + \left(\frac{r^2}{L^2}\right)^{-1} dr^2 + \frac{r^2}{L^2}d\phi^2, \tag{6.4}$$

where we don't have a periodic ϕ, as $\phi \in [-\infty, \infty]$, $t \in [-\infty, \infty]$. The CFT dual to this configuration lives on a plane.

For our case, the physical vacuum is AdS_3 in the Poincaré coordinates as it is continuously connected with both the BTZ black hole and conical singularities. Hence, we can take into account the thermal excitations of the vacuum produced by the black hole with positive mass and also conical singularities which are sourced by pointlike masses.

- **BTZ black hole**
  The BTZ black hole is a solution of the action (6.1) and is given by the metric

$$ds^2 = -\frac{1}{L^2}\left(r^2 - r_+^2\right) dt^2 + \left(r^2 - r_+^2\right)^{-1} L^2 dr^2 + \frac{r^2}{L^2} d\phi^2, \tag{6.5}$$

  where r_+ is the horizon radius. The inverse Hawking temperature (β_H), mass and the Bekenstein-Hawking entropy given by

$$\beta_H = \frac{1}{T_H} = \frac{2\pi L^2}{r_+}, \quad M = \frac{r_+^2}{8G_3 L^2}, \quad S_{BH} = \frac{\mathcal{A}}{4G_3} = \frac{\pi r_+}{2G_3}. \tag{6.6}$$

  This bulk configuration has a compactified t direction and for general values of the periodicity it possess a conical singularity along this t direction. This conical defect is eliminated when $\beta = \beta_H$, resulting in a dual CFT at a finite temperature which lives on the torus $\mathcal{T}(\beta_H, 2\pi L)$ having cycles $\beta_H, 2\pi L$.

  The ground state of this BTZ black hole, which has $r_+ = 0$, $M = 0$ and $T_H = 0$ is represented by the Poincaré patch of AdS_3.

- **AdS_3 with conical singularity in space**
  When we rescale the coordinates in eq. (6.3) as follows

$$t \to \Gamma t, \quad \phi \to \Gamma \phi \quad \text{and} \quad r \to r/\Gamma, \quad \text{where} \quad \Gamma = \frac{r_+}{L}, \tag{6.7}$$

  we get the following metric:

$$ds^2 = -\left(\Gamma^2 + \frac{r^2}{L^2}\right) dt^2 + \left(\Gamma^2 + \frac{r^2}{L^2}\right)^{-1} dr^2 + \frac{r^2}{L^2} d\phi^2, \tag{6.8}$$

  where the range of the coordinates is $t \in [0, \infty], \phi \in [0, 2\pi L], r \in [0, \infty]$. The parameter Γ ranges from $0 \leq \Gamma \leq 1$ where physically it means from Poincaré AdS ($\Gamma = 0$) to global AdS ($\Gamma = 1$). When $\Gamma \neq 1, 0$, then the spatial ϕ direction, is compactified in nature. If the periodicity of ϕ is restricted as $0 \leq \phi \leq 2\pi\Gamma L$ where $\Gamma = r_+/L$, then we have a conical singularity in the spatial direction where the deficit angle is given as $\delta\phi = 2\pi(1 - \Gamma) = 2\pi(1 - r_+/L) = 2\pi(1 - 2\pi L/\beta_{con})$. Here, we have β_{con} which is similar to the inverse Hawking temperature and is given as

$$\beta_{con} \equiv \frac{2\pi L^2}{r_+} = \beta_H. \tag{6.9}$$

  Now, whenever we restrict the coordinates as $t \in [0, \Gamma\beta_{con} = 2\pi L], \phi \in [0, 2\pi\Gamma L], r \in [0, \infty)$, we obtain AdS_3 with a conical singularity whose

conformal boundary is the torus $\mathcal{T}(\Gamma\beta_{con}, 2\pi\Gamma L)$. Accordingly, we also have a dual CFT which lives on the this torus.

Whenever, $\Gamma \neq 0, 1$, we have a conical singularity which is like a geometric distortion produced by the pointlike particle of mass $m = (1-\Gamma)/4G_3$ [95, 109, 110]. Indeed, if we have a stress tensor for a a pointlike mass m, then the eq. (6.8) serves as a solution for the Einstein equations in 3D. It is worthy to note here that our physical vacua of the theory - AdS_3 in the Poincaré coordinates can be extracted from AdS_3 with a conical singularity by putting $\Gamma = 0$, which in turn would imply that $\beta_{con} = \infty$ as we have decompactified the ϕ direction.

- **AdS_3 with conical singularity in time**

  When we have a Euclidean version of the eq. (6.5), then for the periodicities other than β_H, we will have a conical singularity in the time direction. Here, the conical singularity in time is similar to the one in space as we simply exchange the temporal and the spatial direction by having $t \in [0, 2\pi r_+ = 2\pi\Gamma L]$. The conformal boundary of this space is the torus $\mathcal{T}(2\pi\Gamma L, \Gamma\beta_{con})$, which we obatin when we exchange the cycles for the torus related to the conical singularity in space. Accordingly, this spacetime, which is AdS_3 with conical singularity in time also has a dual CFT living on the associated torus.

6.2 Modular transformations

When dealing with 2D CFT lying on the torus, one of the important aspects is invariance of the partition function under the modular transformations [111, 112].

The important part for this modular invariance is the modular parameter $\tau = \omega_2/\omega_1$ where $\omega_{1,2}$ are cycles of the torus. Using this modular parameter τ, we can obtain the various modular transformations, which when combined together, define the modular group $PSL(2,\mathbb{Z})$: $\tau \to (a\tau + b)/(c\tau + d)$ with $ad - bc = 1$.

The three kinds of modular transformations are [111, 112]

$$\begin{array}{l} \mathcal{T} : \tau \to \tau + 1, \\ \mathcal{S} : \tau \to -\frac{1}{\tau}, \\ \mathcal{U} : \tau \to \frac{\tau}{\tau+1}. \end{array} \tag{6.10}$$

We can also have the above transformations by using compositions as follows

$$\begin{array}{l} \mathcal{T} = \mathcal{U}\mathcal{S}\mathcal{U}, \\ \mathcal{U} = \mathcal{T}\mathcal{S}\mathcal{T}, \\ \mathcal{S} = \mathcal{U}\mathcal{T}^{-1}\mathcal{U}, \\ (\mathcal{S}\mathcal{T})^3 = \mathcal{S}^2 = 1. \end{array} \tag{6.11}$$

One can also use the lattice representation for the modular transformations. In this representation, the torus is represented using vectors in the complex plane $(\omega_{1,2})$ and the modular parameter in this representation is $\tau = \frac{\omega_2}{\omega_1} = \tau_1 + i\tau_2$. If we now consider the action of the modular transformation on a unit cell, then for the purpose of simplification we can have $\omega_2 = \tau$ and $\omega_1 = 1$.

Out of all these transformations, it is the modular $\mathcal{S}$ transformation which is important for us and which acts on the complex coordinate present on the torus, $z = t_E + ix_E$ (where x_E, t_E are Euclidean space and time) and on τ, which is the modular parameter for the torus, as follows

$$z \to z' = \frac{z}{\tau}, \qquad \tau \to \tau' = -\frac{1}{\tau}. \tag{6.12}$$

This $\mathcal{S}$ transformation has been used in the AdS_3/CFT_2 correspondence to show that the modular parameter τ_{AdS} corresponding to the 2D CFT dual to the thermal AdS_3 is associated with the modular parameter τ_{BTZ} corresponding to the 2D CFT dual to the BTZ black hole as $\tau_{AdS} = -1/\tau_{BTZ}$ [75,113]. Further, it has also been shown that the modular parameter τ_{con} corresponding to the 2D CFT dual to the AdS_3 with spatial conical singularities is also related to τ_{BTZ} as $\tau_{con} = -1/\tau_{BTZ}$ [33,45].

If we look at the 2D CFT, living on the boundary torus, dual to the AdS space with spatial conical singularity $\mathcal{T}(\Gamma\beta_{con}, 2\pi\Gamma L)$ and with the temporal conical singularity $\mathcal{T}(2\pi\Gamma L, \Gamma\beta_{con})$, then we can see clearly that as their cycles are exchanged, they are related to each other by the modular transformation, $\mathcal{S}$. As we now know that the boundary tori for the various configurations of 2D CFT dual to the AdS_3 space are related to each other by the $\mathcal{S}$ transformation, we can conclude that apart from the vacua, the other four configurations i.e AdS_3 at finite temperature, BTZ black hole, AdS_3 with conical singularities in space, AdS_3 with conical singularities in time need to be in the physical AdS_3 spectrum. This is a non-trivial statement as because generally, AdS_3 with spatial/temporal conical singularity are not included in the spectrum.

When we consider the entanglement entropy for a given subsystem on the torus, as in our case, then we need to consider the action of the $\mathcal{S}$ transformation eq. (6.12) not only on τ but also on z. This happens, because in our case, as dictated by the von Neumann entropy, the accessible subsystem, given by the length l can be either along the spatial or the temporal direction and so, the partition function depends on both τ and z. Infact, using the $\mathcal{S}$ transformation we can exchange the accessible slice l either along the space or the time direction. This happens because, this modular transformation $\mathcal{S}$, when acting upon complex coordinate z can exchange the real with the imaginary part. So, if we take $\omega_1 = 1$, $\tau = \omega_2 = i\alpha$ (where α is a real number) and $z = l$ along Euclidean time direction, then by using eq. (6.12), we have

$$z' = -\frac{il}{\alpha}, \qquad \tau' = \frac{i}{\alpha}. \tag{6.13}$$

So, we see by using $\mathcal{S}$ transformation, we can move from real to the imaginary part of z, hence we can move from Euclidean time to Euclidean space direction and vice-versa. It is possible to have l possessing both real and imaginary part but for simplification purpose, we choose l having either real or imaginary part, meaning it will have either spatial or temporal part.

6.3 Modular transformations for Boundary Cylinders

We start this section by considering the cylinder approximation for the torus $\mathcal{T}(\beta, \alpha)$ (where β is the length of the temporal cycle and α is the length of

the spatial cycle), such that either of the two cycles decompactifies. We do so, because entanglement entropy for CFT on torus does not has a universal form as it depends on the field content of the underlying theory but on the other hand if the CFT lies on an infinite cylinder, then we can have a universal expression for the corresponding entanglement entropy.

This cylinder approximation can be done in the following two ways.

1. When $\beta \gg \alpha$, then the cycle representing the time direction decompactifies leading to the cylinder $\mathcal{C}(\alpha)$. This cylinder, has a compactified space direction whose length is α and a noncompactified time direction.

2. When $\alpha \gg \beta$, then the cycle representing the space direction decompactifies leading to the cylinder $C(\beta)$. This cylinder, has a compactified time direction whose length is β and a noncompactified space direction.

We will now proceed to the see how the $\mathcal{S}$ transformation can be applied to the above obtained cylinders. When we use eq. (6.12) for the torus $\mathcal{T}(\beta, \alpha)$, then we get the modular parameter as $\tau' = i\beta/\alpha$, hence the result is the torus $\mathcal{T}(\alpha, \beta)$.

1. In the first case, when we apply the limit $\beta \gg \alpha$, then the $\mathcal{S}$ will take us from $\mathcal{C}(\alpha) \to C(\alpha)$.

2. In the second case, when we apply the limit $\alpha \gg \beta$, then the $\mathcal{S}$ will take us from $C(\beta) \to \mathcal{C}(\beta)$.

Hence, we see that in the cylinder approximation, the modular transformation $\mathcal{S}$ exchanges the compact with the non compact direction.

As the periodicity of the compact euclidean time direction β gives the inverse temperature for the thermal correlations $\beta = 1/T$, we can say that analogously the periodicity of the compact euclidean space direction α gives the inverse temperature for the quantum correlations $\alpha = 1/T_Q$.

It is worthy to note here the physical relevance of the action of the modular transformation on the cylinders. The map $\mathcal{C}(\alpha) \to C(\alpha)$ takes us from $T << T_Q$ where we have the domination of quantum correlations to $T >> T_Q$ where we have the domination of the thermal correlations and vice-versa for the map $C(\beta) \to \mathcal{C}(\beta)$.

Now, when we use the $\mathcal{S}$ transformation for the cylinders, like $\mathcal{C}(\beta)$ into $C(\beta)$ then it is important to see that this transformation also maps the inaccessible region B from the "*compact*" space to the "*compact*" time direction whereas the vice-versa is true for the other mapping. Here, the inaccessible region remains in the compact/non-compact direction.
But, if we want to move the inaccessible region from the compact to the non-compact direction, then we first need to use the modular $\mathcal{S}$ transformation on the torus and then take the appropriate limit. The cylinders in this case are not connected by the $\mathcal{S}$ transformation.

6.4 Entanglement entropy for CFT on the infinite cylinder

We will now proceed to calculate the entanglement entropy when the boundary CFT lies on the infinite cylinder. We will calculate the entanglement entropy for four different cases as we put the slice in both the Euclidean space and the

Euclidean time direction along both compact and non-compact direction. As stated earlier, we consider the infinite cylinder as results have a universal form unlike the torus where the results depend on the field content of the theory.

To begin with the calculations, we consider the case of free Dirac fermion on the torus and use the S_1 term in the entanglement entropy expression as given in [32]. We consider the S_1 term because when we take the limit for the infinite cylinder, then this term gives us the leading universal contribution. Next, we will use the modular $\mathcal{S}$ transformation to obtain the four different configurations of the slice and the corresponding entanglement entropy on the cylinder.

To obtain the entanglement entropy, we use the von Neumann entropy formula which is obtained by splitting the region of degrees of freedom into two disconnected parts A and B. We then obtain the reduced density matrix for the subsystem A from ρ, which is the density matrix for the entire system by tracing the degrees of freedom in B as $\rho_{\rm A} = {\rm Tr}_{\rm B}\rho$. Entanglement entropy is then given by the von Neumann entropy as ${\rm S_E} = -{\rm Tr}(\rho_{\rm A}{\rm log}\rho_{\rm A})$ [34, 35]. For our case, we start by considering the S_1 term as given in [32] to extract the leading universal term, when we take the limit for the infinite cylinder.

$$S_1 = \frac{c}{3}\,\log\left|\frac{\theta_1(z|\tau)}{2\pi\eta(\tau)^3}\right|, \tag{6.14}$$

where $(z = t_E + ix_E = it_M + ix_M)$ is the complex coordinate for the subsystem A (t_E, x_E denotes the Euclidean coordinates, t_M, x_M denotes the Minkowskian coordinates) and $(\tau = \beta + i\alpha)$ is the modular parameter for the torus. It is important to note here that our z is defined as $(z = t_E + ix_E)$ compared to it's definition in [32] which is $(z = x_E + it_E)$. The periodicities of t_E is β and for x_E, it is α respectively. By θ, we mean the theta function and the Dedekind eta function is given by η. Below, in the figures, when we use the lattice representation for the torus, then the vertical axis gives the real axis and the horizontal axis represents the imaginary axis. It is worth mentioning here, that we are using the formula for the entanglement entropy as given in [32] for both space and time coordinates as compared to it's use in [32] which is only for spatial coordinates.

- **Single interval along the compact time direction**

  We consider a single interval of length l_t along the compact time direction. So, as a result we have $z = l_t$, $\beta = 1$ and $\tau = i\alpha$. Hence, the value of q and y for the purpose of the theta function is now given as

$$\begin{aligned} q &= e^{2\pi i\tau} = e^{-2\pi\alpha}, \\ y &= e^{2\pi iz} = e^{2\pi i l_t}. \end{aligned} \tag{6.15}$$

  The pictorial representation of this configuration is

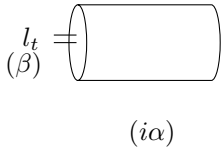

  where the symbol $=$ stands for a single interval.

Now, making use of the above stated values of q and y, we obtain S_1 as

$$S_1 = \frac{c}{3}\log\left|\frac{1}{\pi}\sin(\pi l_t)\prod_{m=1}^{\infty}\frac{(1-yq^m)(1-y^{-1}q^m)}{(1-q^m)^2}\right|. \tag{6.16}$$

We now take the limit $\alpha >> 1$ for the eq. (6.16). Physically, this corresponds to $T >> T_Q$ and the infinite cylinder configuration after the limit is $C(\beta)$. The entanglement entropy for the CFT on this cylinder $C(\beta)$ is now given as

$$S^{(tc)} = \frac{c}{3}\log\left|\frac{\beta}{a\pi}\sin\left(\frac{\pi l_t}{\beta}\right)\right|, \tag{6.17}$$

where a is the UV cutoff and we have restored β as the periodicity for t_E. The above equation gives the entanglement entropy for a single interval along the compact time direction on an infinite cylinder.

- **Single interval along the noncompact space direction**

Applying the modular transformation $\mathcal{S}$ on the above values of z and τ, we get z' and τ' as

$$\begin{aligned} z' &= \tfrac{z}{\tau} = -\tfrac{il_s}{\alpha}, \\ \tau' &= -\tfrac{1}{\tau} = \tfrac{i}{\alpha}, \end{aligned} \tag{6.18}$$

where there has been a change in the subscript from l_t to l_s as the interval is now along the spatial direction.
We now have the new values of q and y as:

$$\begin{aligned} q &= e^{2\pi i\tau} = e^{-2\pi/\alpha}, \\ y &= e^{2\pi iz} = e^{2\pi l_s/\alpha}. \end{aligned} \tag{6.19}$$

As the the $\mathcal{S}$ transformation has moved the interval from real axis to imaginary axis, the pictorial representation of this configuration is

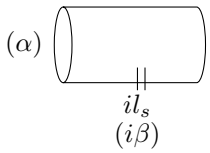

As a result of this modular transformation, the expression for S_1 is now given as

$$S_1 = \frac{c}{3}\log\left|\frac{\alpha}{\pi}e^{-\frac{\pi l^2}{\alpha}}\sinh(\frac{\pi l_s}{\alpha})\prod_{m=1}^{\infty}\frac{(1-yq^m)(1-y^{-1}q^m)}{(1-q^m)^2}\right|. \tag{6.20}$$

We now take the limit $\alpha << 1$ for the eq. (6.20). Physically, this corresponds to $T >> T_Q$ and the infinite cylinder configuration after the limit is $C(\alpha)$. The entanglement entropy for the CFT on this cylinder $C(\alpha)$ is now given as

$$S^{(snc)} = \frac{c}{3}\log\left|\frac{\alpha}{a\pi}\sinh\left(\frac{\pi l_s}{\alpha}\right)\right|. \tag{6.21}$$

The above equation gives the entanglement entropy for a single interval along the non-compact space direction on an infinite cylinder.

- **Single interval along the compact space direction**

  We now use the modular transformation $\mathcal{S}$ to move from the cylinder $C(\beta)$ where the interval is along the compact time direction, to go to the cylinder $\mathcal{C}(\beta)$ where the interval is along the compact space direction. This new configuration looks like

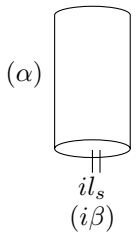

  where, in this new configuration we have l_s instead of l_t.
  This cylinder configuration is true for $\alpha \gg \beta$ which physically means $T \ll T_Q$. The eq. (6.17) remains invariant under the modular map $C(\beta) \to \mathcal{C}(\beta)$ and as a result we obtain the entanglement entropy for a single interval along the compact space direction as

$$S^{(sc)} = \frac{c}{3}\log\left|\frac{\beta}{a\pi}\sin\left(\frac{\pi l_s}{\beta}\right)\right|. \tag{6.22}$$

- **Single interval along the noncompact time direction**

  We now use the modular transformation $\mathcal{S}$ to move from the cylinder $C(\alpha)$ where the interval is along the non-compact space direction, to go to the cylinder $\mathcal{C}(\alpha)$ where the interval is along the non-compact time direction. This new configuration looks like

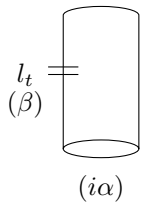

  where, in this new configuration we have l_t instead of l_s.
  This cylinder configuration is true for $\beta \gg \alpha$ which physically means $T \ll T_Q$. The eq. (6.21) remains invariant under the modular map $C(\alpha) \to \mathcal{C}(\alpha)$ and as a result we obtain the entanglement entropy for a single interval along the non-compact time direction as

$$S^{(tnc)} = \frac{c}{3}\log\left|\frac{\alpha}{a\pi}\sinh\left(\frac{\pi l_t}{\alpha}\right)\right|. \tag{6.23}$$

The expressions for the entanglement entropy for the four different cases i.e (6.17),(6.21),(6.22),(6.23) are universal in nature [34–36]. It is important to note here that the eqs. (6.17),(6.21) represent entanglement in time and space respectively, being valid at large temperature when there is domination of the thermal correlations. On the other hand, eqs. (6.22),(6.23) represent entanglement in space and time respectively, being valid at small temperature when there is domination of the quantum correlations

6.4.1 Planar approximation

We can obtain the planar limit, which describes CFT on a plane, for the the above four cases as follows. For eqs. (6.17),(6.22), we take the limit $l_{t,s} << \beta$ and for eqs. (6.21),(6.23), we take the limit $l_{t,s} << \alpha$. After taking the limit, in all the four cases, we obtain the same expression for the entanglement entropy which is

$$S^{(pl)} = \frac{c}{3}\log\left|\frac{l_{s,t}}{a}\right|. \tag{6.24}$$

The above eq. gives the entanglement entropy for a single interval of length l_s/l_t at zero temperature having non-compact space direction.

6.5 Holographic entanglement entropy for the various AdS_3 configurations

In the previous section we have calculated the entanglement entropy of the 2D CFT on the cylinder dual to different 3D bulk configurations for different positions of the interval. In the 2D CFT the information about the actual 3D gravity bulk configuration is just encoded in the position of the interval (along spacelike or timelike direction) and the topology of the spacelike and timelike directions. Our goal is now to associate an entanglement entropy to the bulk gravity configurations. There have been some attempts to calculate the entanglement entropy using holographic methods for various gravitational configurations, but it seems, that there have always been some issues when they are being reduced to the dual CFT calculations [32, 33, 42, 44, 45, 49, 62, 114–116]. To deal with the issue of holographic aspect of entanglement entropy, we will use the results of the previous section, i.e using the entanglement entropy from the CFT perspective, we will associate the holographic entanglement entropy to the dual bulk AdS_3 configurations. To do so, we use the AdS/CFT correspondence, which states that in the large c limit, the 2D CFT is dual to 3D AdS gravity. Using the dual 2D CFT for calculating the entanglement entropy for bulk AdS_3 configurations has advantages over the other methods, for example when entanglement entropy for black holes is calculated using quantum fields in the background of the classical gravity [117, 118], then these results does not seem to be universal but are dependent on the matter fields and the UV cutoff. On the other hand, our holographic method is free from this dependency as central charge c (6.2) of the CFT fixes the number of quantum fields and the UV/IR relation resolves the UV cutoff problem fixing the UV cutoff a of the CFT in terms of the IR cutoff of the AdS spacetime [33, 45]

$$\Lambda = 4\pi^2 L^2/a. \tag{6.25}$$

The AdS/CFT correspondence can be used for calculating the entanglement entropy of bulk gravity configurations as the holographic entanglement entropy in two ways. First, we use the entanglement entropy of CFT on an infinite cylinder, as the results are universal and then use the AdS/CFT dictionary to extract the holographic entanglement entropy for the corresponding bulk configuration. The second method, which we will use in the later section is to use the gravitational tools to extract the holographic entanglement entropy for the various AdS_3 configurations [25, 26, 119, 120].

When we use the CFT results to calculate the holographic entanglement entropy by simply identifying the suitable equations corresponding to the bulk AdS_3 configurations ((6.17),(6.21),(6.22),(6.23)), we encounter the problem of fixing the arbitrary parameters l_t, l_s because correlations in the 3D bulk side are mapped in a non-local fashion onto the boundary CFT and we do no know of any standard way to fix the values of l_t, l_s with reference to the bulk AdS_3 parameters.

A possible solution to this problem was proposed in [33, 45], where the authors had conjectured $l_s = 2\pi L$ for the BTZ black hole, using the UV/IR relation. We will now validate this conjecture not only for the BTZ black hole but for also for other configurations when we calculate the holographic entanglement entropy below.

- **AdS_3 with conical singularity in space**

  The solution describing AdS_3 with conical singularity in space is given by the metric (6.8). It's dual CFT lies on the torus $\mathcal{T}(2\pi L, 2\pi r_+)$. We can say here, that for $r_+ < L$, the conical defect is a result of having an accessible interval of length $(2\pi r_+)$ in the spatial cycle, when the total length of the spatial cycle is $(2\pi L)$ for the torus $\mathcal{T}(2\pi r_+, 2\pi L)$. It is to be noted that $\mathcal{T}(2\pi r_+, 2\pi L)$ is obtained by modular transformation of the original torus. Here, the conical singularity is removed when $r_+ = 0$, on the bulk side it pertains to the AdS_3 vacua in the Poincaré coordinates as it corresponds to $T = 0$ state on the boundary CFT.

  We can obtain the torus $\mathcal{T}^{cs}(2\pi L, \beta_{con})$, when we rescale the lenghts by L/r_+. Further, for $r_+ << L$, we get the cylinder $\mathcal{C}^{cs}(\beta_{con})$ with the interval length now being $l_s = 2\pi L$. Now, using (6.22), we can have the holographic entanglement entropy for AdS_3 with the conical singularity in space, as

  $$S^{(cs)} = \frac{c}{3}\log\left|\frac{\beta_{con}}{a\pi}\sin\left(\frac{2\pi^2 L)}{\beta_{con}}\right)\right|, \tag{6.26}$$

  where we have used $\beta = \beta_{con} = 2\pi L^2/r_+$ and $l_s = 2\pi L$.
  As expected, this result is true for small temperatures i.e for
  $T = 1/\beta_{con} << T_Q = 1/(2\pi L)$.

- **AdS_3 with conical singularity in time**

  When we apply the modular $\mathcal{S}$ transformation to $\mathcal{T}^{cs}(2\pi L, \beta_{con})$, having interval of length $l_s = 2\pi L$, we obtain $\mathcal{T}^{ct}(\beta_{con}, 2\pi L)$ having interval of length $l_t = 2\pi L$. This torus $\mathcal{T}^{ct}(\beta_{con}, 2\pi L)$ is related to the bulk configuration of AdS_3 with conical singularity in time. Also, in the limit

$L >> r_+$, the cylinder $\mathcal{C}^{cs}(\beta_{con})$ having interval of length $l_s = 2\pi L$ related to AdS_3 with conical singularity in space, under $\mathcal{S}$ transformation maps to, $C^{ct}(\beta_{con})$ having interval of length $l_t = 2\pi L$, associated with AdS_3 with conical singularity in time. Now, using (6.17), we can have the holographic entanglement entropy for AdS_3 with the conical singularity in time, as

$$S^{(ct)} = \frac{c}{3}\log\left|\frac{\beta_{con}}{a\pi}\sin\left(\frac{2\pi^2 L_t}{\beta_{con}}\right)\right|, \tag{6.27}$$

where $L_t \equiv L$ as we now have L_t as the length for the *euclidean time* cycle. This result is valid for $T >> T_Q$.

It is to be noted that even though for the Euclidean case, $L_t = L$ and the expression for the holographic entanglement entropy for AdS_3 with conical singularity in space is same as for AdS_3 with conical singularity in time, their physical meaning is different. The holographic entanglement entropy for AdS_3 with conical singularity in space given by the eq. (6.26) is true when the quantum correlations dominate whereas the holographic entanglement entropy for AdS_3 with conical singularity in time given by the eq. (6.27) is true when the thermal correlations dominate.

- **BTZ black hole**

  The boundary torus associated with AdS_3 with a conical singularity in space, $\mathcal{T}^{cs}(2\pi L, \beta_{con})$ is related by the modular $\mathcal{S}$ transformation with $\mathcal{T}^{BTZ}(\beta_H, 2\pi L)$, which is the boundary torus associated with the BTZ black hole [33, 45]. In the limit, $r_+ >> L$ and using the modular $\mathcal{S}$ transformation we can have the map $\mathcal{C}^{cs}(\beta_{con}) \to C^{BTZ}(\beta_H)$, where each of the cylinders have an interval of length $2\pi L$ along the compact space and non-compact space respectively. Now, using (6.21), with $\alpha = \beta_H$ and $l_s = 2\pi L$, we can have the holographic entanglement entropy for the BTZ black hole, as

$$S^{(BTZ)} = \frac{c}{3}\log\left|\frac{\beta_H}{a\pi}\sinh\left(\frac{2\pi^2 L}{\beta_H}\right)\right|. \tag{6.28}$$

  This result is true for $T >> T_Q$ and matches with the result obtained in [33, 45].

  Next, we again use the modular transformation to move from $C^{BTZ}(\beta_H)$ which has the interval along the non compact space direction to $\mathcal{C}^{BTZ}(\beta_H)$ which has the interval along the the noncompact time direction. Now, using (6.23), with $\alpha = \beta_H$ and $l_t = 2\pi L$, we have

$$S_{ET}^{(BTZ)} = \frac{c}{3}\log\left|\frac{\beta_H}{a\pi}\sinh(\frac{2\pi^2 L_t}{\beta_H})\right|. \tag{6.29}$$

  This result which is valid for $T << T_Q$ gives the holographic entanglement entropy for the BTZ black hole for the Euclidean time correlations.

  Here, also $L_t \equiv L$ for we now have a *euclidean time* cycle. It is worthy note here that eq. (6.28) gives the holographic entanglement entropy of the BTZ black hole for spatial correlations, when thermal correlations

dominate whereas eq. (6.29) gives the holographic entanglement entropy of the BTZ black hole for temporal correlations, when quantum correlations dominate.

- **AdS_3 vacuum**

  For the holographic entanglement entropy for the AdS_3 vacua we take the limit ($r_+ << L$) in eqs. (6.26) and in (6.29) and use (6.25) to get

$$S^{vac} = \frac{c}{3}\log\left(\frac{2\pi L}{a}\right) = \frac{c}{3}\log\left(\frac{\Lambda}{L}\right). \tag{6.30}$$

  Another way to get the above result is to put $l_{s,t} = 2\pi L$ in the eq. (6.24) and then use (6.25). It is to be noted that we cannot get this result from (6.27) or (6.28) as they are valid in the large temperature limit ($r_+ >> L$).

Summarising the results of this section we can state that from the entanglement entropy point of view, taking into account modular symmetry of the boundary CFT, the bulk configurations can be reduced to only three configurations :-
1. Spacetime with an event horizon - BTZ black hole
2. Spacetime with a conical singularity
3. AdS vacuum

When we extract the values for the holographic entanglement entropy for the above two configurations, we have the following results :-

1. The 2D CFT's which are dual to the spacetime with an event horizon, live on the infinite cylinder, in which case the inaccessible region belongs to the non-compact direction and the corresponding holographic entanglement entropy (6.28),(6.29) behaves exponentially.
2. The 2D CFT's which are dual to the spacetime with a conical singularity, live on the infinite cylinder, in which case the inaccessible region belongs to the compact direction and the corresponding holographic entanglement entropy (6.26),(6.27) behaves periodically.
3. The 2D CFT which are dual to the AdS vacuum live on a plane and the inaccessible region belongs to the non compact dimension. The corresponding holographic entanglement entropy (6.30) scales logarithmically.

6.6 Holographic entanglement entropy using gravitational tools

As mentioned in the previous section, we can also obtain the holographic entanglement entropy for the various AdS_3 configurations using direct gravitational tools and the AdS/CFT dictionary. So, in this section, we will explore the gravitational route by using various methods so as to cross-check the results of the previous section. The first of these methods is the Ryu-Takayanagi prescription [25, 26]. The Ryu-Takayanagi formula affirms that the holographic entanglement entropy for a subsystem A belonging to a d-dimensional CFT, is given by the minimal area of γ_A which is a $d-1$ dimensional surface in the bulk

in AdS_{d+1}

$$S_A = \frac{\text{Area}(\gamma_A)}{4G_N^{d+1}}, \tag{6.31}$$

where γ_A is defined such that A has a $d-2$ dimensional boundary ∂A which coincides with the boundary of γ_A given by $\partial\gamma_A$. The other methods are the extensions/modifications of this Ryu-Takayanagi formula like differential entropy [119] and complexified geodesics [120]. Let us now calculate the entanglement entropy for the CFT's dual to the various 3D bulk configurations, using the different holographic methods.

- **BTZ black hole**

  The holographic entanglement entropy for the CFT dual to the BTZ black hole has already been calculated, using the Ryu-Takayanagi prescription [32]. Here, the minimal area $\text{Area}(\gamma_A)$ is the length of the geodesic between the two ends of the one dimensional interval l_s lying on the boundary. It was noted that in this case, when the interval length l_s is large, the subsystem A spreads large enough to almost cover the conformal boundary. As a result, the geodesic breaks into two disjoint parts, one piece warps around the black hole and is of finite nature, the other piece which is $\propto \frac{c}{3}\log(\epsilon/a)$ is close to the boundary and diverges. The term which represents the geodesic wrapping around the horizon gives the holographic entanglement entropy of the BTZ black hole and the other term gives the holographic entanglement entropy for the AdS_3 vacuum (6.30).

  In our case for the cylinder approximation, in the limit $\beta << 2\pi L$, ϕ can be seen as a coordinate on the universal cover of S^1, so the geodesic wrapping around the horizon corresponds to $l_s = 2\pi L$. Using this value of $l_s = 2\pi L$ and $\alpha = \beta_H$ in the eq. (6.21), we get the holographic entanglement entropy for the BTZ black hole as obtained in eq. (6.28).

- **AdS_3 with conical singularity in space**

  The holographic entanglement entropy for CFT dual to AdS_3 with conical singularity in space has already been calculated in [119]. Considering a system of size R, we have a subsystem whose size in terms of angular coordinates is $\Gamma\phi$ and whose holographic entanglement entropy is

$$S_{con} = \frac{c}{3}\log\left|\frac{R}{\pi(\Gamma\mu)}\sin(\Gamma\phi)\right|, \tag{6.32}$$

  where μ is the UV cutoff.

  Previously, we saw that when we take the limit $r_+ << L$ in the cylinder approximation, conical singularity is the outcome of having an accessible length $2\pi r_+$ from the total length $2\pi L$.
  So, if we put $R = 2\pi L$, $\Gamma\phi = \pi r_+/L$, $\Gamma\mu = a r_+/L$ in eq. (6.32) and use the expression for β_{con} as given in (6.9), then we recover the result as given in the eq. (6.26).

- **AdS_3 with conical singularity in time**

  In the AdS space, it is a well known fact that the timelike geodesics do not reach the boundary. So, as our interval on the boundary is now having timelike separated endpoints, we will use the approach of complexified geodesics [120] to calculate the holographic entanglement entropy.

  We consider an interval Δt_E (t_E stands for Euclidean time) in the background of BTZ black hole, the complexified, renormalized, geodesic length for this interval is then given as

  $$\mathcal{L} = 2\,\ln\left[\frac{2L}{r_+}\sin(\frac{r_+\Delta t_E}{2L^2})\right], \tag{6.33}$$

  where 2π is the periodicities for the Euclidean time cycle.
  The expression in the eq. (6.33) is true for two cases, first is the regular Euclidean manifold, i.e the case without the conical defects and after we rescale t_E, the expression is valid for the second case which is the manifold with the conical singularity.

  Now, if we use $\Delta t_E = 2\pi L$ and a suitable UV cutoff a in the eq. (6.33), then we recover the result as given in eq. (6.27).

6.7 Leading and sub-leading terms in the entanglement entropy expansion

As previously shown, the holographic entanglement entropy for AdS_3 can be categorized in three classes including the vacuum. So, in this section we will analyse the leading and sub-leading terms in the entanglement entropy expansion for the two types of solutions.

We start with the BTZ black hole case, whose holographic entanglement entropy is given by Eqs. (6.28). Using the limit $r_+/L >> 1$ in the eq. (6.28), we get

$$\Delta S \equiv S^{BTZ} - S^{vac} = \frac{\pi r_+}{2G_3} - \frac{L}{2G_3}\ln\frac{\pi r_+}{L} + O(1) = S_{BH} - \frac{L}{2G_3}\ln S_{BH} + O(1). \tag{6.34}$$

In the above expression, we have already removed the contribution from the AdS_3 vacua S^{vac} (6.30) and S_{BH} stands for the Bekenstein-Hawking entropy of the BTZ black hole.

The above equation showcases the large T behaviour when there is the domination of the thermal correlations over the quantum correlations. The leading term which is the measure of the thermal entropy and the subleading $\ln S_{BH}$ term are as expected [118, 121, 122].

From the gravitational perspective, the leading term in eq. (6.34) is positive, scales like an area term and satisfies the area law for the black hole. Therefore, we can say that the existence of the horizon in the gravitational configuration increases the entanglement entropy of the vacua and possess a holographic nature.

From the CFT perspective, using eq. (6.21), we have the regulated, leading term in the large T regime as

$$S^{snc} - S^{vac} = \frac{c}{3}\frac{\pi l_s}{\beta}. \tag{6.35}$$

Now, if we put $l_s = 2\pi L$ in the above equation, we will obtain the Gibbs entropy $S_{Gibbs} = (2/3)c\pi^2 LT$. So, we see that the leading term in this case, has an extensive, thermal nature. Further, if we put $\beta = \beta_H$, then we recover the Bekenstein-Hawking entropy for the BTZ black hole.

We now consider the second class of solution, i.e the holographic entanglement entropy for AdS_3 with a conical singularity in space which is given by the (6.26). Here, we consider the limit $r_+/L << 1$, which is below the Hawking-Page phase transition, where the thermal AdS_3 is preferred for stability issues. As we are focussing on conical singularities, we disregard the stability aspect. So, using the limit $r_+/L << 1$ in the eq. (6.26), we get

$$\Delta S = -\frac{c\,\pi^2}{18}\Gamma^2 = -\frac{\pi^2}{12G_3}\frac{r_+^2}{L}. \tag{6.36}$$

The above equation showcases the small T behaviour when there is the domination of the spatial quantum correlations over the thermal correlations.

From the gravitational perspective, the leading term in eq. (6.36) is negative, scales like a volume term. Therefore, we can say that the existence of the spatial conical singularity in the gravitational configuration reduces the entanglement entropy of the vacua by contribution a volume term and possess a holographic nature. This reduction of the entanglement entropy because of matter contribution has been mentioned in [7]. Further, it has also been seen that the entanglement entropy can also scale as volume when the subsystem size is very small in [123].

From the CFT perspective, using eq. (6.22) we have the leading term as

$$\Delta S = -\frac{c}{18}\left(\frac{\pi l_s}{\beta}\right)^2 = -\frac{c}{18}\pi^2 l_s^2 T_Q^2, \tag{6.37}$$

where $T_Q = 1/\beta$ is the "quantum" temperature, as previously introduced. So, we see that the leading term in this case, has a super-extensive scaling nature.

For timelike correlations, when we use the limit $r_+/L >> 1$ for the case considered in the eq. (6.29) and the limit $r_+/L << 1$ for the case considered in the eq. (6.27), we have non-trivial results, hence discussed in the next section.

6.8 Aspects of the entanglement entropy in the Minkowski space

As seen previously, we have used the Euclidean time for the calculation of the holographic entanglement entropy, now we will analyze the effects of the Wick rotation ($t_E = it$), i.e. when we move from the Euclidean to the Minkowski space.

When we consider the interval in terms of the spatial coordinates, then the eqs. (6.21), (6.22), (6.26), (6.28) remain invariant under the Wick rotation. The physical interpretation of such a result is that we are considering correlations in an equilibrium thermal CFT.

But the situation is different, when we consider the interval in terms of the temporal coordinates, then the eqs. (6.17), (6.23), (6.27), (6.29) do not

remain invariant under the Wick rotation. When we are only dealing with the Euclidean variables where space x_E and time t_E are looked upon in the same fashion, then on interchanging $(t_E \leftrightarrow x_E)$, the eqs. having temporal coordinates are easily related to the ones having spatial coordinates i.e. eqs. (6.21), (6.22), (6.26), (6.28). When, we are dealing with the Minkowskian variables, then the Wick rotation $(l_t \rightarrow il_t)$ and $(L_t \rightarrow iL_t)$ affects the equations in the following manner. When applied to the eqs. (6.17) and (6.27), their original periodic nature in the Euclidean spacetime changes to the exponential nature in the Minkowskian spacetime. The physical interpretation of such a situation can be that after applying the Wick rotation, the eqs. (6.17) and (6.27) are expressing correlations in a non-equilibrium thermal QFT, wherein there is the domination of thermal correlations. This result for the entanglement entropy seems to be similar to the calculation of the two-point function for the timelike separated interval [120].

Next, when we apply the Wick rotation to the eqs. (6.23), (6.29), their original exponential nature in the Euclidean spacetime changes to the periodic nature in the Minkowskian spacetime. We do not have an explicit physical interpretation for this case as the eqs. are valid for $T << T_Q$ wherein there is the domination of the quantum correlations and thermal description will not be applicable. It seems that in this case, we might be looking at "entanglement in time" as also discussed in [124, 125]. This aspect requires further study.

6.9 Aspects of causality related to the holographic entanglement entropy

Calculation of the entanglement entropy in the CFT framework, i.e using the replica trick ensures locality and causality on the boundary CFT but the same is not true when we use the Ryu-Takayangi prescription for the calculation of the holographic entanglement entropy. In the Ryu-Takayanagi picture, the mechanism through which the bulk information is captured by the minimal surfaces and codified on the boundary is not explicit. An attempt to investigate this issue was made by the authors in [126]. They constructed the causal information surface whose proper area gives the causal holographic information, in a manner similar to the Ryu-Takayanagi method. It so happens that for two of the configurations that we are dealing with, in this chapter, i.e the Global AdS_3 and the BTZ black hole, the causal holographic information matches with the holographic entanglement entropy. Hence, we are assured of the preservation of the causality for these two cases as obtained in our results (6.30), (6.28), where the result in eq. (6.30) is related to the Global AdS_3 by rescaling and planar approximation.

Going ahead, the authors in [127] have put forward the idea of differential entropy which combines this proposal of the causal holographic information with the bulk configuration of a hole in AdS. Further, this differential entropy method has also been used to calculate the holographic entanglement entropy for AdS_3 with a conical singularity in space in [127]. Since, the differential entropy method takes into account the causal aspects for the holographic entanglement entropy for conical singularity in space and it matches with our results (6.26), hence for this configuration also, we are assured of the causality aspects for our

result.

However, when we consider the holographic entanglement entropy in terms of the temporal correlations, as given in the eqs. (6.27) and (6.29), then these causality aspects are not completely clear. The authors in [128] have presented the doubtful picture of causality associated with the approach of the complexified geodesics as this method does not assures an explicit causal relation between the bulk and the boundary. So, as a result this approach of the complexified geodesics, presently, can be considered just as a mathematical way for the calculation of the holographic entanglement entropy in terms of the temporal correlations. Another method to calculate the temporal holographic entanglement entropy can be the image prescription [128] but unfortunately in this case also, causality is not inherently present as the method of image prescription is modified to incorporate causality. It has been put forward that to explore the regime of physics untouched by the minimal geodesics, for example the interior region of the black holes, one can use the idea of entwinement as proposed in [119]. While considering the idea of the temporal entanglement entropy, one possibility is that, it can be seen as a result of entwinement, wherein the embedding space for AdS may give birth to the internal degree of freedom. This possible relation between the temporal entanglement entropy and entwinement needs further investigation.

6.10 Conclusion

In this chapter, which is based on [108], we have explained the mechanism through which one can make use of the AdS/CFT correspondence and modular transformations of the torus to calculate first the universal form of the holographic entanglement entropy for the various bulk AdS_3 configurations wherein the boundary torus was approximated to the cylinder configuration by taking the appropriate limits. The solutions for the various bulk configurations can be classified into three main types : One for the BTZ black hole/bulk gravity having a horizon, a second for AdS_3 with a conical singularity/bulk gravity having localised matter and finally a third for the AdS_3 vacuum.

When one considers the bulk gravity solutions with a horizon, then from the expression of the holographic entanglement entropy, we can extract the following information:

1. The region which is not accessible to the observer lies along the non-compact direction of the boundary cylinder.
2. The holographic entanglement entropy has an exponential behaviour.
3. Leading term in the expansion of the holographic entanglement entropy is positive and scales as area and correponds to an extensive, thermal piece on the boundary CFT.
4. Presence of the horizon in the bulk enhances the holographic entanglement entropy of the AdS_3 Poincaré vacuum.

On the other hand, when we consider the bulk gravity with localized matter, then from the expression of the holographic entanglement entropy, we can extract the following information:

1. The region which is not accessible to the observer lies along the compact direction of the boundary cylinder.
2. The holographic entanglement entropy has a periodic behaviour.

3. Leading term in the expansion of the holographic entanglement entropy is negative and scales as volume and corresponds to a super-extensive term on the boundary CFT.
4. Presence of the localised matter in the bulk reduces the holographic entanglement entropy of the AdS_3 Poincaré vacuum.

It is to be noted here that we have chosen the physical vacuum of the theory to be AdS_3 in the Poincaré patch as because, unlike the vacua in global coordinates, it is continuously related to the BTZ black hole spectrum and also with the spectrum of the conical singularity.

Also, another aspect which is worth noting here is related to the Hawking-Page phase transition which occurs at the critical point $r_+ \sim L$. It is well known, that below this critical point the gravitational configuration of the BTZ black hole becomes unstable, hence thermal AdS_3 is preferred. Now, the two limits, i.e $r_+ >> L$ and $r_+ << L$, that we use for the cylinder approximation, are away from the previously mentioned critical point $r_+ \sim L$. So, even though the physics for the limit $r_+ >> L$ is clear, as it is dominated by the BTZ black hole, the physics for the other limit $r_+ << L$ is not completely understood. This lack of clarity for the physics in the limit $r_+ << L$, is due to the fact that generally conical singularities are not considered as possible candidates for the Euclidean quantum gravity partition function. Also, it is not possible to describe conical singularities in a regular geometric description for spacetime.

As a future development of our investigations, one can analyze the generalization from 3D to four or higher dimensions. It would be interesting to see, for example, how our derivation is affected when we have in 4D naked curvature singularity produced by the localized sources which have negative mass. We expect this aspect to be non-trivial as in 3D gravity itself, we have used specific features for our calculations.

Chapter 7

Holographic entanglement negativity conjecture for adjacent intervals in AdS_3/CFT_2

Recently, quantum entanglement has been used in various aspects of theoretical physics ranging from condensed matter physics to quantum gravity [1, 2, 8, 15, 129]. One of the key features of the quantum entanglement is the entanglement entropy. If we have a bipartite quantum system in a pure state then the entanglement entropy is given by the von Neumann entropy for the corresponding reduced density matrix. This entanglement entropy for a 2D CFT has been calculated by Calabrese *et al* using the replica trick [34, 35]. Futher, it was put forward by Ryu-Takayanagi that the universal term in the expression for the entanglement entropy for a CFT can also be obtained using the AdS/CFT correspondence [25, 26, 42].

Unfortunately, entanglement entropy fails as a measure of entanglement when we consider mixed states. In case of mixed states, entanglement entropy contains information both on thermal and quantum corelations. Therefore a new quantity is required to have an appropriate measure for the distillable entanglement. To solve this issue, the authors in [54] proposed "entanglement negativity" which could serve as a measure for the distillable entanglement. The non convex property for the entanglement negativity was given by Plenio [55]. Entanglement negativity for CFT has been calculated by Calabrese *et al*, where they used a modified version of the replica trick. The holographic version of the entanglement negativity was put forth in [61–63], wherein the authors have proposed a conjecture for a single interval on the boundary CFT. This holographic entanglement negativity turns out to be proportional to sum of the holographic mutual information for the corresponding partitioning of the system.

Motivated by the holographic entanglement negativity conjecture for a single interval, we consider here a distinct configuration of two adjacent intervals. Note that the entanglement negativity for the single interval configuration character-

izes the entanglement of the interval with the rest of the system and describes a pure state at zero temperature and a mixed state at finite temperature. In contrast the entanglement negativity for the adjacent intervals characterizes the entanglement between the two intervals and describes a mixed state even at zero temperature due to the information about the rest of the system being traced over. This makes it an interesting configuration to investigate both at zero and finite temperatures. Hence the holographic entanglement negativity conjecture for two adjacent intervals has no advantage or improvement over the single interval conjecture as these two conjectures are dealing with two completely distinct configurations

In this chapter, which is based on the ref. [130], we will discuss the holographic entanglement negativity for two adjacent intervals on the boundary CFT, for various cases. We will start this chapter by reviewing entanglement negativity for two adjacent intervals in the CFT perspective and then discuss the holographic entanglement negativity for two adjacent intervals in the background of AdS_3/CFT_2, finally we will end this chapter with the summary and some discussion related to our results.

7.1 Entanglement Negativity

We start this section by reviewing the definition of the logarithmic negativity as presented in [54]. For furture purpose we will use the term "entanglement negativity" in place of "logarithmic negativity". We start by considering tripartition of a system as A_1, A_2 and B where $A = A_1 \cup A_2$ and $B = A^c$ is the remaining part of the system. The Hilbert space $\mathcal{H}$ for the subsystem A is given as $\mathcal{H} = \mathcal{H}_1 \otimes \mathcal{H}_2$, where $\mathcal{H}_1, \mathcal{H}_2$ are the Hilbert spaces for A_1 and A_2 respectively. Moving on, we define the partial transpose of the reduced density matrix $\rho_A = \mathrm{Tr}_{A^c}(\rho)$ as

$$\langle e_i^{(1)} e_j^{(2)} | \rho_A^{T_2} | e_k^{(1)} e_l^{(2)} \rangle = \langle e_i^{(1)} e_l^{(2)} | \rho_A | e_k^{(1)} e_j^{(2)} \rangle, \tag{7.1}$$

where $|e_i^{(1)}\rangle$ and $|e_j^{(2)}\rangle$ are the bases for the Hilbert spaces $\mathcal{H}_1$ and $\mathcal{H}_2$ respectively. We can now define the entanglement negativity between the two subsystems A_1 and A_2 as

$$\mathcal{E} = \ln \mathrm{Tr} |\rho_A^{T_2}|, \tag{7.2}$$

where $\mathrm{Tr}|\rho_A^{T_2}|$ is the trace norm and is defined as the sum of absolute eigenvalues of $\rho_A^{T_2}$.

7.1.1 Entanglement negativity in 2D CFT

We will now present the calculation of the entanglement negativity for mixed states in 2D CFT when the configuration is of two disjoint intervals [56,57]. We consider the tripartition of the system as given earlier and represented by the Fig. 10 below :

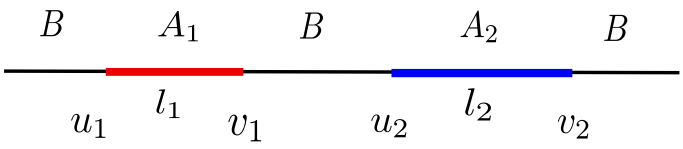

Figure 10 : Schematic of two disjoint intervals A_1 and A_2 in a (1+1)-dimensional CFT .

In the above configuration, A_1 has length l_1 and is given as $(A_1 \in [u_1, v_1])$ and A_2 has length l_2 and is given as $(A_2 \in [u_2, v_2])$. The remaining system is given as $B = A^c$. To calculate the entanglement negativity through the replica method, we need $\mathrm{Tr}(\rho_A^{T_2})^{n_e}$ which is given in terms of the twist/anti-twist fields as follows

$$\mathrm{Tr}(\rho_A^{T_2})^{n_e} = \langle \mathcal{T}_{n_e}(u_1)\overline{\mathcal{T}}_{n_e}(v_1)\overline{\mathcal{T}}_{n_e}(u_2)\mathcal{T}_{n_e}(v_2)\rangle_{\mathbb{C}}, \tag{7.3}$$

where the four point function is on the complex plane.
Now, considering the analytic continuation $n_e \to 1$ for the above equation, we can now define the entanglement negativity as

$$\mathcal{E} = \lim_{n_e \to 1} \ln \mathrm{Tr}(\rho_A^{T_2})^{n_e}. \tag{7.4}$$

It is worthy to note here that this analytic continuation is an involved calculation and is till date possible for some simplified models of conformal field theories [51, 58, 131, 132].

7.1.2 Two adjacent intervals in the vacuum

To calculate the entanglement negativity for mixed states having the configuration of two adjacent intervals in vacuum [56, 57], we begin by taking the limit $v_1 \to u_2$ in the Fig. 10 to obtain the desired configuration in Fig. 11 below :

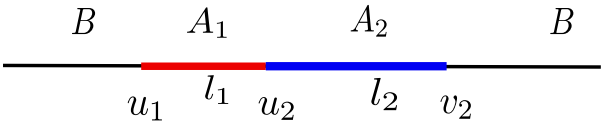

Figure 11 : Schematic of two adjacent intervals A_1 and A_2 in a (1+1)-dimensional CFT .

In the limit $v_1 \to u_2$, $\mathrm{Tr}(\rho_A^{T_2})^{n_e}$ (7.3) can now be written as a three point function of the twist/anti-twist fields as follows

$$\mathrm{Tr}(\rho_A^{T_2})^{n_e} = \langle \mathcal{T}_{n_e}(-l_1)\overline{\mathcal{T}}^2_{n_e}(0)\mathcal{T}_{n_e}(l_2)\rangle. \tag{7.5}$$

We now make use of the eqs. (7.4) and (7.5) to extract the desired entanglement negativity as

$$\mathcal{E} = \frac{c}{4} \ln \left[\frac{l_1 l_2}{(l_1 + l_2)a} \right] + const, \tag{7.6}$$

where a is the UV cut off and c is the central charge for the corresponding CFT. It is worthy to note here that the first term is universal in nature whereas the '*const* ' term depends on the operator content of the theory.

7.1.3 Two adjacent intervals in vacuum - Finite Size

We now proceed to calculate the entanglement negativity for mixed states which are at zero temperature and having the configuration of two adjacent intervals when the system is finite and has periodic boundary conditions [56]. For the calculation of the entanglement negativity, we need the three point function (7.5) on a system which has finite length L. To realize this configuration, we use the conformal map $z \to w = \frac{iL}{2\pi} \ln z$, which takes us from the complex plane, where we have the coordinates labelled by z to the cylinder having circumference L, on which the coordinates are labelled by w. Using this map and eq. (7.4), we can now obtain the entanglement negativity as

$$\mathcal{E} = \frac{c}{4} \ln \left[\Big(\frac{L}{\pi a} \Big) \frac{\sin(\frac{\pi l_1}{L}) \sin(\frac{\pi l_2}{L})}{\sin \frac{\pi (l_1+l_2)}{L}} \right] + const, \tag{7.7}$$

where the first term is of universal nature and the '*const* ' term is of non-universal nature.

7.1.4 Two adjacent intervals - Finite Temperature

We can extend the above analysis to calculate the entanglement negativity for two adjacent intervals for mixed states which are at finite temperature. For the calculation of the entanglement negativity at a finite temperature, we need the three point function (7.5) on a cylinder, having the circumference β, where $\beta = \frac{1}{T}$ gives the inverse temperature. To realize this configuration, we use the conformal map $z \to w = \frac{\beta}{2\pi} \ln z$, which takes us from the complex plane, where we have the coordinates labelled by z to the cylinder having circumference β, on which the coordinates are labelled by w. Using this map and eq. (7.4), we can now obtain the entanglement negativity as

$$\mathcal{E} = \frac{c}{4} \ln \left[\Big(\frac{\beta}{\pi a} \Big) \frac{\sinh(\frac{\pi l_1}{\beta}) \sinh(\frac{\pi l_2}{\beta})}{\sinh \frac{\pi (l_1+l_2)}{\beta}} \right] + const, \tag{7.8}$$

where the first term is of universal nature and the '*const* ' term is of non-universal nature.

7.1.5 Entanglement negativity behaviour in the large central charge limit

The AdS_3/CFT_2 correspondence, tells us that when we take the large central limit i.e. $c \to \infty$ for the 2D boundary CFT, then this limit corresponds to the semiclassical regime of the dual bulk gravity i.e we have the Newton's constant $G_N^{(3)} \to 0$. This happens because of the connection between the central charge c and the Newton's constant $G_N^{(3)}$ which is given by the Brown-Henneaux formula as $c = \frac{3R}{2G_N^{(3)}}$ Note that henceforth R stands for the AdS_3 radius as compared to L previously.

Using the monodromy method, the authors in [133] analysed the large central charge behaviour of the four point function as given in the eq. (7.3), to ascertain the conformal blocks that provided the dominant contribution. Their analysis led to the result that in the case of the two adjacent intervals corresponding to the limit $v_1 \to u_2$, as shown in the Fig. 11, the four point function as given in the eq. (7.3) receives the dominant contribution from the conformal block related to the intermediate operator $\overline{\mathcal{T}}^2$. Hence, in the limit of the large central charge, the expression for the entanglement negativity can be given as

$$\mathcal{E} = \frac{c}{4} \ln \Big[\frac{l_1 l_2}{(l_1 + l_2)a} \Big]. \tag{7.9}$$

We see that the above result matches with the universal term for the entanglement negativity as given in the eq. (7.6).

Also, it was shown that the entanglement negativity goes to zero, as the disjoint intervals move away from each other. In the next section, we will talk about the holographic entanglement negativity conjecture for two adjacent intervals and show that it matches with the CFT results in the large central charge limit.

It is interesting to note here that the monodromy method has also been used previously to study the large central charge behaviour of the entanglement entropy for the case of multiple disjoint intervals in [52](using a different method in [51]). The analysis led to the result that in the large central charge limit, the entanglement entropy has a universal nature and matches with the results of the holographic entanglement entropy conjecture given by Ryu-Takayanagi.

7.2 Holographic entanglement negativity conjecture for two adjacent intervals in $\mathbf{AdS_3/CFT_2}$

As we had indicated in the earlier section, in the limit of the large central charge, it is possible to have a holographic description of the entanglement negativity using the AdS/CFT correspondence. So to begin with, we consider the mixed state configuration of $A_1 \cup A_2$ as shown in the Fig. 11, where we have the two adjacent intervals A_1 and A_2, having lengths l_1 and l_2 respectively. It is already known that in this case we need the three point correlation function (7.5) whose conformally invariant form is as follows

$$\langle \mathcal{T}_{n_e}(z_1) \overline{\mathcal{T}}^2_{n_e}(z_2) \mathcal{T}_{n_e}(z_3) \rangle = \frac{c_n^2 \; C_{\mathcal{T}_{n_e} \overline{\mathcal{T}}^2_{n_e} \mathcal{T}_{n_e}}}{|z_{12}|^{\Delta_{\mathcal{T}^2_{n_e}}} |z_{23}|^{\Delta_{\mathcal{T}^2_{n_e}}} |z_{13}|^{2\Delta_{\mathcal{T}_{n_e}} - \Delta_{\mathcal{T}^2_{n_e}}}}, \tag{7.10}$$

where the normalization constants are given by c_n and the structure constant pertaining to the given OPE is $C_{\mathcal{T}_{n_e} \overline{\mathcal{T}}^2_{n_e} \mathcal{T}_{n_e}}$. Also, $\Delta_{\mathcal{T}_{n_e}}$ and $\Delta_{\mathcal{T}^2_{n_e}}$ represent the scaling dimensions for the twist operators $\mathcal{T}_{n_e}$ and $\mathcal{T}^2_{n_e}$ respectively and are given as

$$\begin{aligned} \Delta_{\mathcal{T}_{n_e}} &= \frac{c}{12}\Big(n_e - \frac{1}{n_e}\Big), \\ \Delta_{\mathcal{T}^2_{n_e}} = 2\Delta_{\mathcal{T}_{\frac{n_e}{2}}} &= \frac{c}{6}\Big(\frac{n_e}{2} - \frac{2}{n_e}\Big). \end{aligned} \tag{7.11}$$

We can now write the leading universal term for the expression given in the eq. (7.10) as

$$\langle \mathcal{T}_{n_e}(z_1)\overline{\mathcal{T}}^2_{n_e}(z_2)\mathcal{T}_{n_e}(z_3)\rangle = \frac{\big\langle \mathcal{T}_{n_e}(z_1)\overline{\mathcal{T}}_{n_e}(z_3)\big\rangle\big\langle \mathcal{T}_{\frac{n_e}{2}}(z_1)\overline{\mathcal{T}}_{\frac{n_e}{2}}(z_2)\big\rangle\big\langle \mathcal{T}_{\frac{n_e}{2}}(z_2)\overline{\mathcal{T}}_{\frac{n_e}{2}}(z_3)\big\rangle}{\big\langle \mathcal{T}_{\frac{n_e}{2}}(z_1)\overline{\mathcal{T}}_{\frac{n_e}{2}}(z_3)\big\rangle} + O[\frac{1}{c}], \tag{7.12}$$

where we have used the following equation as given in [56, 57]

$$\langle \mathcal{T}^2_{n_e}(u)\overline{\mathcal{T}}^2_{n_e}(v)\rangle_{\mathbb{C}} = \big\langle \mathcal{T}_{\frac{n_e}{2}}(z_i)\overline{\mathcal{T}}_{\frac{n_e}{2}}(z_j)\big\rangle^2_{\mathbb{C}} \tag{7.13}$$

and ignored the contribution from the non-universal terms as we are considering the large central charge limit.

Using the $\mathrm{AdS}_3/\mathrm{CFT}_2$ dictionary, we can now correlate the two point function in terms of the twist fields at z_i, z_j pertaining to the boundary CFT with the geodesic length in the bulk, $\mathcal{L}_{ij}$ whose end points are also anchored at z_i, z_j at the boundary, as follows

$$\big\langle \mathcal{T}_{n_e}(z_k)\overline{\mathcal{T}}_{n_e}(z_l)\big\rangle_{\mathbb{C}} \sim e^{-\frac{\Delta_{n_e}\mathcal{L}_{kl}}{R}}, \tag{7.14}$$

$$\big\langle \mathcal{T}_{\frac{n_e}{2}}(z_i)\overline{\mathcal{T}}_{\frac{n_e}{2}}(z_j)\big\rangle_{\mathbb{C}} \sim e^{-\frac{\Delta_{\frac{n_e}{2}}\mathcal{L}_{ij}}{R}}. \tag{7.15}$$

Next, we use eqs. (7.14) and eq. (7.15) in eq. (7.12), to rewrite the the three point correlation function as

$$\langle \mathcal{T}_{n_e}(z_1)\overline{\mathcal{T}}^2_{n_e}(z_2)\mathcal{T}_{n_e}(z_3)\rangle = \exp\left[\frac{-\Delta_{\mathcal{T}_{n_e}}\mathcal{L}_{13} - \Delta_{\mathcal{T}_{\frac{n_e}{2}}}(\mathcal{L}_{12}+\mathcal{L}_{23}-\mathcal{L}_{13})}{R}\right], \tag{7.16}$$

where we have $(z_1 = -l_1, z_2 = 0, z_3 = l_2)$.

Before proceeding ahead with the replica limit, it is important to mention here that first, one needs to consider the large central charge limit, as we have already done and then only consider the replica limit. As seen earlier, the replica limit is similar to the concept of analytic continuation.

Next, when we consider the replica limit ($n_e \to 1$), the scaling dimensions take up the values as $\Delta_{\mathcal{T}_{n_e}} \to 0$ and $\Delta_{\mathcal{T}_{\frac{n_e}{2}}} \to -\frac{c}{8}$. Using the above values, we can now obtain the holographic entanglement negativity for the mixed state configuration of the two adjacent intervals as

$$\mathcal{E} = \frac{3}{16G_N^3}(\mathcal{L}_{12}+\mathcal{L}_{23}-\mathcal{L}_{13}), \tag{7.17}$$

wherein we have made use of the Brown-Henneaux formula $c = \frac{3R}{2G_N^3}$ [95]. Since the above expression is written in terms of the geodesic lengths, we now use the Ryu-Takayanagi conjecture [25] which states that the holographic entanglement entropy S_A for a subsystem A in a dual CFT_{d+1} is given as

$$S_A = \frac{\mathrm{Area}(\gamma_\mathrm{A})}{4G_N^{(d+2)}}. \tag{7.18}$$

In the above expression γ_A is a co-dimension two space like static minimal surface in the bulk AdS_{d+2} homologous to the subsystem A and $G_N^{(d+2)}$ is the

$d+2$ dimensional Newton constant. Using the Ryu-Takayanagi conjecture, we can re-express equation (7.17) as

$$\mathcal{E} = \frac{3}{4}(S_{A_1} + S_{A_2} - S_{A_1 \cup A_2}) = \frac{3}{4}\mathcal{I}(A_1, A_2), \tag{7.19}$$

where we have identified the labels 12 with interval A_1, 23 with interval A_2 and 13 with $A_1 \cup A_2$ and $\mathcal{I}(A_1, A_2)$ represents the holographic mutual information between the two adjacent intervals. This is depicted pictorially in Fig. 12 below:

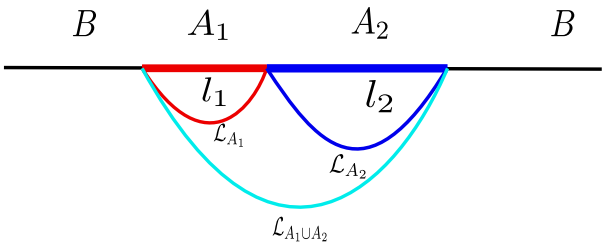

Figure 12 : Schematic of bulk geodesics anchored on the subsystems A_1 , A_2 and $A_1 \cup A_2$ in a (1+1)-dimensional boundary CFT .

Note here that whereas the mutual information gives the upper bound on the total correlation existing in a bipartite system, the entanglement negativity gives the upper bound on the distillable entanglement. However, for the given case, in the large central charge limit the universal terms from both of these two quantities turns to be the same. Also, this kind of similarity has also been seen in the cases of local and global quench problems in [134, 135]

This entire exercise clearly shows that in the setup of AdS_3/CFT_2, we can have a holographic representation of the entanglement negativity for the given mixed state configuration of the two adjacent intervals. We will now move on to calculate the holographic entanglement negativity for various scenarios.

7.2.1 Two adjacent intervals in the vacuum

Using the conjecture as proposed above, we will now calculate the holographic entanglement negativity for the mixed states at zero temperature having the configuration of two adjacent intervals on the boundary 2D CFT. As dictated by the AdS_3/CFT_2 correspondence, in this case, the bulk configuration is the AdS_3 vacuum which is described in the Poincaré coordinates as follows

$$ds^2 = -\left(\frac{r^2}{R^2}\right) dt^2 + \left(\frac{r^2}{R^2}\right)^{-1} dr^2 + \frac{r^2}{R^2} dx^2, \tag{7.20}$$

where the AdS_3 radius is given by R and for the coordinate x, we have the condition $x \in \mathbb{R}$. For the boundary interval γ, whose length is l_γ on the 2D CFT, we have the corresponding geodesic whose length $\mathcal{L}_\gamma$ in the bulk AdS_3, given as [25, 26, 33, 45]

$$\mathcal{L}_\gamma = 2R \ln \frac{l_\gamma}{a}, \tag{7.21}$$

where the UV cut off is denoted by a.
Using eq. (7.19), we can now obtain the holographic entanglement negativity as

$$\mathcal{E} = \frac{3R}{8G_N^3} \ln \left[\frac{l_1 l_2}{(l_1 + l_2)a} \right]. \tag{7.22}$$

After using the Brown-Henneaux formula in the above equation, the result for the holographic entanglement negativity matches with the CFT result in the large central charge limit (7.6), hence validating the conjecture in this case.

7.2.2 Two adjacent intervals in vacuum - Finite Size

We will now move on with the calculation of the holographic entanglement negativity for the mixed states at zero temperature when the system is of finite size of length L. This pertains to the configuration of two adjacent intervals on the boundary 2D CFT which lies on an infinite cylinder having the circumference L. As dictated by the AdS_3/CFT_2 correspondence, in this case, the bulk configuration is the AdS_3 vacuum which is now described by the global coordinates as follows [25, 26, 33, 45]

$$ds^2 = R^2(-\cosh^2 \rho dt^2 + d\rho^2 + \sinh^2 \rho d\phi^2), \tag{7.23}$$

where the coordinate ϕ is periodic in nature having a periodicity of 2π. In this case for the boundary interval γ, whose length is l_γ on the 2D CFT, the corresponding geodesic length $\mathcal{L}_\gamma$ in the bulk AdS_3, is given as [25, 26, 33, 45]

$$\mathcal{L}_\gamma = 2R \ln \Big(\frac{L}{\pi a} \sin \frac{\pi l_\gamma}{L} \Big). \tag{7.24}$$

Using the expression for the geodesic length as given by the eq. (7.24) in the eq. (7.17), we can now obtain the holographic entanglement negativity as

$$\mathcal{E} = \frac{3R}{8G_N^3} \ln \left[\Big(\frac{L}{\pi a} \Big) \frac{\sin(\frac{\pi l_1}{L}) \sin(\frac{\pi l_2}{L})}{\sin \frac{\pi(l_1+l_2)}{L}} \right]. \tag{7.25}$$

In this case also, after using the Brown-Henneaux formula in the above equation, the result for the holographic entanglement negativity matches with the CFT result in the large central charge limit (7.7), hence validating the conjecture in this case also.

7.2.3 Two adjacent intervals - Finite Temperature

We will now proceed with the calculation of the holographic entanglement negativity for the mixed states at finite temperature. This pertains to the configuration of two adjacent intervals on the boundary 2D CFT which lies on a cylinder whose spatial direction is non-compactified and infinite in range whereas the temporal direction which is Euclidean in nature lies along the compactified circle whose circumference is β. As dictated by the AdS_3/CFT_2 correspondence, in this case, the bulk configuration is the (uncharged, non-rotating) Euclidean BTZ black hole which is at the Hawking temperature $T = \frac{1}{\beta}$ and the corresponding metric is given as [25, 26, 33, 45]

$$ds^2 = \frac{(r^2 - r_h^2)}{R^2} d\tau^2 + \frac{R^2}{(r^2 - r_h^2)} dr^2 + \frac{r^2}{R^2} d\phi^2, \tag{7.26}$$

where τ stands for the Euclidean time and the the event horizon is denoted by $r = r_h$. In this case for the boundary interval γ, whose length is l_γ on the 2D CFT, the corresponding geodesic length $\mathcal{L}_\gamma$ in the bulk AdS_3, is given as [25, 26, 33, 45]

$$\mathcal{L}_\gamma = 2R \ln\Big(\frac{\beta}{\pi a}\sinh\frac{\pi l_\gamma}{\beta}\Big), \tag{7.27}$$

where $\beta = 2\pi R^2/r_h$ denotes the inverse Hawking temperature. Using the expression for the geodesic length as given by the eq. (7.27) in the eq. (7.17), we can now obtain the holographic entanglement negativity as

$$\mathcal{E} = \frac{3R}{8G_N^3}\ln\Bigg[\Big(\frac{\beta}{\pi a}\Big)\frac{\sinh(\frac{\pi l_1}{\beta})\sinh(\frac{\pi l_2}{\beta})}{\sinh\frac{\pi(l_1+l_2)}{\beta}}\Bigg]. \tag{7.28}$$

In this case of finite temperature, after using the Brown-Henneaux formula in the above equation, the result for the holographic entanglement negativity matches with the CFT result in the large central charge limit (7.8). Hence we get a validation of the conjecture in the case of finite temperature also.

7.3 Conclusion

In this chapter, which is based on the Ref. [130], we have used the AdS_3/CFT_2 correspondence to establish a holographic prescription for the calculation of the entanglement negativity for the mixed state configuration of two adjacent intervals for both zero and at finite temperature. In this case, the entanglement is between the two adjacent intervals as the degrees of freedom pertaining to the remaining system is traced over. The holographic prescription makes use of the lengths of the geodesics in the bulk AdS_3 whose endpoints are anchored on two adjacent intervals lying on the boundary 2D CFT and as a result the holographic entanglement negativity can also be expressed as the holographic mutual information between the two adjacent intervals.

The calculation for the holographic entanglement negativity is done for 3 cases :-
1. First, when the boundary CFT is at zero temperature and lies on an infinite plane then the corresponding bulk configuration is the AdS_3 vacuum in the Poincaré patch.
2. Second, when the boundary CFT is at zero temperature and lies on an infinite cylinder having the circumference L as it's spatial direction is compactified and finite in length. This is the case when the system is at zero temperature and has finite size. The corresponding bulk configuration is the AdS_3 vacuum in the global coordinates.
3. Third, when the boundary CFT is at finite temperature and lies on an infinite cylinder having the circumference β as it's (Euclidean) temporal direction is compactified and the spatial direction is infinite in length. The corresponding bulk configuration is the Euclidean BTZ black hole.
In all the above 3 cases, the holographic results matches with the CFT results in the large central charge limit.

The holographic entanglement negativity conjecture as proposed in [130] can be generalized to the AdS_{d+1}/CFT_d case. In this case, then we will have two adjacent subsystems on the boundary d-dimensional CFT. The holographic entan-

glement negativity in this case will now involve an algebraic combination of the areas of the co-dimension two minimal surfaces residing in the bulk and whose endpoints are anchored on the two boundary subsystems. In this case also, the holographic entanglement negativity can be expressed as the holographic mutual information between the two adjacent subsystems in the following fashion

$$\mathcal{E} = \frac{3}{16G_N^{(d+1)}}\big(\mathcal{A}_1 + \mathcal{A}_2 - \mathcal{A}_{12}\big) = \frac{3}{4}\mathcal{I}(A_1, A_2). \tag{7.29}$$

However, this generalization needs to be validated and maybe one can use the reasonings similar to [11].

This conjecture for the $\mathrm{AdS}_3/\mathrm{CFT}_2$ setup furnishes a neat way to calculate the holographic entanglement negativity for two adjacent intervals for both zero and finite temperature scenarios. This holographic entanglement negativity can be applied to various fields like condensed matter physics, topological phases, quantum phase transitions, quantum gravity etc. These applications constitute an interesting future research arena.

Chapter 8

Holographic Entanglement Negativity for Conformal Field Theories with a Conserved Charge

Currently, quantum entanglement is playing a major role in many fields of physics like many body theory, quantum gravity, black hole physics. Quantum entanglement for pure states is characterized by the measure called entanglement entropy. In quantum information theory, entanglement entropy is given by the von Neumann entropy of the corresponding reduced density matrix. In conformal field theory, entanglement entropy has been calculated using the replica trick [34, 35]. Using the AdS/CFT correspondence, Ryu and Takayanagi had proposed the holographic entanglement entropy [25, 26, 42] which makes use of the area of the bulk co dimension two minimal surface.

However, entanglement entropy fails as a measure when we deal with the mixed state configurations. To solve this problem, Vidal and Werner [54] proposed the measure called as entanglement negativity which serves as an upper bound on the distillable entanglement and this measure was capable to capture entanglement in a given mixed state. The non-convexity of the entanglement negativity and it's monotone nature was shown in [55]. Also, entanglement negativity has been calculated for conformal field theories using a modified version of the replica trick [56–58].

As it was already known that the entanglement entropy has a holographic counterpart, so attempts were made to extract a holographic counterpart for the entanglement negativity as well [59, 60]. A clear solution to this issue was given in [61–63] where the authors had proposed the holographic entanglement negativity conjecture for a given single interval on the boundary CFT. Compared to the holographic entanglement entropy, this conjecture for the holographic entanglement negativity involved an algebraic combination of the areas of the bulk co-dimension two minimal surfaces. The results from this conjecture agreed with the universal term for the corresponding CFT results in the large central charge limit, further the reasonings for this conjecture was given a firmer footing

in [64].

Recently, another conjecture for the holographic entanglement negativity was proposed in [130]. This conjecture dealt with the case of two adjacent intervals on the boundary CFT as compared to the single interval case in the previously stated conjecture. This conjecture for two adjacent intervals involved lengths of the bulk geodesics and as a result the holographic entanglement negativity could be expressed as the holographic mutual information between the two adjacent intervals. Interestingly, this relation between the universal piece of the entanglement negativity and the corresponding mutual information for the case of two adjacent intervals has also been noticed in [134, 135]. Similar to the previous conjecture for a single interval, in this case of two adjacent intervals also, the holographic result agreed with the universal term of the CFT results in the large central charge limit.

The generalization for the conjecture of two adjacent intervals to the case of $\text{AdS}_{d+1}/\text{CFT}_d$ was put forth in [65]. This generalization involved areas of co-dimension two bulk minimal surfaces whose endpoints were anchored on the corresponding subsystem residing on the boundary d-dimensional CFT. The calculations were done for pure AdS_{d+1} and AdS_{d+1}-Schwarzschild black hole. It was noticed that in the finite temperature case which correponds to the AdS_{d+1}-Schwarzschild black hole in the bulk, in the high temperature approximation, the volume/thermal terms are cancelled out leaving behind area dependent terms. Hence, it was concluded that the holographic entanglement negativity scales as the area and not volume compared to the entanglement entropy [47]. This area law for the case of entanglement negativity has also been noticed in [66, 67]. Further, a covariant version for the holographic entanglement negativity for two adjacent intervals was put forth in [68].

In this chapter, which is based on [136], we will study the application of the $\text{AdS}_{d+1}/\text{CFT}_d$ version of the holographic entanglement negativity conjecture for two adjacent intervals to the case of RN-AdS black holes. The dual CFT's which correspond to the RN-AdS black hole in the bulk have a conserved charge. We will begin this chapter with a review of the $\text{AdS}_{d+1}/\text{CFT}_d$ version of the holographic entanglement negativity conjecture. We will then move to study the holographic entanglement negativity for two adjacent intervals for various configurations of RN-$\text{AdS}_4/\text{CFT}_3$ setup followed by RN-$\text{AdS}_{d+1}/\text{CFT}_d$ setup. Finally, we will end this chapter with some discussion on the results.

8.1 Holographic entanglement negativity conjecture for two adjacent intervals

In this section, we will review the holographic entanglement negativity conjecture for two adjacent intervals. We will first begin with $\text{AdS}_3/\text{CFT}_2$ case as described in [130] and then describe the $\text{AdS}_{d+1}/\text{CFT}_d$ version [65].

In case of conformal field theories, entanglement negativity is calculated using a modified version of the replica trick [56–58]. We start by considering tripartition of the system in A_1, A_2, A^c where $A = A_1 \cup A_2$ and the remaining part of the system is $A^c = (A_1 \cup A_2)^c$. We then define the entanglement negativity as follows

$$\mathcal{E} = \lim_{n_e \to 1} \ln \text{Tr}(\rho_A^{T_2})^{n_e}, \tag{8.1}$$

where the partial transpose of the reduced density matrix ρ_A with respect to the interval A_2 is given as $\rho_A^{T_2}$. Further, $n_e \to 1$ is the replica limit, wherein we consider the analytic continuation for even n i.e. n_e.

In the above equation, $\mathrm{Tr}(\rho_A^{T_2})^{n_e}$ is a three point correlation function which is given as

$$\mathrm{Tr}(\rho_A^{T_2})^{n_e} = \langle \mathcal{T}_{n_e}(z_1)\overline{\mathcal{T}}^2_{n_e}(z_2)\mathcal{T}_{n_e}(z_3)\rangle = c_n^2 \frac{C_{\mathcal{T}_n\overline{\mathcal{T}}^2_n\mathcal{T}_n}}{|z_{12}|^{\Delta_{\mathcal{T}^2_{n_e}}}|z_{23}|^{\Delta_{\mathcal{T}^2_{n_e}}}|z_{13}|^{2\Delta_{\mathcal{T}_{n_e}}-\Delta_{\mathcal{T}^2_{n_e}}}}, \tag{8.2}$$

where $|z_{ij}| = |z_i - z_j|$ and the scaling dimension for $\tau^2_{n_e}$, τ_{n_e} is $\Delta_{\tau^2_{n_e}}$ and $\Delta_{\tau_{n_e}}$ respectively.

Now, using the fact that in the setup of AdS_3/CFT_2 correspondence and in the large central charge limit the above three point function of twist fields (8.2) residing on the CFT can be alternatively expressed in terms of the bulk geodesics whose endpoints are anchored on the intervals, we get [130]

$$\langle \mathcal{T}_{n_e}(z_1)\overline{\mathcal{T}}^2_{n_e}(z_2)\mathcal{T}_{n_e}(z_3)\rangle = \exp\left[\frac{-\Delta_{\mathcal{T}_{n_e}}\mathcal{L}_{13} - \Delta_{\mathcal{T}_{\frac{n_e}{2}}}(\mathcal{L}_{12}+\mathcal{L}_{23}-\mathcal{L}_{13})}{R}\right], \tag{8.3}$$

here the endpoints of the adjacent intervals are $(z_1 = -l_1, z_2 = 0, z_3 = l_2)$. Now, after making use of the Brown-Henneaux formula $c = \frac{3R}{2G_N^3}$ [95], the holographic entanglement negativity can be written as

$$\mathcal{E} = \frac{3}{16G_N^3}(\mathcal{L}_{12}+\mathcal{L}_{23}-\mathcal{L}_{13}), \tag{8.4}$$

In the case of $\mathrm{AdS}_{d+1}/\mathrm{CFT}_d$, holographic entanglement negativity will involve $\mathcal{A}_i$ which is the area of bulk co-dimension 2 static minimal surface and can be expressed as [65]

$$\mathcal{E} = \frac{3}{16G_N^{(d+1)}}\big(\mathcal{A}_1+\mathcal{A}_2-\mathcal{A}_{12}\big) \tag{8.5}$$

Now, applying the Ryu-Takayanagi conjecture [25] to the above eqs (8.4), (8.5) we can finally express the holographic entanglement negativity for two adjacent subsystems as

$$\mathcal{E} = \frac{3}{4}(S_{A_1}+S_{A_2}-S_{A_1\cup A_2}) = \frac{3}{4}[\mathcal{I}(A_1,A_2)], \tag{8.6}$$

where S_{A_i} is the holographic entanglement entropy of the subsystem A_i. The expression $\mathcal{I}(A_1,A_2)$ in the above (8.6) is the holographic mutual information between the two adjacent subsystems. Next, we will use this holographic conjecture to evaluate the entanglement negativity for two adjacent subsystems in the subsequent sections.

8.2 Holographic entanglement negativity in the setup of RN-AdS$_4$/CFT$_3$

In this section we will study the holographic entanglement negativity for two adjacent subsystems when we have mixed state configuration in the form of

rectangular strip geometry on the boundary 3 dimensional CFT (having a conserved charge) which is dual to the RN-AdS$_4$ black holes in the bulk. We will consider both extremal and non-extremal cases.

8.2.1 Area of the minimal surface for RN-AdS$_4$ black holes

In this subsection, we will review the perturbative method of calculation of the area of the bulk co-dimension two static minimal surface in the case of RN-AdS$_4$ black hole [47, 49] as it is pertinent to the calculation of holographic entanglement negativity later.

The metric for the RN-AdS$_4$ black hole having a planar horizon is

$$ds^2 = -r^2 f(r) dt^2 + \frac{1}{r^2 f(r)} dr^2 + r^2(dx^2 + dy^2), \tag{8.7}$$

$$f(r) = 1 - \frac{M}{r^3} + \frac{Q^2}{r^4}, \tag{8.8}$$

where the AdS radius $R = 1$.
The lapse function vanishes at the horizon ($r = r_h$) and we get the following relation between mass, charge and horizon radius

$$f(r_h) = 0 \Rightarrow M = \frac{r_h^4 + Q^2}{r_h}. \tag{8.9}$$

Effectively, we can now re-express the lapse function (8.8) as

$$f(r) = 1 - \frac{r_h^3}{r^3} - \frac{Q^2}{r^3 r_h} + \frac{Q^2}{r^4}. \tag{8.10}$$

The Hawking temperature in the case of RN-AdS_4 black hole is given as

$$T = \left.\frac{f'(r)}{4\pi}\right|_{r=r_h} = \frac{3r_h}{4\pi}(1 - \frac{Q^2}{3r_h^4}). \tag{8.11}$$

and when $T = 0$, we have what is called as an extremal black hole characterized by the extremality condition

$$r_h = \frac{\sqrt{Q}}{3^{\frac{1}{4}}}. \tag{8.12}$$

We will now move towards the calculation for the area of the bulk co-dimension two static minimal surface. The endpoints of these surfaces are anchored on the boundary 3D CFT which is dual to the RN-AdS$_4$ black hole in the bulk. The subsystems A on the boundary CFT$_3$ have a rectangular strip geometry and is described as

$$x \in [-\frac{l}{2}, \frac{l}{2}], \qquad y \in [-\frac{L}{2}, \frac{L}{2}]. \tag{8.13}$$

The area $\mathcal{A}_A$ of the bulk co-dimension two bulk static minimal surface is then given as

$$\mathcal{A}_A = 2L \int_{r_c}^{\infty} \frac{dr}{\sqrt{f(r)(1 - \frac{r_c^4}{r^4})}}. \tag{8.14}$$

where r_c is a constant of integration and defines the turning point of the minimal surface in the bulk and it can be obtained by inverting the equation of motion which is

$$\frac{l}{2} = \int_{r_c}^{\infty} \frac{r_c^2 dr}{r^4 \sqrt{f(r)(1-\frac{r_c^4}{r^4})}}, \tag{8.15}$$

where l is the length of the rectangular strip along the x direction.
Once we have the value of r_c from (8.15), we subsitute it in (8.14) to obtain the area of the extremal surface. This is the outline of the method to obtain the area.

Now, for the purpose of the perturbative analysis, using the fact that the lapse function vanishes at the horizon, we can use (8.10) instead of (8.8) in (8.14). To solve the above integrals, we change the coordinate from r to $u = \frac{r_c}{r}$, to get the following expressions

$$f(u) = 1 - \frac{{r_h}^3 u^3}{{r_c}^3} - \frac{Q^2 u^3}{{r_c}^3 r_h} + \frac{Q^2 u^4}{{r_c}^4}, \tag{8.16}$$

$$l = \frac{2}{r_c} \int_0^1 \frac{u^2 f(u)^{-\frac{1}{2}}}{\sqrt{1-u^4}} du, \tag{8.17}$$

$$\mathcal{A}_A = 2Lr_c \int_0^1 \frac{f(u)^{-\frac{1}{2}}}{u^2\sqrt{1-u^4}} du, \tag{8.18}$$

The required area of the minimal surface can now be obtained by using the above equations and doing a perturbative analysis in the various limits of the charge Q and the temperature T.

In the following section, we will calculate the holographic entanglement negativity for two adjacent subsystems having a mixed state configuration for the RN-AdS$_4$/CFT$_3$ scenario. The two adjacent subsystems A_1, A_2 have a rectangular strip geometry and are described as

$$x \in [-\tfrac{l_1}{2}, \tfrac{l_1}{2}], \qquad y \in [-\tfrac{L}{2}, \tfrac{L}{2}], \tag{8.19}$$

$$x \in [-\tfrac{l_2}{2}, \tfrac{l_2}{2}], \qquad y \in [-\tfrac{L}{2}, \tfrac{L}{2}], \tag{8.20}$$

respectively. This configuration is depicted below in the Fig. 13.
In this case of two adjacent subsystems, one can now obtain the turning point by using l_1 and l_2 instead of l in the eq. (8.17) and finally obtain the area by then making using of the eq. (8.18).

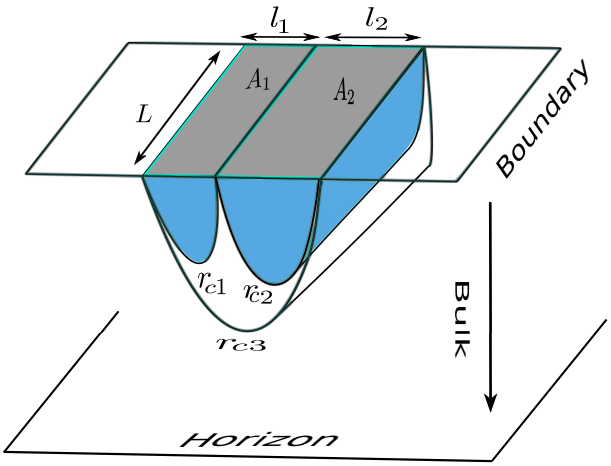

Figure 13 : Schematic of the bulk static minimal surfaces that are anchored on the subsystems A_1 , A_2 and $A_1 \cup A_2$ on the boundary CFT_3 dual to the RN-AdS_4 black hole.

8.2.2 Non-extremal RN-AdS_4 black holes

We will first consider the case of the non-extremal RN-AdS_4 black hole which means that the black hole is at a finite, non-vanishing temperature. At the boundary CFT_3 which is dual to the RN-AdS_4 black hole, we will consider the mixed state configuration of the two adjacent subsystems having rectangular strip geometries as shown in the Fig. 13. We first use a perturbative method to calculate the area of the static minimal surface in the bulk and then use the conjecture to calculate the holographic entanglement negativity. In the following subsections, we will perform this exercise in the various limits of the charge and temperature.

Small charge and low temperature

In this scenario we consider the case when the black hole has a small charge and is at low temperature. In this case r_h can be given as

$$r_h \geq \frac{\sqrt{Q}}{3^{\frac{1}{4}}}. \tag{8.21}$$

In this case, because both the charge and the temperature are small, $Q/r_h^2 \sim 1$ and using the fact that $r_h << r_c$ we can do a Taylor expansion for $f(u)^{-\frac{1}{2}}$ around $\frac{r_h}{r_c} = 0$ to the leading order in $\mathcal{O}[(\frac{r_h}{r_c}u)^3]$. The approximated form of the lapse function (8.16) is [49]

$$f(u)^{-\frac{1}{2}} \approx 1 + \frac{1+\alpha}{2}\left(\frac{r_h}{r_c}\right)^3 u^3, \tag{8.22}$$

where $\alpha = \frac{Q^2}{r_h^4}$.
Now, using (8.22), (8.17), (8.18) we get the following expression for the area of

the bulk co-dimension two static minimal surface [49]

$$\mathcal{A}_A = \mathcal{A}_A^{div} + \mathcal{A}_A^{finite}, \tag{8.23}$$

where the $\mathcal{A}_A^{div}$ is the divergent part and $\mathcal{A}_A^{finite}$ is the finite part of $\mathcal{A}_A$ given as

$$\mathcal{A}_A^{div} = 2\Big(\frac{L}{a}\Big), \tag{8.24}$$

$$\mathcal{A}_A^{finite} = k_1\frac{L}{l} + k_2 r_h^3(1+\alpha)l^2 + \mathcal{O}(r_h^4 l^3). \tag{8.25}$$

The constants k_1, k_2 in the above equation are expressed as

$$k_1 = -\frac{4\pi\Gamma(\frac{3}{4})^2}{\Gamma(\frac{1}{4})^2}, \tag{8.26}$$

$$k_2 = \frac{\Gamma(\frac{1}{4})^2}{32\Gamma(\frac{3}{4})^2}. \tag{8.27}$$

Next, using the conjecture (8.5), we can now obtain the holographic entanglement negativity as

$$\mathcal{E} = \frac{3}{16G_N^{3+1}}\Big[\Big(\frac{2L}{a}\Big) + k_1(\frac{L}{l_1}+\frac{L}{l_2}-\frac{L}{l_1+l_2}) - 2k_2 ML\ l_1 l_2\Big] + \ldots, \tag{8.28}$$

where $M = r_h^3(1+\alpha) = r_h^3(1+\frac{Q^2}{r_h^4})$ and the ellipses denotes sub leading corrections for the given case.
In the above equation, the first term gives the divergent piece for the holographic entanglement negativity, the second term gives the finite term for the holographic entanglement negativity at zero temperature for the given mixed state configuration of two adjacent subsystems on the CFT_3, which corresponds to the geometry of pure AdS_4 in the bulk. The third term gives the corrections due to the presence of charge and the temperature. We see here, that as the temperature was low, there seems to be no thermal contribution towards the holographic entanglement entropy, hence the holographic entanglement negativity in this case does not exhibits thermal piece separation.

Small charge and high temperature

In this case we consider the scenario when the black hole has a small charge and is at high temperature. Now, as $r_h >> 1$, we have $\frac{Q}{\sqrt{3}r_h^2} << 1$ and using this fact we can do a Taylor expansion of $f(u)^{-\frac{1}{2}}$ around $\delta = 0$ where $\delta = \frac{Q}{\sqrt{3}r_h^2}$. The approximated form of the lapse function [49] is

$$f(u)^{-\frac{1}{2}} \approx \frac{1}{\sqrt{1-\frac{{r_h}^3u^3}{{r_c}^3}}} + \frac{3}{2}\left(\frac{r_h}{r_c}\right)^3 \frac{\delta^2u^3(1-\frac{r_hu}{r_c})}{(1-\frac{{r_h}^3u^3}{{r_c}^3})^{3/2})}. \tag{8.29}$$

Now using the eqs. (8.29),(8.17) and (8.18) we get the following expression for the finite term of the area as [49]

$$\mathcal{A}_A^{finite} = Llr_h^2 + Lr_h(k_1+\delta^2k_2) + Lr_h\epsilon\Big[k_3 + \delta^2(k_4+k_5\log\epsilon)\Big] + O[\epsilon^2], \tag{8.30}$$

where the value of the constants k_1, k_2, k_3, k_4 and k_5 for the above equation are given in the Appendix (A.1) in the eqs. labelled as (A.1), (A.2), (A.3), (A.4) and (A.5) respectively. The parameter ϵ appearing in the eq. (8.30) is expressed as

$$\epsilon = \frac{1}{3}\exp\Big(-\sqrt{3}(lr_h - c_1 - c_2\delta^2)\Big), \tag{8.31}$$

where the constants c_1, c_2 for the above equation are given in the Appendix (A.1) in eqs. labelled as (A.6) and (A.7) respectively. Now, using the conjecture, we obtain the holographic entanglement negativity for the given case as

$$\begin{aligned}\mathcal{E} &= \frac{3}{16G_N^{3+1}}\Bigg[\frac{2L}{a} + Lr_h\Big\{(k_1+\delta^2 k_2) + k_3(\epsilon_1+\epsilon_2-\epsilon_{12}) \\ &\quad +\delta^2 k_4(\epsilon_1+\epsilon_2-\epsilon_{12}) + \delta^2 k_5\big(\log\epsilon_1 + \log\epsilon_2 - \log\epsilon_{12}\big)\Big\}\Bigg] + ...\end{aligned} \tag{8.32}$$

where $\epsilon_1, \epsilon_2, \epsilon_{12}$ corresponds to the subsystems A_1, A_2 and $A_1 \cup A_2$ respectively.

We see that in the above equation the holographic entanglement negativity depends on a single parameter L, which is the length common to both the two adjacent subsystems on the boundary CFT. On the bulk side this L turns out to be the area of the minimal surface which in the given case of RN-AdS$_4$/CFT$_3$ turns out to be the length. It is interesting to compare this to the holographic entanglement entropy which scales as the volume for the given limit (area in the case of RN-AdS$_4$/CFT$_3$) [49] whereas holographic entanglement negativity scales as the area for the given limit (length in the case of RN-AdS$_4$/CFT$_3$). In the case of holographic entanglement negativity, as the temperature is high, even though the volume terms which represent thermal correlations are present, they are cancelled out and so we are left with only area dependent terms (length in the case of RN-AdS$_4$/CFT$_3$). This conforms to the expectations coming from the domain of quatum information theory. This elimination of the thermal terms is similar to the AdS$_3$/CFT$_2$ scenario [61,130] suggesting that maybe the absence of the thermal terms is an universal aspect of the holographic entanglement negativity.

Large charge and high temperature

We now consider the case when the black hole has a large charge and is at high temperature. Now, in this case the turning point of the minimal surface in the bulk is close to the horizon so we have $r_c \sim r_h$, $u_0 = \frac{r_c}{r_h} \sim 1$ and using this fact we can do a Taylor expansion of $f(u)^{-\frac{1}{2}}$ around u_0. The approximated form of the lapse function is [49]

$$f(u) \approx \Big(3 - \frac{Q^2}{r_h^4}\Big)\Big(1 - \frac{r_h}{r_c}u\Big). \tag{8.33}$$

Now, using the eqs. (8.33), (8.17), (8.18) we get the following expression for the finite term of the area as [49]

$$\mathcal{A}_A^{finite} = Llr_h^2 + \frac{Lr_h}{2\sqrt{\delta}}\Big[K_1' + K_2'\epsilon + \mathcal{O}(\epsilon^2)\Big], \tag{8.34}$$

where ϵ is as given in the eq. ((8.31)) and the constants K_1' and K_2' in the above equation are given in the Appendix (A.2) in the eqs. labelled as (A.8) and (A.9) respectively.

Using the holographic entanglement negativity conjecture, we obtain

$$\mathcal{E} = \frac{3}{8G_N^{3+1}}\left[\left(\frac{L}{a}\right) + \frac{Lr_h}{\sqrt{\delta}}\Big\{K_1' + K_2'(\epsilon_1 + \epsilon_2 - \epsilon_{12})\Big\}\right] + \ldots, \tag{8.35}$$

where $\epsilon_1, \epsilon_2, \epsilon_{12}$ corresponds to the subsystems A_1, A_2 and $A_1 \cup A_2$ respectively.

In this case also even though because of the high temperature, thermal contributions from the holographic entanglement entropy are present, they are removed by the holographic entanglement negativity and the resulting holographic entanglement negativity then scales as the area (length in the case of RN-AdS$_4$/CFT$_3$) of the minimal surface conforming to the expectations from quantum information theory. As a result we again witness the similarity of the elimination of the thermal terms between this case and the AdS$_3$/CFT$_2$ scenario, receiving hints that maybe removal of the thermal contribution is an universal aspect of the holographic entanglement negativity.

8.2.3 Extremal RN-AdS$_4$ black holes

We now move on towards the calculation of the holographic entanglement negativity of mixed states at zero temperature. We consider the configuration of the two adjacent subsystems having rectangular strip geometries and residing on the boundary CFT$_3$ dual to the extremal RN-AdS$_4$ black hole in the bulk. We will perform calculations in a pertubative method for both the limits of small charge and large charge.

Small charge

In this case we consider the scenario when the black hole has a small charge and is at zero temperature. We use equation (8.12) in the lapse function (8.16) and then observing the fact that for a small r_h, we can do the Taylor expansion of the $f(u)^{-\frac{1}{2}}$ around $\frac{r_h}{r_c} = 0$, we get the approximated form for the lapse function in the leading order in $\mathcal{O}[(\frac{r_h}{r_c}u)^3]$ as follows [49]

$$f(u)^{-\frac{1}{2}} \approx 1 + 2\frac{r_h^3}{r_c^3}u^3, \tag{8.36}$$

Using the eqs. (8.36), (8.17), (8.18) leads to the following expression for the finite part of the area as [49]

$$\mathcal{A}_A^{finite} = k_1\frac{L}{l} + k_2 r_h^3 L l^2 + \mathcal{O}(r_h^4 l^3), \tag{8.37}$$

where the constants k_1, k_2 appearing in the above equation are given as

$$\begin{aligned} k_1 &= -\frac{4\pi\Gamma(\frac{3}{4})^2}{4\Gamma(\frac{1}{4})^2}, \\ k_2 &= \frac{4\Gamma(\frac{1}{4})^2}{32\Gamma(\frac{3}{4})^2}. \end{aligned}$$

Using the holographic entanglement negativity conjecture, we obtain

$$\mathcal{E} = \frac{3}{16G_N^{3+1}}\Big[\Big(\frac{2L}{a}\Big) + k_1(\frac{L}{l_1} + \frac{L}{l_2} - \frac{L}{l_1+l_2}) - 2k_2 r_h^3 L l_1 l_2\Big] + \dots . \tag{8.38}$$

In this case, since the black hole is at zero temperature, no thermal contributions are present in the holographic entanglement entropy and this fact is clearly reflected in the holographic entanglement negativity which shows no thermal piece separation. The second term in the above equation expresses the finite piece of the holographic entanglement negativity for mixed state at zero temperature having the configuration of two adjacent subsystems on the boundary CFT_3 which is dual to the pure AdS_4 in the bulk. The third term gives the correction due to the presence of the conserved charge of the extremal RN-AdS_4 black hole.

Large charge

In this case we consider the situation when the black hole has a large charge and is at zero temperature. Now, as $r_c \sim r_h$, we have $u_0 = \frac{r_c}{r_h} \sim 1$ and using this fact we can do a Taylor expansion of $f(u)^{-\frac{1}{2}}$ around u_0. The approximated form of the lapse function is [49]

$$f(u) \approx 6\Big(1 - \frac{r_h}{r_c}u\Big)^2 . \tag{8.39}$$

Now using the eqs. (8.39), (8.17) and (8.18), we get the following expression for the finite term of the area as [49]

$$\mathcal{A}_A^{finite} = Llr_h^2 + Lr_h\Big(K_1 + K_2\sqrt{\epsilon} + K_3\epsilon + \mathcal{O}(\epsilon^{\frac{3}{2}})\Big), \tag{8.40}$$

where the constants K_1, K_2 and K_3 in the above equation are given in the Appendix (A.3) in the eqs. labelled as (A.10), (A.11) and (A.12) respectively.

Now, using the holographic entanglement negativity conjecture, we obtain

$$\mathcal{E} = \frac{3}{16G_N^{3+1}}\left[\Big(\frac{2L}{a}\Big) + Lr_h\Big\{K_1 + K_2(\sqrt{\epsilon_1} + \sqrt{\epsilon_2} - \sqrt{\epsilon_{12}}) + K_3(\epsilon_1 + \epsilon_2 - \epsilon_{12})\Big\}\right] + \dots , \tag{8.41}$$

where $\epsilon_1, \epsilon_2, \epsilon_{12}$ corresponds to the subsystems A_1, A_2 and $A_1 \cup A_2$ respectively.

In this case as the black hole is at zero temperature, the volume contribution (area in the RN-$\text{AdS}_4/\text{CFT}_3$ scenario) to the holographic entanglement entropy comes from the degeneracy of the ground state and finally gets removed by the holographic entanglement negativity. Hence, the holographic entanglement negativity scales as the area (length in the RN-$\text{AdS}_4/\text{CFT}_3$ scenario). conforming to the expectations from quantum information theory.

8.3 Holographic entanglement negativity in the setup of RN-$\text{AdS}_{d+1}/\text{CFT}_d$

In the previous section, we saw that the holographic entaglement negativity conjecture in the case of $RN - AdS_4$ produces results as expected i.e. whenever the

holographic entanglement entropy has thermal contributions for non-extremal cases, thermal contributions are separated from quantum correlations which in turn are described by the holographic entanglement negativity. It is interesting to note that the holographic entanglement negativity can also differentiate between quantum and "unreal" thermal contributions for extremal large charge case. This separation makes it evident that the CFT dual to extremal black hole is in a mixed state even though it is at zero temperature. It is the large charge of the black hole that leads to a large radius of horizon, finally resulting in an extensive thermal-like term which reflects the fact that the black hole has an effective thermal-like temperature. The exercise in the previous section strengthens the validity of the conjecture for RN-AdS$_4$/CFT$_3$ even when the black hole carries charge and is static. Now, as the authors in [65] have already proved the validity of the conjecture for the case of AdS$_{\rm d+1}$ − Schwarzschild, it becomes important to investigate if this conjecture still holds for charged and static black holes in AdS$_{d+1}$ and produces results similar to RN-AdS$_4$.

In this section we will proceed towards the calculation of the holographic entanglement negativity for mixed states having the configuration of the two adjacent subsystems on the boundary CFT$_d$ dual to the RN-AdS$_{d+1}$ black hole in the bulk. The boundary subsystems have a rectangular strip geometry. This scenario requires a perturbative calculation of the the area of the bulk co-dimension two static minimal surface in the various limits of the temperature T and the chemical potential μ related to the charge Q of the RN-AdS$_{d+1}$ black hole. However, it turns out that in the RN-AdS$_{d+1}$/CFT$_d$ setup it is suitable to express the holographic entanglement negativity in terms of another set of parameters called as effective temperature $T_{\rm eff}$ and a dimensionless energy parameter ε. Both these parameters $T_{\rm eff}$ and ε are functions of the temperature and chemical potential. The parameter $T_{\rm eff}$ counts the number of microstates of the system for a specific temperature and chemical potential whereas the parameter ε is a dimensionless measure for the energy of the system [137].

8.3.1 Area of the minimal surface for RN-AdS$_{d+1}$ black holes

We will start with the metric for the RN-AdS$_{d+1}$ ($d \geq 3$) black hole which is

$$\begin{aligned} ds^2 =& \frac{1}{z^2}\left(-f(z)dt^2 + \frac{dz^2}{f(z)} + d\vec{x}^2\right), \\ f(z) =& 1 - Mz^d + \frac{(d-2)Q^2}{(d-1)}z^{2(d-1)}, \\ A_t =& Q(z_H^{d-2} - z^{d-2}), \end{aligned} \tag{8.42}$$

where the AdS radius $R = 1$ and z_H is the location of the horizon, given by the smallest real root when the lapse function vanishes $f(z) = 0$. Q, M are the charge and the mass of the black hole respectively. The chemical potential is given by

$$\mu \equiv \lim_{z\to 0} A_t(z) = Qz_H^{d-2}, \tag{8.43}$$

and the Hawking temperature is given as

$$T = -\frac{1}{4\pi}\frac{d}{dz}f(z)\Big|_{z_H} = \frac{d}{4\pi z_H}\left(1 - \frac{(d-2)^2Q^2z_H^{2(d-1)}}{d(d-1)}\right). \tag{8.44}$$

Next, the lapse function, chemical potential and temperature can be rewritten as

$$f(z) = 1-\varepsilon\left(\frac{z}{z_H}\right)^d+(\varepsilon-1)\left(\frac{z}{z_H}\right)^{2(d-1)}, \tag{8.45}$$

$$\mu = \frac{1}{z_H}\sqrt{\frac{(d-1)}{(d-2)}(\varepsilon-1)}, \tag{8.46}$$

$$T = \frac{2(d-1)-(d-2)\varepsilon}{4\pi z_H}. \tag{8.47}$$

Here, ε having limits $1 \geq \varepsilon \geq \frac{2(d-1)}{d-2}$ is a dimensionless quantity, which represents energy of the system and is given as [137]

$$\varepsilon(T,\mu) = b_0 - \frac{2n}{1+\sqrt{1+\frac{d^2}{2\pi^2 b_0 b_1}\left(\frac{\mu^2}{T^2}\right)}}, \tag{8.48}$$

Here b_0, b_1 are constants which depend on spacetime dimensions and are given as

$$b_0 = \frac{2(d-1)}{d-2}\ , \qquad b_1 = \frac{d}{d-2}. \tag{8.49}$$

The effective temperature T_{eff} defined earlier is given as [137]

$$T_{\text{eff}}(T,\mu) \equiv \frac{d}{4\pi z_H} = \frac{T}{2}\left[1+\sqrt{1+\frac{d^2}{2\pi^2 b_0 b_1}\left(\frac{\mu^2}{T^2}\right)}\right]. \tag{8.50}$$

In order to calculate the area of the bulk co-dimension two static minimal surface we consider a rectangular strip geometry for the subsystems on the boundary CFT which is defined as

$$x \equiv x^1 \in \left[-\frac{l}{2},\frac{l}{2}\right],\ x^i \in \left[-\frac{L}{2},\frac{L}{2}\right], \qquad i=2,...,d-2, \tag{8.51}$$

where $L \to \infty$. The radial U.V. cutoff a is given as $z(\pm\ell/2) = a$.
In the first step, we need to find the turning point z_* of the minimal surface in the bulk from the following equation

$$\frac{l}{2} = \int_0^{z_*} \frac{dz}{\sqrt{f(z)[(z_*/z)^{2(d-1)}-1]}}, \tag{8.52}$$

where we see the relation between the turning point z_* of the minimal surface in the bulk and l, the length of the strip in the x^1 direction.
We now use the value of the turning point z_* in the following expression to obtain the area of the extremal surface.

$$\mathcal{A} = 2L^{d-2}z_*^{d-1}\int_0^{l/2}\frac{dx}{z(x)^{2(d-1)}} = 2L^{d-2}z_*^{d-1}\int_a^{z_*}\frac{dz}{z^{d-1}\sqrt{f(z)[z_*^{2(d-1)}-z^{2(d-1)}]}}, \tag{8.53}$$

where the UV cutoff is denoted by a.

Alternatively, we can also express eq. (8.52) as a double sum [137]

$$l = \frac{z_*}{d-1}\sum_{n=0}^{\infty}\sum_{k=0}^{n}\frac{\Gamma\left[\frac{1}{2}+n\right]\Gamma\left[\frac{d(n+k+1)-2k}{2(d-1)}\right]\varepsilon^{n-k}(1-\varepsilon)^k}{\Gamma[1+n-k]\Gamma[k+1]\Gamma\left[\frac{d(n+k+2)-2k-1}{2(d-1)}\right]}\left(\frac{z_*}{z_H}\right)^{nd+k(d-2)}. \tag{8.54}$$

and as a result we can also express the eq. for the area (8.53) as a double sum [137]

$$\begin{aligned}\mathcal{A} = {} & \frac{2}{d-2}\left(\frac{L}{a}\right)^{d-2} + 2\frac{L^{d-2}}{z_*^{d-2}}\left[\frac{\sqrt{\pi}\Gamma\left(-\frac{d-2}{2(d-1)}\right)}{2(d-1)\Gamma\left(\frac{1}{2(d-1)}\right)}\right] \\ & + \frac{L^{d-2}}{(d-1)z_*^{d-2}}\left[\sum_{n=1}^{\infty}\sum_{k=0}^{n}\frac{\Gamma\left[\frac{1}{2}+n\right]\Gamma\left[\frac{d(n+k-1)-2k+2}{2(d-1)}\right]\varepsilon^{n-k}(1-\varepsilon)^k}{\Gamma[1+n-k]\Gamma[k+1]\Gamma\left[\frac{d(n+k)-2k+1}{2(d-1)}\right]}\left(\frac{z_*}{z_H}\right)^{nd+k(d-2)}\right].\end{aligned} \tag{8.55}$$

As a result of the above two eqs. (8.54), (8.55), we will now be able to perform the pertubative analysis in the various limits of the temperature T and the chemical potential μ to extract the turning point and the area in terms of the parameters T_{eff} and ε.

We will now move on towards the calculation of the holographic entanglement negativity for the two adjacent subsystems having a mixed state configuration for the RN-AdS$_{d+1}$/CFT$_d$ scenario. For this purpose, we shall use the above stated perturbative method for the turning point and the area. The two adjacent subsystems A_1, A_2 have a rectangular strip geometry and are described as

$$x^1 \in [-\tfrac{l_1}{2}, \tfrac{l_1}{2}], \qquad x^i \in [-\tfrac{L}{2}, \tfrac{L}{2}], \tag{8.56}$$

$$x^1 \in [-\tfrac{l_2}{2}, \tfrac{l_2}{2}], \qquad x^i \in [-\tfrac{L}{2}, \tfrac{L}{2}], \tag{8.57}$$

respectively. This configuration is as depicted in the Fig. 13 where in this case the length L is the length of the strip geometry in the other $(d-2)$ directions. In this case of two adjacent subsystems, one can now obtain the turning point by using l_1 and l_2 instead of l in the eq. (8.52) and finally obtain the area by then making using of the eq. (8.53).

8.3.2 Non-extremal RN-AdS$_{d+1}$ black holes

We will first consider the case of the non-extremal RN-AdS$_{d+1}$ black hole which means that the black hole is at a finite temperature. At the boundary CFT$_d$ which is dual to the RN-AdS$_{d+1}$ black hole, we will consider the mixed state configuration of the two adjacent subsystems having rectangular strip geometries as shown in the Fig. 13. We first use a perturbative method to calculate the area of the static minimal surface in the bulk and then use the conjecture to calculate the holographic entanglement negativity. In the following subsections, we will perform this exercise in the various limits of the chemical potential μ and the temperature T.

Small chemical potential and low temperature

The case of small chemical potential and low temperature is governed by the limits $\mu l \ll 1$ and $Tl \ll 1$ respectively. Now, it so happens that the area of the bulk minimal surface is also affected by the length of the strip in the x^1 direction wherein the lengths in the remaining x^i directions is a constant L. As a result, we need to modify the limits for the case of small chemical potential and low temperature as $T \ll \mu$ or $T \gg \mu$ [137] and hence we will calculate the holographic entanglement negativity for both these two limits.

(i) $Tl \ll \mu l \ll 1$

We will first consider the case in which $Tl \ll 1$, $\mu l \ll 1$ and $T \ll \mu$ or alternatively these limits can be combined and re-expressed as $Tl \ll \mu l \ll 1$.
When $T \ll \mu$, one can use the Taylor expansion for the $T_{\text{eff}}(T,\mu)$ (8.50) and $\varepsilon(T,\mu)$ (8.48) around $\frac{T}{\mu} = 0$ and obtain the following expression in the leading order [137]

$$T_{\text{eff}} \approx \frac{1}{2}\left(\frac{\mu d}{\pi\sqrt{2b_0 b_1}} + T\right), \tag{8.58}$$

$$\varepsilon \approx b_0 - \frac{2n\pi\sqrt{2b_0 b_1}}{d}\left(\frac{T}{\mu}\right). \tag{8.59}$$

From the two limits $Tl \ll 1$ and $\mu l \ll 1$ one can infer that the turning point of the entangling surface in the bulk is faraway from the horizon i.e $z_* \ll z_H$. Hence, it is now possible to perform an expansion for the eq. (8.54) in the leading order in $(\frac{l}{z_H})^d$ to obtain the turning point as

$$z_* = \frac{l\,\Gamma\left[\frac{1}{2(d-1)}\right]}{2\sqrt{\pi}\Gamma\left[\frac{d}{2(d-1)}\right]}\left[1 - \frac{1}{2(d+1)}\frac{2^{\frac{1}{d-1}-d}\Gamma\left(1+\frac{1}{2(d-1)}\right)\Gamma\left(\frac{1}{2(d-1)}\right)^{d+1}}{\pi^{\frac{d+1}{2}}\Gamma\left(\frac{1}{2}+\frac{1}{d-1}\right)\Gamma\left(\frac{d}{2(d-1)}\right)^{d}}\varepsilon\left(\frac{l}{z_H}\right)^{d} + \mathcal{O}\left(\frac{l}{z_H}\right)^{2(d-1)}\right]. \tag{8.60}$$

Subsequently, one can perform an expansion for the eq. (8.55) in the leading order in $(\frac{l}{z_H})^d$ to obtain the area and then re-express it in terms of T_{eff} and ε as follows [137]

$$\mathcal{A}_A = \left[\frac{2}{d-2}\left(\frac{L}{a}\right)^{d-2} + \mathcal{S}_0\left(\frac{L}{l}\right)^{d-2} + \varepsilon\mathcal{S}_0\mathcal{S}_1\left(\frac{4\pi T_{\text{eff}}}{d}\right)^{d} L^{d-2}l^2\right] + \mathcal{O}\Big(T_{\text{eff}}l\Big)^{2(d-1)}. \tag{8.61}$$

Using the holographic entanglement negativity conjecture, we obtain

$$\mathcal{E} = \frac{3}{16G_N^{d+1}}\left[\frac{2}{d-2}\left(\frac{L}{a}\right)^{d-2} + \mathcal{S}_0 L^{d-2}\left(\frac{1}{l_1^{d-2}} + \frac{1}{l_2^{d-2}} - \frac{1}{(l_1+l_2)^{d-2}}\right) - \varepsilon\mathcal{S}_0\mathcal{S}_1\left(\frac{4\pi T_{\text{eff}}}{d}\right)^{d} L^{d-2}2l_1 l_2\right] + \ldots. \tag{8.62}$$

The above equation gives the holographic entanglement negativity for mixed state at a finite temperature. Note that in the above equation the first two terms pertain to the holographic entanglement negativity for the mixed state at zero temperature on the boundary CFT_d which in turn is dual to the pure AdS_{d+1} in the bulk. The third term gives the corrections arising out of the chemical potential and the temperature of the black hole.

(ii) $\boldsymbol{\mu l \ll T l \ll 1}$

We will now consider the second case in which $Tl \ll 1$, $\mu l \ll 1$ and $T \gg \mu$ or alternatively these limits can be combined and re-expressed as $\mu l \ll Tl \ll 1$. When $T \gg \mu$ one can use the Taylor expansion for the $T_{\text{eff}}(T,\mu)$ (8.50) and $\varepsilon(T,\mu)$ (8.48) around $\frac{\mu}{T} = 0$ and obtain the following expression in the leading order [137]

$$T_{\text{eff}} = T\left[1 + \frac{d(d-2)^2}{16\pi^2(d-1)}\left(\frac{\mu}{T}\right)^2 + \mathcal{O}\left(\frac{\mu}{T}\right)^4\right] , \tag{8.63}$$

$$\varepsilon = 1 + \frac{d^2(d-2)}{16\pi^2(d-1)}\left(\frac{\mu}{T}\right)^2 + \mathcal{O}\left(\frac{\mu}{T}\right)^4 . \tag{8.64}$$

As in this case also, we have $Tl \ll 1$ and $\mu l \ll 1$ one can infer that the turning point of the entangling surface in the bulk is faraway from the horizon i.e $z_* \ll z_H$. Hence, it is possible to perform an expansion for the eq. (8.54) to the leading order in $(\frac{l}{z_H})^d$ to obtain the turning point which turns out to be the same expression as given in the eq. eq.(8.60).

Subsequently, one can perform an expansion for the eq. (8.55) in the leading order in $(\frac{l}{z_H})^d$ to obtain the area and then re-express it in terms of T_{eff} and ε as follows [137]

$$\mathcal{A}_A = \Big[\frac{2}{d-2}\left(\frac{L}{a}\right)^{d-2} + \mathcal{S}_0\left(\frac{L}{l}\right)^{d-2} + \varepsilon\mathcal{S}_0\mathcal{S}_1\left(\frac{4\pi T_{\text{eff}}}{d}\right)^d L^{d-2}l^2\Big] + \mathcal{O}\Big(T_{\text{eff}}l\Big)^{2(d-1)}, \tag{8.65}$$

where the value of the numerical constants $\mathcal{S}_0$ and $\mathcal{S}_1$ is given in the Appendix (B.1) in the eqs. labelled as (B.1) and (B.2) respectively.
It is important to note here that even though the expression for the area (8.65) in this case of $\mu l \ll Tl \ll 1$ is similar to the above case of $Tl \ll \mu l \ll 1$ (8.61), the expression for T_{eff} and ε is different in both the cases.

Now, using the conjecture, we obtain the holographic entanglement negativity for the given case as

$$\mathcal{E} = \frac{3}{16G_N^{d+1}}\Big[\frac{2}{d-2}\left(\frac{L}{a}\right)^{d-2} + \mathcal{S}_0L^{d-2}\left(\frac{1}{l_1^{d-2}} + \frac{1}{l_2^{d-2}} - \frac{1}{(l_1+l_2)^{d-2}}\right) - \varepsilon\mathcal{S}_0\mathcal{S}_1\left(\frac{4\pi T_{\text{eff}}}{d}\right)^d L^{d-2}2l_1l_2\Big] + \ldots . \tag{8.66}$$

The above equation gives the holographic entanglement negativity for mixed state at a finite temperature. Note that in the above equation the first two terms pertain to the holographic entanglement negativity for the mixed state at zero temperature on the boundary CFT_d which in turn is dual to the pure AdS_{d+1} in the bulk. The third term gives the corrections arising out of the chemical potential and the temperature of the black hole.

Small chemical potential and high temperature

The case of small chemical potential and high temperature is governed by the limits $\mu \ll T$ and $Tl \gg 1$ as given in [137]. When $\mu \ll T$ one can use the Taylor expansion for the $T_{\text{eff}}(T,\mu)$ (8.50) and $\varepsilon(T,\mu)$ (8.48) around $\frac{\mu}{T}=0$ and obtain the same expression for T_{eff} (8.63) and ε (8.64) in the leading order in $\frac{\mu}{T}$ as given in the previous case [137].

However, as compared to the previous case, the limit $Tl \gg 1$ dictates the fact that the turning point of the entangling surface in the bulk is near the horizon i.e $z_* \sim z_H$. Hence, in this case one can do a perturbative expansion of the eq. (8.55) around $\frac{z_*}{z_H}=1$ and obtain the area as

$$\mathcal{A}_A = \Big[\frac{2}{d-2}\left(\frac{L}{a}\right)^{d-2} + V\left(\frac{4\pi T_{\text{eff}}}{d}\right)^{d-1} + L^{d-2}\left(\frac{4\pi T_{\text{eff}}}{d}\right)^{d-2}\gamma_d\left(\frac{\mu}{T}\right)\Big], \quad (8.67)$$

where $V = L^{d-2}l$ gives the volume of the strip and $\gamma_d\Big(\frac{\mu}{T}\Big)$ is a perturbative expression in terms of $\frac{\mu}{T}$ as stated in the Appendix (B.2) in the eq. labelled as (B.3).

Now, using the conjecture, we obtain the holographic entanglement negativity for the given case as

$$\mathcal{E} = \frac{3}{16G_N^{d+1}}\Big[\frac{2}{d-2}\left(\frac{L}{a}\right)^{d-2} + L^{d-2}\left(\frac{4\pi T_{\text{eff}}}{d}\right)^{d-2}\gamma_d\left(\frac{\mu}{T}\right)\Big]. \quad (8.68)$$

In this case, when the temperature is high, mixed state behaviour comes into play and thermal contributions are reflected in the holographic entanglement entropy in the form of volume term which gets removed by the holographic entanglement negativity. Hence, the leading term in the above eq. for the holographic entanglement negativity is an area term. This exercise reproduces the result of the RN-AdS$_4$/CFT$_3$ scenario conforming to the expectations of the quantum information theory.

Large chemical potential and low temperature

The case of large chemical potential and low temperature is governed by the limits $\mu l \gg 1$ and $T \ll \mu$. When $T \ll \mu$, one can use the Taylor expansion for the $T_{\text{eff}}(T,\mu)$ (8.50) and $\varepsilon(T,\mu)$ (8.48) around $\frac{T}{\mu}=0$ and obtain the same expression in the leading order as given by the eq.(8.58) and eq.(8.59) respectively. [137]. Using the limit $\mu l \gg 1$, we can infer that the turning point of the entangling surface in the bulk is near the horizon i.e $z_* \sim z_H$. Hence, in this case one can do a perturbative expansion of the eq. (8.55) around $\frac{z_*}{z_H}=1$ and obtain the area as [137]

$$\mathcal{A}_A = \Big[\frac{2}{d-2}\left(\frac{L}{a}\right)^{d-2} + V\left(\frac{4\pi T_{\text{eff}}}{d}\right)^{d-1} + L^{d-2}\left(\frac{4\pi T_{\text{eff}}}{d}\right)^{d-2}\Big(N_0 + N_1(b_0-\varepsilon)\Big) + \mathcal{O}\left(\frac{T}{\mu}\right)\Big], \quad (8.69)$$

where $V = L^{d-2}l$ gives the volume of the strip and the value of the numerical constants appearing in the above equation N_0 and N_1 are given in the Appendix (B.3) in the eqs. labelled as (B.5) and (B.6) respectively.

Now, using the conjecture, we obtain the holographic entanglement negativity for the given case as

$$\mathcal{E} = \frac{3}{16G_N^{d+1}}\Big[\frac{2}{d-2}\left(\frac{L}{a}\right)^{d-2} + L^{d-2}\left(\frac{4\pi T_{\text{eff}}}{d}\right)^{d-2}\Big(N_0 + N_1(b_0-\varepsilon)\Big)\Big] + \dots . \tag{8.70}$$

The above equation gives the holographic entanglement negativity for mixed state at a finite temperature. We see that in this case also thermal correlations are contributing towards the holographic entanglement entropy which gets cancelled out by the holographic entanglement negativity. Hence, the holographic entanglement negativity depends on the area term. This exercise reproduces the result of the RN-AdS$_4$/CFT$_3$ scenario conforming to the expectations of the quantum information theory.

8.3.3 Extremal RN-AdS$_{d+1}$ black holes

In the previous subsection we calculated the holographic entanglement negativity for the mixed states which were at a finite temperature on the boundary CFT$_d$ which in turn was dual to the non-extremal RN-AdS$_{d+1}$ black hole in the bulk. We now move towards the computation of the holographic entanglement negativity for the mixed states which were at zero temperature on the boundary CFT$_d$ which in turn is dual to the extremal RN-AdS$_{d+1}$ black hole in the bulk which implies we have the following parameters [137]

$$Q^2 = d(d-1)L^2/(d-2)^2 z_H^{2(d-1)}, \tag{8.71}$$

$$\varepsilon = b_1, \tag{8.72}$$

$$\mu = \frac{1}{z_H}\sqrt{\frac{b_0 b_1}{2}} = \frac{1}{z_H}\sqrt{\frac{d(d-1)}{(d-2)^2}}, \tag{8.73}$$

$$T_{\text{eff}} = \frac{\mu d}{2\pi\sqrt{2b_0 b_1}}, \tag{8.74}$$

where Q is the charge of the extremal RN-AdS$_{d+1}$ black hole T_{eff} represents the effective temperature as described previously. In the case of extremal RN-AdS$_{d+1}$ black hole we consider the boundary subsystem having a rectangular strip geometry. Using the above mentioned parameters we will first calculate the area of the bulk co-dimension two static minimal surface in a perturbative fashion and then make use of the conjecture to obtain the corresponding holographic entanglement negativity. We will do these calculations for the both the limits of small and large chemical potential.

Small chemical potential

The case of small chemical potential for extremal RN-AdS$_{d+1}$ black hole is governed by the limit $\mu l \ll 1$. In this limit, the turning point of the entangling surface in the bulk is faraway from the horizon i.e $z_* \ll z_H$. Hence, we can do a perturbative expansion for the eq. (8.54) in the leading order in $(\frac{l}{z_H})^d$ to obtain the turning point as previously obtained in the eq. (8.60) [137].

Hence, in this case to obtain the area one can do a perturbative expansion of the eq. (8.55) to the leading order in $(l/z_H)^d$ and then re-express it in terms

of μ as given in [137]

$$\mathcal{A}_A = \Big[\frac{2}{d-2}\left(\frac{L}{a}\right)^{d-2} + \mathcal{S}_0\left(\frac{L}{l}\right)^{d-2} + \mathcal{S}_0\mathcal{S}_1\frac{2(d-1)}{d-2}\left(\frac{(d-2)\mu}{\sqrt{d(d-1)}}\right)^{d} L^{d-2}l^2 + \mathcal{O}[(\mu l)^{2(d-1)}]\Big], \tag{8.75}$$

where the value of the numerical constants $\mathcal{S}_0,\ \mathcal{S}_1$ in the above equation is the same as given in the Appendix (B.1) in the eqs. labelled as (B.1) and (B.2) respectively.

Now, using the conjecture, we obtain the holographic entanglement negativity for the given case as

$$\begin{aligned}\mathcal{E} = \frac{3}{16G_N^{d+1}}\Big[\frac{2}{d-2}\left(\frac{L}{a}\right)^{d-2} + \mathcal{S}_0 L^{d-2}\left(\frac{1}{l_1^{d-2}} + \frac{1}{l_2^{d-2}} - \frac{1}{(l_1+l_2)^{d-2}}\right) \\ -\mathcal{S}_0\mathcal{S}_1\frac{2(d-1)}{d-2}\left(\frac{(d-2)\mu}{\sqrt{d(d-1)}}\right)^{d} L^{d-2}2l_1l_2\Big] + \ldots.\end{aligned} \tag{8.76}$$

Note that the first two terms in the above equation pertain to the holographic entanglement negativity for the mixed state at zero temperature on the boundary CFT_d which in turn is dual to the pure AdS_{d+1} in the bulk. The third term gives the corrections arising out of the chemical potential of the black hole.

Large chemical potential

The case of large chemical potential for extremal RN-AdS_{d+1} black hole is governed by the limit $\mu l \gg 1$. Hence, from the eq. (8.71) we can infer that the value of the horizon radius is large and so the turning point of the entangling surface in the bulk is near the horizon i.e $z_* \to z_H$. Hence, in this case one can do a perturbative expansion of the eq. (8.55) around $z_*/z_H = 1$ and obtain the area as

$$\mathcal{A}_A = \Big[\frac{2}{d-2}\left(\frac{L}{a}\right)^{d-2} + V\mu^{d-1}\left(\frac{d-2}{\sqrt{d(d-1)}}\right)^{d-1} + L^{d-2}N(b_0)\left(\frac{d-2}{\sqrt{d(d-1)}}\right)^{d-2}\mu^{d-2}\Big], \tag{8.77}$$

where $V = L^{d-2}l$ gives the volume of the strip and $N(b_0)$ gives the value of $N(\varepsilon)$ when $\varepsilon = b_0$.

Now, using the conjecture, we obtain the holographic entanglement negativity for the given case as

$$\mathcal{E} = \frac{3}{16G_N^{d+1}}\Big[\frac{2}{d-2}\left(\frac{L}{a}\right)^{d-2} + L^{d-2}N(b_0)\left(\frac{d-2}{\sqrt{d(d-1)}}\right)^{d-2}\mu^{d-2}\Big]. \tag{8.78}$$

In this case as the black hole is at zero temperature, the volume contribution towards the holographic entanglement entropy comes from the degeneracy of the ground state and finally gets removed by the holographic entanglement negativity. Hence, the holographic entanglement negativity scales as an area term. This exercise reproduces the result of the RN-$\mathrm{AdS}_4/\mathrm{CFT}_3$ scenario conforming to the expectations of the quantum information theory.

8.4 Summary and Conclusion

In this chapter, which is based on [136], we have used the conjecture as given in [65,130] to calculate the holographic entanglement negativity for mixed state having the configuration of the two adjacent subsystems on the boundary CFT which are dual to the RN-AdS black hole in the bulk. We have considered both the non-extremal and the extremal RN-AdS black hole. The configuration of the two adjacent subsystems on the boundary is considered to have a rectangular strip geometry. The calculations are first performed for the case of RN-AdS_4/CFT_3 and then for a general RN-AdS_{d+1}/CFT_d setup. This exercise showcases the non trivial nature of the perturbative calculation of the holographic entanglement negativity in the various relevant limits.

In the first case of the RN-AdS_4/CFT_3 scenario, we can summarize the results as follows :-

1. When we have the mixed state at a finite temperature on the boundary CFT_3 dual to the non-extremal RN-AdS_4 black hole, then we perform the calculations for various limits of the charge and the temperature of the black hole.

a. When we have the limit of small charge and low temperature, then the leading contribution to the holographic entanglement negativity comes from the mixed state at zero temperature on the boundary CFT_3 which in turn is dual to the pure AdS_4 in the bulk. The subleading term represents the corrections due to the charge and the temperature of the black hole. This reflects the fact that in this case the entangling surface in the bulk is faraway from the black hole horizon, so the leading contributing comes from the near boundary pure AdS_4 configuration.

b. When we encounter limits having large charge and/or large temperature, then the leading contribution to the holographic entanglement negativity scales as an area (length in the case of RN-AdS_4/CFT_3) as the volume terms (area in the case of RN-AdS_4/CFT_3) are completely eliminated. This reflects the fact that in this case the entangling surface in the bulk is near the black hole horizon, so the leading contributing comes from the degrees of freedom of the entangling surface which is shared between the two adjacent subsystems.

2. When we have the mixed state at zero temperature on the boundary CFT_3 dual to the extremal RN-AdS_4 black hole, then we perform the calculations for various limits of the charge of the black hole.

a. In the case of small charge, the leading contribution to the holographic entanglement negativity comes from the mixed state at zero temperature on the boundary CFT_3 which in turn is dual to the pure AdS_4 in the bulk. The subleading term represents the corrections due to the charge of the black hole.

b. In the case of large charge, the leading contribution towards the holographic entanglement negativity scales as an area (length in the case of RN-AdS_4/CFT_3) as the volume terms (area in the case of RN-AdS_4/CFT_3) arising out of the vacuum degeneracy are completely eliminated.

In the second case of the RN-AdS_{d+1}/CFT_d scenario, another set of parameters

called as effective temperature T_{eff} and a dimensionless energy parameter ε were introduced. We can summarize the results as follows :-

1. When we have the mixed state at a finite temperature on the boundary CFT_d dual to the non-extremal RN-AdS_{d+1} black hole, then we perform the calculations for various limits of the chemical potential and the temperature of the black hole.

a. When we have the limit of small chemical potential and low temperature, then the leading contribution to the holographic entanglement negativity comes from the mixed state at zero temperature on the boundary CFT_d which in turn is dual to the pure AdS_{d+1} in the bulk. The subleading term represents the corrections due to the chemical potential and the temperature of the black hole. This reflects the fact that in this case the entangling surface in the bulk is far-away from the black hole horizon, so the leading contributing comes from the near boundary pure AdS_{d+1} configuration.

b. When we encounter limits having large chemical potential and/or large temperature, then the leading contribution to the holographic entanglement negativity scales as an area as the volume terms are completely eliminated. This reflects the fact that in this case the entangling surface in the bulk is near the black hole horizon, so the leading contributing comes from the degrees of freedom of the entangling surface which is shared between the two adjacent subsystems.

2. When we have the mixed state at the zero temperature on the boundary CFT_d dual to the extremal RN-AdS_{d+1} black hole, then we perform the calculations for various limits of the chemical potential of the black hole.

a. In the case of small chemical potential, the leading contribution towards the holographic entanglement negativity comes from the mixed state at zero temperature on the boundary CFT_d which in turn is dual to the pure AdS_{d+1} in the bulk. The subleading term represents the corrections due to the chemical potential of the black hole.

b. In the case of large chemical potential, the leading contribution towards the holographic entanglement negativity scales as an area as the volume terms arising out of the vacuum degeneracy are completely eliminated.

We see that in the case of RN-AdS black hole when the leading term for the holographic entanglement entropy is a volume term then in the case of the holographic entanglement negativity the leading term is an area term. This discrepancy between the leading terms is due to the fact that in the case of the holographic entanglement negativity the volume terms are completely eliminated due to the specific algebraic combination of the involved holographic entanglement entropies. This dominance of the area term in case of the holographic entanglement negativity justifies the expectations from the quatum information theory. Also, it is worth noting that this elimination of the volume terms in the holographic entanglement negativity is also observed in the $\text{AdS}_3/\text{CFT}_2$ scenario and so we may think of this "removal of volume terms" from the holographic entanglement negativity as an universal aspect.

It is interesting to note that even when the black hole is at zero temperature,

the dual CFT exhibits mixed state nature and this happens only for extremal-large charge case. The holographic entanglement negativity is able to detect this mixed state nature for extremal case also as it removes the volume term from the corresponding holographic entanglement entropy. This extremal state result holds not just for RN $-$ AdS_4 but also for RN $-$ AdS_{d+1} as demonstrated in this paper. In the future, it would be further interesting to understand how entanglement negativity is able to differentiate between extensive and non-extensive terms for the extremal-large charge case as both the terms are facets of quantum correlations.

This entire exercise further pushes the credibility of our conjecture [65, 130] for a charged, static black hole. In the future, it would be interesting to investigate the proof for this conjecture similar to the [11] and study further applications of this conjecture.

Conclusion

In this thesis we have addressed from a holographic perspective and making large use of the AdS/CFT correspondence, the problem of the relationship between thermality and quantum entanglement for a large class of AdS black holes. This is a crucial issue for understanding many hot open problems in black hole physics and quantum gravity, such as the microscopic origin of black hole entropy, the loss of information in the black hole evaporation and the emergence of spacetime out of an underlying microscopic quantum theory of gravity. The concepts that are relevant in this framework are those of thermal and entanglement entropy, entanglement negativity (the amount of distillable quantum information in a mixed state) and their relationship to spacetime structures like horizons and minimal surfaces. In our thesis we have investigated these concepts and their relationship with spacetime structures for the case of 3D AdS gravity (the BTZ black hole), 4D AdS gravity (RN-AdS_4 black hole) and also D+1-dimensional AdS Gravity (RN-AdS_{d+1} black hole).

In the case of BTZ black hole, it has been shown that the horizon and the conical singularity are related to each other [33]. Hence, it becomes important to understand how the entanglement entropy differentiates between horizon and conical singularity and this issue has been dealt in chapter 6. Using the modular symmetries of the boundary 2D CFT we have extracted the universal part of the entanglement entropy for the CFT on the torus and we have identified it as the entanglement entropy of the relevant 3D bulk configurations (the BTZ black hole and 3D spacetime with conical singularities). We have seen that the entanglement entropy keeps information of the spacetime structure of the bulk theory. More precisely, in the black hole case :-
(i) The inaccessible region lies along the non-compact direction of the boundary cylinder.
(ii) The holographic entanglement entropy shows an exponential behaviour.
(iii) The leading term in the expansion is positive and scales as an area term.
(iv) Enhancement of the holographic entanglement entropy of the AdS_3 Poincaré vacuum.
In case of the conical singularity :-
(i) The inaccessible region lies along the compact direction of the boundary cylinder.
(ii) The holographic entanglement entropy shows a periodic behaviour.
(iii) The leading term in the expansion is negative and scales as a volume term.
(iv) Reduction of the holographic entanglement entropy of the AdS_3 Poincaré vacuum.

When we deal with the entanglement for conformal field theories at a finite

temperature dual to a black hole in the bulk, then it turns out that the "entanglement entropy" is not the correct measure as it fails to separate classical and quantum correlations. It was shown that the correct measure is "entanglement negativity" which serves as an upper bound on the distillable entanglement and can separate classical and quantum correlations. The holographic version of this entanglement negavtivity for two adjacent intervals has been the subject for the chapter 7. We have used the AdS_3/CFT_2 setup to put forth a conjecture for the holographic entanglement negativity for two adjacent intervals and performed calculations for various scenarios to validate the conjecture. In this case, the entanglement is between the two adjacent intervals as we trace over the degrees of freedom for the remaining part of the system. The holographic prescription involves the lengths of the geodesics present in the bulk AdS_3 wherein the endpoints of these geodesics are anchored on the two adjacent intervals lying on the boundary 2D CFT and as a result we can express the holographic entanglement negativity for the case of two adjacent intervals as the holographic mutual information between these two adjacent intervals. The calculations have been performed for 3 cases (i) Mixed state at zero temperature dual to the AdS_3 vacua in Poincaré coordinates (ii) Mixed state at zero temperature dual to the AdS_3 vacua in global coordinates (iii) Mixed state at finite temperature dual to the Euclidean BTZ black hole. We have shown that in all the three cases the holographic results match with the corresponding CFT results in the large central charge limit, thereby providing a strong support for our conjecture. We have also generalized the conjecture for the AdS_{d+1}/CFT_d scenario wherein we have two adjacent subsystems on the boundary d-dimensional CFT and which now involves the areas of the bulk co-dimension two static minimal surfaces instead of the lengths of the geodesics as considered previously for the case of AdS_3/CFT_2. In this case, we now express the holographic entanglement negativity as the holographic mutual information between the two adjacent subsystems.

We have generalised the results for the entanglement negativity to the case of RN-AdS black holes in four and generic D+1 dimensions. We have considered both the extremal and the non-extremal black holes. We first deal with the RN-AdS_4/CFT_3 case and then with the generalized RN-AdS_{d+1}/CFT_d case wherein both the cases the two adjacent subsystems on the boundary have a rectangular strip geometry. The calculation in both the RN-AdS_4/CFT_3 and RN-AdS_{d+1}/CFT_d scenarios involves non trivial perturbative expansion of the holographic entanglement negativity in different limits of the relevant parameters. In the case of RN-AdS_4/CFT_3, the parameters involved in the perturbative expansion are the charge and the temperature of the black hole whereas in the case of RN-AdS_{d+1}/CFT_d, the parameters involved in the perturbative expansion are the chemical potential and the temperature of the black hole.

1. For the case of the non-extremal black hole, when the mixed states are at a finite temperature on the boundary CFT, we have the following results :-
a. In the limit of small charge/small chemical potential and low temperature, the dominant contribution for the holographic entanglement negativity is governed by the mixed state at zero temperature dual to the pure AdS bulk configuration. The subleading terms represents the corrections due to the charge/chemical potential and the temperature of the black hole. The physical interpretation of this result is that the minimal surface in the bulk is far from the horizon therefore the dominant contributions are given by the near boundary pure AdS bulk

configuration.
b. In the limit of large charge/chemical potential and/or high temperature, the dominant contribution for the holographic entanglement negativity scales as area as the volume terms are completely cancelled out. The physical interpretation of this result is that the minimal surface in the bulk is near the horizon therefore the dominant contributions are given by the degrees of freedom of the minimal surface shared between the two adjacent subsystems.

2. For the case of the extremal black hole, when the mixed states are at a zero temperature on the boundary CFT, we have the following results :-
a. In the limit of small charge/small chemical potential, the dominant contribution for the holographic entanglement negativity is governed by the mixed state at zero temperature dual to the pure AdS bulk configuration. The subleading terms represents the corrections due to the charge/chemical potential of the black hole.
b. In the limit of large charge/large chemical potential, the dominant contribution for the holographic entanglement negativity scales as area as the volume terms coming from the vacuum degeneracy are completely cancelled out.

The cancellation of the volume terms representing thermal correlations observed for the RN-AdS black holes has also been noticed in the AdS_3/CFT_2 scenario and is result of the specific algebraic combination of the involved holographic entangle- ment entropies. The dominant contribution for the holographic entanglement negativity for two adjacent intervals scales as area conforms to the quantum information theory expectations and stimulates the fact that this elimination of volume terms might be a universal feature of the holographic entanglement negativity for two adjacent intervals. This entire exercise further provides support to the conjecture for the holographic entanglement negativity for two adjacent intervals when we have a charged, static black hole.

As a plan for future research one can use the results from the chapter 6 to better understand the aspects related to the Hawking-Page phase transition, entanglement in time, holographic entanglement entropy of conical singularity in higher dimensions, entwinement, the leading term in the expansion of the holographic entanglement entropy for conical singularity being negative, scaling as volume and showing super-extensive behaviour, "quantum" temperature, β_{con}. The results from the chapters 7 and 8 can be used in the future to better understand the aspects related to the holographic entanglement negativity in the case of extremal black holes, bulk proof of the conjecture whose reasoning is similar to [11], checking the validity of the conjecture when the CFT lives on a torus, entanglement negativity for AdS_3 with a conical singularity.

Appendix A

Non-extremal and extremal RN-AdS$_4$

A.1 Non-extremal RN-AdS$_4$ (Small charge - high temperature)

The constants k_1, k_2, k_3, k_4 and k_5 in the eq. (8.30) are given as follows

$$k_1 = \sum_{n=1}^{\infty}\left(\frac{1}{3n-1}\frac{\Gamma(n+\frac{1}{2})}{\Gamma(n+1)}\frac{\Gamma(\frac{3n+3}{4})}{\Gamma(\frac{3n+5}{4})} - \frac{2}{3\sqrt{3}n^2}\right) + \frac{\pi^2}{9\sqrt{3}} + \frac{\sqrt{\pi}\Gamma(-\frac{1}{4})}{\Gamma(\frac{1}{4})}, \quad \text{(A.1)}$$

$$k_2 = \frac{3\pi}{8} - \frac{3\Gamma(\frac{3}{2})\Gamma(\frac{7}{4})}{\Gamma(\frac{9}{4})} + 3\sum_{n=1}^{\infty}\left(\frac{1}{3n+2}\frac{\Gamma(n+\frac{3}{2})}{\Gamma(n+1)}\frac{\Gamma(\frac{3n+6}{4})}{\Gamma(\frac{3n+8}{4})} - \frac{1}{3\sqrt{3}n}\right)$$
$$- 3\sum_{n=1}^{\infty}\left(\frac{2}{3n+3}\frac{\Gamma(n+\frac{3}{2})}{\Gamma(n+1)}\frac{\Gamma(\frac{3n+7}{4})}{\Gamma(\frac{3n+9}{4})} - \frac{2}{3\sqrt{3}n}\right), \quad \text{(A.2)}$$

$$k_3 = \frac{-2}{\sqrt{3}} + \frac{\pi^2}{9\sqrt{3}}, \quad \text{(A.3)}$$

$$k_4 = \frac{2}{\sqrt{3}} - \frac{2}{\sqrt{3}}\log[3] + \frac{3\sqrt{\pi}\Gamma(\frac{3}{2})\Gamma(\frac{7}{4})}{\Gamma(\frac{9}{4})}, \quad \text{(A.4)}$$

$$k_5 = \frac{-2}{\sqrt{3}}. \quad \text{(A.5)}$$

The constants c_1 and c_2 appearing in the eq. (8.31) are given as follows

$$c_1 = \frac{\sqrt{\pi}}{2}\frac{\Gamma(\frac{3}{4})}{\Gamma(\frac{5}{4})} + \sum_{n=1}^{\infty}\left(\frac{\Gamma(n+\frac{1}{2})}{2\Gamma(n+1)}\frac{\Gamma(\frac{3n+3}{4})}{\Gamma(\frac{3n+5}{4})} - \frac{1}{\sqrt{3}n}\right), \quad \text{(A.6)}$$

$$c_2 = \frac{1}{\sqrt{3}} - \frac{3}{2}\sum_{n=0}^{\infty}\left(\frac{\Gamma(n+\frac{3}{2})}{\Gamma(n+1)}\frac{\Gamma(\frac{3n+6}{4})}{\Gamma(\frac{3n+8}{4})} - \frac{2}{\sqrt{3}}\right) + \frac{3}{2}\sum_{n=0}^{\infty}\left(\frac{\Gamma(n+\frac{3}{2})}{\Gamma(n+1)}\frac{\Gamma(\frac{3n+7}{4})}{\Gamma(\frac{3n+9}{4})} - \frac{2}{\sqrt{3}}\right). \quad \text{(A.7)}$$

A.2 Non-extremal RN-AdS$_4$ (Large charge - high temperature)

The constants K_1' and K_2' in the eq. (8.34) are given as follows

$$K_1' = -\frac{2\sqrt{\pi}\Gamma(\frac{3}{4})}{\Gamma(\frac{1}{4})} + \frac{\log[4]-10}{8} + \frac{1}{2}\sum_{n=2}^{\infty}\left(\frac{1}{n-1}\frac{\Gamma(n+\frac{1}{2})}{\Gamma(n+1)}\frac{\Gamma(\frac{n+3}{4})}{\Gamma(\frac{n+5}{4})} - \frac{2}{n^2}\right) + \frac{\pi^2}{6}, \tag{A.8}$$

$$K_2' = \frac{\pi^2}{6} - \frac{3}{2}. \tag{A.9}$$

A.3 Extremal RN-AdS$_4$ (Large charge)

The constants K_1, K_2 and K_3 in the eq. (8.40) are given as follows

$$\begin{aligned} K_1 &= \frac{2}{\sqrt{6}}\Bigg[-2\frac{\sqrt{\pi}\Gamma(\frac{3}{4})}{\Gamma(\frac{1}{4})} + \frac{\log[4]}{4} - \frac{1+2\sqrt{\pi}}{2} + \sqrt{\pi}\zeta\left(\frac{3}{2}\right) \\ &+ \frac{\sqrt{\pi}}{2}\sum_{n=2}^{\infty}\left(\frac{1}{n-1}\frac{\Gamma(\frac{n+3}{4})}{\Gamma(\frac{n+5}{4})} - \frac{2}{n\sqrt{n}}\right)\Bigg], \end{aligned} \tag{A.10}$$

$$K_2 = -\frac{2\pi}{\sqrt{6}}, \tag{A.11}$$

$$K_3 = \frac{2}{\sqrt{6}}\left[1-\sqrt{\pi}+\sqrt{\pi}\zeta\left(\frac{3}{2}\right)\right]. \tag{A.12}$$

Appendix B

Non-extremal and extremal RN-AdS$_{d+1}$

B.1 Non-extremal RN-AdS$_{d+1}$ (Small chemical potential - low temperature)

The constants $\mathcal{S}_0$ and $\mathcal{S}_1$ appearing in the eq. (8.65) are given as follows

$$\mathcal{S}_0 = \frac{2^{d-2}\pi^{\frac{d-1}{2}}\Gamma\left(-\frac{d-2}{2(d-1)}\right)}{(d-1)\Gamma\left(\frac{1}{2(d-1)}\right)}\left(\frac{\Gamma\left(\frac{d}{2(d-1)}\right)}{\Gamma\left(\frac{1}{2(d-1)}\right)}\right)^{d-2}, \tag{B.1}$$

$$\mathcal{S}_1 = \frac{\Gamma\left(\frac{1}{2(d-1)}\right)^{d+1}2^{-d-1}\pi^{-\frac{d}{2}}}{\Gamma\left(\frac{d}{2(d-1)}\right)^{d}\Gamma\left(\frac{1}{2}+\frac{1}{d-1}\right)}\left(\frac{\Gamma\left(\frac{1}{d-1}\right)}{\Gamma\left(-\frac{d-2}{2(d-1)}\right)}+\frac{2^{\frac{1}{d-1}}(d-2)\Gamma\left(1+\frac{1}{2(d-1)}\right)}{\sqrt{\pi}(d+1)}\right). \tag{B.2}$$

B.2 Non-extremal RN-AdS$_{d+1}$ (Small chemical potential - high temperature)

The function $\gamma_d\left(\frac{\mu}{T}\right)$ appearing in the eq. (8.67) is given as follows

$$\gamma_d\left(\frac{\mu}{T}\right) = N(1)+\frac{d^2(d-2)}{16\pi^2(d-1)}\left(\frac{\mu}{T}\right)^2\int_0^1 dx\left(\frac{x\sqrt{1-x^{2(d-1)}}}{\sqrt{1-x^d}}\right)\left(\frac{1-x^{d-2}}{1-x^d}\right)+\mathcal{O}\left(\frac{\mu}{T}\right)^4, \tag{B.3}$$

where the numerical constant $N(\varepsilon)$ is given as

$$N(\varepsilon) = 2\left[\frac{\sqrt{\pi}\Gamma\left(-\frac{d-2}{2(d-1)}\right)}{2(d-1)\Gamma\left(\frac{1}{2(d-1)}\right)}\right]+2\int_0^1 dx\left(\frac{\sqrt{1-x^{2(d-1)}}}{x^{d-1}\sqrt{f(z_H x)}}-\frac{1}{x^{d-1}\sqrt{1-x^{2(d-1)}}}\right). \tag{B.4}$$

B.3 Non-extremal RN-AdS$_{d+1}$(Large chemical potential - low temperature)

The numerical constants N_0, N_1 in the eq. (8.69) are given as follows

$$N_0 = 2\left[\frac{\sqrt{\pi}\Gamma\left(-\frac{d-2}{2(d-1)}\right)}{2(d-1)\Gamma\left(\frac{1}{2(d-1)}\right)}\right] + 2\int_0^1 dx\left(\frac{\sqrt{1-x^{2(d-1)}}}{x^{d-1}\sqrt{1-b_0x^d+b_1x^{2(d-1)}}} - \frac{1}{x^{d-1}\sqrt{1-x^{2(d-1)}}}\right), \tag{B.5}$$

$$N_1 = \int_0^1 dx\left(\frac{x\sqrt{1-x^{2(d-1)}}}{\sqrt{1-b_0x^d+b_1x^{2(d-1)}}}\right)\left(\frac{1-x^{d-2}}{1-b_0x^d+b_1x^{2(d-1)}}\right). \tag{B.6}$$

Bibliography

[1] B. Swingle, "Entanglement Renormalization and Holography," *Phys. Rev.* **D86** (2012) 065007, arXiv:0905.1317 [cond-mat.str-el].

[2] M. Van Raamsdonk, "Building up spacetime with quantum entanglement," *Gen. Rel. Grav.* **42** (2010) 2323–2329, arXiv:1005.3035 [hep-th]. [Int. J. Mod. Phys.D19,2429(2010)].

[3] G. Evenbly and G. Vidal, "Tensor network states and geometry," *Journal of Statistical Physics* **145** no. 4, (Nov, 2011) 891–918. https://doi.org/10.1007/s10955-011-0237-4.

[4] T. Faulkner, M. Guica, T. Hartman, R. C. Myers, and M. Van Raamsdonk, "Gravitation from Entanglement in Holographic CFTs," *JHEP* **03** (2014) 051, arXiv:1312.7856 [hep-th].

[5] T. Faulkner, F. M. Haehl, E. Hijano, O. Parrikar, C. Rabideau, and M. Van Raamsdonk, "Nonlinear gravity from entanglement in conformal field theories," *Journal of High Energy Physics* **2017** no. 8, (Aug, 2017) 57. https://doi.org/10.1007/JHEP08(2017)057.

[6] B. Czech, L. Lamprou, S. McCandlish, and J. Sully, "Tensor networks from kinematic space," *Journal of High Energy Physics* **2016** no. 7, (Jul, 2016) 100. https://doi.org/10.1007/JHEP07(2016)100.

[7] E. P. Verlinde, "Emergent Gravity and the Dark Universe," *SciPost Phys.* **2** no. 3, (2017) 016, arXiv:1611.02269 [hep-th].

[8] M. Van Raamsdonk, "Comments on quantum gravity and entanglement," arXiv:0907.2939 [hep-th].

[9] B. Swingle and M. Van Raamsdonk, "Universality of Gravity from Entanglement," arXiv:1405.2933 [hep-th].

[10] H. Casini, M. Huerta, and R. C. Myers, "Towards a derivation of holographic entanglement entropy," *JHEP* **05** (2011) 036, arXiv:1102.0440 [hep-th].

[11] A. Lewkowycz and J. Maldacena, "Generalized gravitational entropy," *JHEP* **08** (2013) 090, arXiv:1304.4926 [hep-th].

[12] A. Almheiri, X. Dong, and D. Harlow, "Bulk Locality and Quantum Error Correction in AdS/CFT," *JHEP* **04** (2015) 163, arXiv:1411.7041 [hep-th].

[13] F. Pastawski, B. Yoshida, D. Harlow, and J. Preskill, "Holographic quantum error-correcting codes: Toy models for the bulk/boundary correspondence," *JHEP* **06** (2015) 149, arXiv:1503.06237 [hep-th].

[14] F. Sanches and S. J. Weinberg, "Holographic entanglement entropy conjecture for general spacetimes," *Phys. Rev.* **D94** no. 8, (2016) 084034, arXiv:1603.05250 [hep-th].

[15] J. Maldacena and L. Susskind, "Cool horizons for entangled black holes," *Fortsch. Phys.* **61** (2013) 781–811, arXiv:1306.0533 [hep-th].

[16] L. Susskind, "Entanglement is not enough," *Fortsch. Phys.* **64** (2016) 49–71, arXiv:1411.0690 [hep-th].

[17] C. Cao, S. M. Carroll, and S. Michalakis, "Space from hilbert space: Recovering geometry from bulk entanglement," *Phys. Rev. D* **95** (Jan, 2017) 024031. https://link.aps.org/doi/10.1103/PhysRevD.95.024031.

[18] N. Bao, C. Cao, S. M. Carroll, and A. Chatwin-Davies, "De Sitter Space as a Tensor Network: Cosmic No-Hair, Complementarity, and Complexity," *Phys. Rev.* **D96** no. 12, (2017) 123536, arXiv:1709.03513 [hep-th].

[19] T. Jacobson, "Entanglement Equilibrium and the Einstein Equation," *Phys. Rev. Lett.* **116** no. 20, (2016) 201101, arXiv:1505.04753 [gr-qc].

[20] T. Jacobson, "Thermodynamics of space-time: The Einstein equation of state," *Phys. Rev. Lett.* **75** (1995) 1260–1263, arXiv:gr-qc/9504004 [gr-qc].

[21] E. P. Verlinde, "On the Origin of Gravity and the Laws of Newton," *JHEP* **04** (2011) 029, arXiv:1001.0785 [hep-th].

[22] T. Padmanabhan, "Thermodynamical Aspects of Gravity: New insights," *Rept. Prog. Phys.* **73** (2010) 046901, arXiv:0911.5004 [gr-qc].

[23] A. Strominger and C. Vafa, "Microscopic origin of the Bekenstein-Hawking entropy," *Phys. Lett.* **B379** (1996) 99–104, arXiv:hep-th/9601029 [hep-th].

[24] J. M. Maldacena, "The Large N limit of superconformal field theories and supergravity," *Int. J. Theor. Phys.* **38** (1999) 1113–1133, arXiv:hep-th/9711200 [hep-th]. [Adv. Theor. Math. Phys.2,231(1998)].

[25] S. Ryu and T. Takayanagi, "Holographic derivation of entanglement entropy from AdS/CFT," *Phys. Rev. Lett.* **96** (2006) 181602, arXiv:hep-th/0603001 [hep-th].

[26] S. Ryu and T. Takayanagi, "Aspects of Holographic Entanglement Entropy," *JHEP* **08** (2006) 045, arXiv:hep-th/0605073 [hep-th].

[27] A. Almheiri, D. Marolf, J. Polchinski, and J. Sully, "Black Holes: Complementarity or Firewalls?," *JHEP* **02** (2013) 062, arXiv:1207.3123 [hep-th].

[28] M. Srednicki, "Entropy and area," *Phys. Rev. Lett.* **71** (1993) 666–669, arXiv:hep-th/9303048 [hep-th].

[29] L. Bombelli, R. K. Koul, J. Lee, and R. D. Sorkin, "A Quantum Source of Entropy for Black Holes," *Phys. Rev.* **D34** (1986) 373–383.

[30] L. Susskind and J. Uglum, "Black hole entropy in canonical quantum gravity and superstring theory," *Phys. Rev.* **D50** (1994) 2700–2711, arXiv:hep-th/9401070 [hep-th].

[31] T. M. Fiola, J. Preskill, A. Strominger, and S. P. Trivedi, "Black hole thermodynamics and information loss in two-dimensions," *Phys. Rev.* **D50** (1994) 3987–4014, arXiv:hep-th/9403137 [hep-th].

[32] T. Azeyanagi, T. Nishioka, and T. Takayanagi, "Near Extremal Black Hole Entropy as Entanglement Entropy via AdS(2)/CFT(1)," *Phys. Rev.* **D77** (2008) 064005, arXiv:0710.2956 [hep-th].

[33] M. Cadoni and M. Melis, "Holographic entanglement entropy of the BTZ black hole," *Found. Phys.* **40** (2010) 638–657, arXiv:0907.1559 [hep-th].

[34] P. Calabrese and J. L. Cardy, "Entanglement entropy and quantum field theory," *J. Stat. Mech.* **0406** (2004) P06002, arXiv:hep-th/0405152 [hep-th].

[35] P. Calabrese and J. Cardy, "Entanglement entropy and conformal field theory," *J. Phys.* **A42** (2009) 504005, arXiv:0905.4013 [cond-mat.stat-mech].

[36] C. Holzhey, F. Larsen, and F. Wilczek, "Geometric and renormalized entropy in conformal field theory," *Nucl. Phys.* **B424** (1994) 443–467, arXiv:hep-th/9403108 [hep-th].

[37] C. G. Callan, Jr. and F. Wilczek, "On geometric entropy," *Phys. Lett.* **B333** (1994) 55–61, arXiv:hep-th/9401072 [hep-th].

[38] G. Vidal, J. I. Latorre, E. Rico, and A. Kitaev, "Entanglement in quantum critical phenomena," *Phys. Rev. Lett.* **90** (2003) 227902, arXiv:quant-ph/0211074 [quant-ph].

[39] A. R. Its, B.-Q. Jin, and V. E. Korepin, "Entanglement in the xy spin chain," *Journal of Physics A: Mathematical and General* **38** no. 13, (2005) 2975. http://stacks.iop.org/0305-4470/38/i=13/a=011.

[40] A. Kitaev and J. Preskill, "Topological entanglement entropy," *Phys. Rev. Lett.* **96** (2006) 110404, arXiv:hep-th/0510092 [hep-th].

[41] H. Casini and M. Huerta, "A Finite entanglement entropy and the c-theorem," *Phys. Lett.* **B600** (2004) 142–150, arXiv:hep-th/0405111 [hep-th].

[42] T. Nishioka, S. Ryu, and T. Takayanagi, "Holographic Entanglement Entropy: An Overview," *J. Phys.* **A42** (2009) 504008, arXiv:0905.0932 [hep-th].

[43] V. E. Hubeny, M. Rangamani, and T. Takayanagi, "A Covariant holographic entanglement entropy proposal," *JHEP* **07** (2007) 062, arXiv:0705.0016 [hep-th].

[44] T. Takayanagi, "Entanglement Entropy from a Holographic Viewpoint," *Class. Quant. Grav.* **29** (2012) 153001, arXiv:1204.2450 [gr-qc].

[45] M. Cadoni and M. Melis, "Entanglement Entropy of AdS Black Holes," *Entropy* **12** no. 11, (2010) 2244–2267.

[46] D. D. Blanco, H. Casini, L.-Y. Hung, and R. C. Myers, "Relative Entropy and Holography," *JHEP* **08** (2013) 060, arXiv:1305.3182 [hep-th].

[47] W. Fischler and S. Kundu, "Strongly Coupled Gauge Theories: High and Low Temperature Behavior of Non-local Observables," *JHEP* **05** (2013) 098, arXiv:1212.2643 [hep-th].

[48] W. Fischler, A. Kundu, and S. Kundu, "Holographic Mutual Information at Finite Temperature," *Phys. Rev.* **D87** no. 12, (2013) 126012, arXiv:1212.4764 [hep-th].

[49] P. Chaturvedi, V. Malvimat, and G. Sengupta, "Entanglement thermodynamics for charged black holes," *Phys. Rev.* **D94** no. 6, (2016) 066004, arXiv:1601.00303 [hep-th].

[50] D. V. Fursaev, "Proof of the holographic formula for entanglement entropy," *JHEP* **09** (2006) 018, arXiv:hep-th/0606184 [hep-th].

[51] M. Headrick, "Entanglement Renyi entropies in holographic theories," *Phys. Rev.* **D82** (2010) 126010, arXiv:1006.0047 [hep-th].

[52] T. Hartman, "Entanglement Entropy at Large Central Charge," arXiv:1303.6955 [hep-th].

[53] T. Faulkner, "The Entanglement Renyi Entropies of Disjoint Intervals in AdS/CFT," arXiv:1303.7221 [hep-th].

[54] G. Vidal and R. F. Werner, "Computable measure of entanglement," *Phys. Rev. A* **65** (Feb, 2002) 032314. https://link.aps.org/doi/10.1103/PhysRevA.65.032314.

[55] M. B. Plenio, "Logarithmic Negativity: A Full Entanglement Monotone That is not Convex," *Phys. Rev. Lett.* **95** no. 9, (2005) 090503, arXiv:quant-ph/0505071 [quant-ph].

[56] P. Calabrese, J. Cardy, and E. Tonni, "Entanglement negativity in extended systems: A field theoretical approach," *J. Stat. Mech.* **1302** (2013) P02008, arXiv:1210.5359 [cond-mat.stat-mech].

[57] P. Calabrese, J. Cardy, and E. Tonni, "Entanglement negativity in quantum field theory," *Phys. Rev. Lett.* **109** (2012) 130502, arXiv:1206.3092 [cond-mat.stat-mech].

[58] P. Calabrese, J. Cardy, and E. Tonni, "Finite temperature entanglement negativity in conformal field theory," *J. Phys.* **A48** no. 1, (2015) 015006, arXiv:1408.3043 [cond-mat.stat-mech].

[59] M. Rangamani and M. Rota, "Comments on Entanglement Negativity in Holographic Field Theories," *JHEP* **10** (2014) 060, arXiv:1406.6989 [hep-th].

[60] E. Perlmutter, M. Rangamani, and M. Rota, "Central Charges and the Sign of Entanglement in 4D Conformal Field Theories," *Phys. Rev. Lett.* **115** no. 17, (2015) 171601, arXiv:1506.01679 [hep-th].

[61] P. Chaturvedi, V. Malvimat, and G. Sengupta, "Holographic Quantum Entanglement Negativity," arXiv:1609.06609 [hep-th].

[62] P. Chaturvedi, V. Malvimat, and G. Sengupta, "Entanglement negativity, Holography and Black holes," arXiv:1602.01147 [hep-th].

[63] P. Chaturvedi, V. Malvimat, and G. Sengupta, "Covariant holographic entanglement negativity," arXiv:1611.00593 [hep-th].

[64] V. Malvimat and G. Sengupta, "Entanglement negativity at large central charge," arXiv:1712.02288 [hep-th].

[65] P. Jain, V. Malvimat, S. Mondal, and G. Sengupta, "Holographic Entanglement Negativity for Adjacent Subsystems in AdS_{d+1}/CFT_d," arXiv:1708.00612 [hep-th].

[66] C. De Nobili, A. Coser, and E. Tonni, "Entanglement negativity in a two dimensional harmonic lattice: Area law and corner contributions," *J. Stat. Mech.* **1608** no. 8, (2016) 083102, arXiv:1604.02609 [cond-mat.stat-mech].

[67] N. E. Sherman, T. Devakul, M. B. Hastings, and R. R. P. Singh, "Nonzero-temperature entanglement negativity of quantum spin models: Area law, linked cluster expansions, and sudden death," *Phys. Rev. E* **93** (Feb, 2016) 022128. https://link.aps.org/doi/10.1103/PhysRevE.93.022128.

[68] P. Jain, V. Malvimat, S. Mondal, and G. Sengupta, "Covariant Holographic Entanglement Negativity Conjecture for Adjacent Subsystems in AdS_{d+1}/CFT_d," arXiv:1710.06138 [hep-th].

[69] V. E. Hubeny, "Extremal surfaces as bulk probes in AdS/CFT," *JHEP* **07** (2012) 093, arXiv:1203.1044 [hep-th].

[70] E. Tonni, "Holographic entanglement entropy: near horizon geometry and disconnected regions," *JHEP* **05** (2011) 004, arXiv:1011.0166 [hep-th].

[71] P. Caputa, G. Mandal, and R. Sinha, "Dynamical entanglement entropy with angular momentum and U(1) charge," *JHEP* **11** (2013) 052, arXiv:1306.4974 [hep-th].

[72] S. A. H. Mansoori, B. Mirza, M. D. Darareh, and S. Janbaz, "Entanglement Thermodynamics of the Generalized Charged BTZ Black Hole," *Int. J. Mod. Phys.* **A31** no. 12, (2016) 1650067, arXiv:1512.00096 [gr-qc].

[73] C. Park, "Holographic entanglement entropy in the nonconformal medium," *Phys. Rev.* **D91** no. 12, (2015) 126003, arXiv:1501.02908 [hep-th].

[74] S. He, J.-R. Sun, and H.-Q. Zhang, "On Holographic Entanglement Entropy with Second Order Excitations," *Nucl. Phys.* **B928** (2018) 160–181, arXiv:1411.6213 [hep-th].

[75] O. Aharony, S. S. Gubser, J. M. Maldacena, H. Ooguri, and Y. Oz, "Large N field theories, string theory and gravity," *Phys. Rept.* **323** (2000) 183–386, arXiv:hep-th/9905111 [hep-th].

[76] J. Maldacena, "The Gauge/gravity duality," in *Black holes in higher dimensions*, G. T. Horowitz, ed., pp. 325–347. 2012. arXiv:1106.6073 [hep-th]. https://inspirehep.net/record/916620/files/arXiv:1106.6073.pdf.

[77] H. Năstase, *Introduction to the AdS/CFT Correspondence*. Cambridge University Press, 2015.

[78] R. Blumenhagen, D. Lüst, and S. Theisen, *Basic concepts of string theory*. Springer, Heidelberg, Germany, 2013.

[79] G. W. Gibbons, "Anti-de-Sitter spacetime and its uses," in *Mathematical and quantum aspects of relativity and cosmology. Proceedings, 2nd Samos Meeting on cosmology, geometry and relativity, Pythagoreon, Samos, Greece, August 31-September 4, 1998*, pp. 102–142. 2011. arXiv:1110.1206 [hep-th].

[80] E. P. Ralph Blumenhagen, *Introduction to Conformal Field Theory*. Springer-Verlag Berlin Heidelberg, 2009.

[81] M. Banados, C. Teitelboim, and J. Zanelli, "The Black hole in three-dimensional space-time," *Phys. Rev. Lett.* **69** (1992) 1849–1851, arXiv:hep-th/9204099 [hep-th].

[82] M. Banados, M. Henneaux, C. Teitelboim, and J. Zanelli, "Geometry of the (2+1) black hole," *Phys. Rev.* **D48** (1993) 1506–1525, arXiv:gr-qc/9302012 [gr-qc]. [Erratum: Phys. Rev.D88,069902(2013)].

[83] S. Carlip, "Conformal field theory, (2+1)-dimensional gravity, and the BTZ black hole," *Class. Quant. Grav.* **22** (2005) R85–R124, arXiv:gr-qc/0503022 [gr-qc].

[84] E. Papantonopoulos, *From Gravity to Thermal Gauge Theories: The AdS/CFT Correspondence*. Springer-Verlag Berlin Heidelberg, 2011.

[85] J. D. Bekenstein, "How does the entropy / information bound work?," *Found. Phys.* **35** (2005) 1805–1823, arXiv:quant-ph/0404042 [quant-ph].

[86] A. Zaffaroni, "Introduction to the AdS-CFT correspondence," *Class. Quant. Grav.* **17** (2000) 3571–3597.

[87] Jan de Boer, "Introduction to the AdS/CFT Correspondence,". http://www-library.desy.de/preparch/desy/proc/proc02-02/Proceedings/pl.6/deboer_pr.pdf.

[88] M. Ammon and J. Erdmenger, *Gauge/Gravity Duality: Foundations and Applications*. Cambridge University Press, 2015.

[89] M. Natsuume, "AdS/CFT Duality User Guide," *Lect. Notes Phys.* **903** (2015) pp.1–294, arXiv:1409.3575 [hep-th].

[90] T. Mohaupt, "Introduction to string theory," *Lect. Notes Phys.* **631** (2003) 173–251, arXiv:hep-th/0207249 [hep-th]. [,173(2002)].

[91] T. Jacobson, "Black hole entropy and induced gravity," arXiv:gr-qc/9404039 [gr-qc].

[92] S. N. Solodukhin, "The Conical singularity and quantum corrections to entropy of black hole," *Phys. Rev.* **D51** (1995) 609–617, arXiv:hep-th/9407001 [hep-th].

[93] S. N. Solodukhin, "On 'Nongeometric' contribution to the entropy of black hole due to quantum corrections," *Phys. Rev.* **D51** (1995) 618–621, arXiv:hep-th/9408068 [hep-th].

[94] D. V. Fursaev and S. N. Solodukhin, "On one loop renormalization of black hole entropy," *Phys. Lett.* **B365** (1996) 51–55, arXiv:hep-th/9412020 [hep-th].

[95] J. D. Brown and M. Henneaux, "Central Charges in the Canonical Realization of Asymptotic Symmetries: An Example from Three-Dimensional Gravity," *Commun. Math. Phys.* **104** (1986) 207–226.

[96] E. Witten, "Anti-de Sitter space and holography," *Adv. Theor. Math. Phys.* **2** (1998) 253–291, arXiv:hep-th/9802150 [hep-th].

[97] L. Susskind and E. Witten, "The Holographic bound in anti-de Sitter space," arXiv:hep-th/9805114 [hep-th].

[98] J. M. Maldacena and A. Strominger, "AdS(3) black holes and a stringy exclusion principle," *JHEP* **12** (1998) 005, arXiv:hep-th/9804085 [hep-th].

[99] R. F. Werner, "Quantum states with einstein-podolsky-rosen correlations admitting a hidden-variable model," *Phys. Rev. A* **40** (Oct, 1989) 4277–4281. https://link.aps.org/doi/10.1103/PhysRevA.40.4277.

[100] A. Peres, "Separability criterion for density matrices," *Phys. Rev. Lett.* **77** (Aug, 1996) 1413–1415. https://link.aps.org/doi/10.1103/PhysRevLett.77.1413.

[101] M. Horodecki, P. Horodecki, and R. Horodecki, "Mixed-state entanglement and distillation: Is there a "bound" entanglement in nature?," *Phys. Rev. Lett.* **80** (Jun, 1998) 5239–5242. https://link.aps.org/doi/10.1103/PhysRevLett.80.5239.

[102] M. Cadoni and S. Mignemi, "Entropy of 2-D black holes from counting microstates," *Phys. Rev.* **D59** (1999) 081501, arXiv:hep-th/9810251 [hep-th].

[103] S. N. Solodukhin, "Entanglement entropy of black holes," *Living Rev. Rel.* **14** (2011) 8, arXiv:1104.3712 [hep-th].

[104] S. Das, S. Shankaranarayanan, and S. Sur, "Black hole entropy from entanglement: A Review," arXiv:0806.0402 [gr-qc].

[105] H. Terashima, "Entanglement entropy of the black hole horizon," *Phys. Rev.* **D61** (2000) 104016, arXiv:gr-qc/9911091 [gr-qc].

[106] R. Brustein, M. B. Einhorn, and A. Yarom, "Entanglement interpretation of black hole entropy in string theory," *JHEP* **01** (2006) 098, arXiv:hep-th/0508217 [hep-th].

[107] M. Cadoni, "Emergent gravity and entanglement entropy of black holes," *J. Phys. Conf. Ser.* **174** (2009) 012061.

[108] M. Cadoni and P. jain, "How is the Presence of Horizons and Localized Matter Encoded in the Entanglement Entropy?," *Int. J. Mod. Phys.* **A32** no. 15, (2017) 1750083, arXiv:1703.02505 [hep-th].

[109] S. Deser, R. Jackiw, and G. 't Hooft, "Three-Dimensional Einstein Gravity: Dynamics of Flat Space," *Annals Phys.* **152** (1984) 220.

[110] S. Deser and R. Jackiw, "Three-Dimensional Cosmological Gravity: Dynamics of Constant Curvature," *Annals Phys.* **153** (1984) 405–416.

[111] P. Di Francesco, P. Mathieu, and D. Senechal, *Conformal Field Theory*. Graduate Texts in Contemporary Physics. Springer-Verlag, New York, 1997. http://www-spires.fnal.gov/spires/find/books/www?cl=QC174.52.C66D5::1997.

[112] R. Blumenhagen and E. Plauschinn, "Introduction to conformal field theory," *Lect. Notes Phys.* **779** (2009) 1–256.

[113] S. Carlip and C. Teitelboim, "Aspects of black hole quantum mechanics and thermodynamics in (2+1)-dimensions," *Phys. Rev.* **D51** (1995) 622–631, arXiv:gr-qc/9405070 [gr-qc].

[114] S. N. Solodukhin, "Entanglement entropy of black holes and AdS/CFT correspondence," *Phys. Rev. Lett.* **97** (2006) 201601, arXiv:hep-th/0606205 [hep-th].

[115] M. Cadoni, "Entanglement entropy of two-dimensional Anti-de Sitter black holes," *Phys. Lett.* **B653** (2007) 434–438, arXiv:0704.0140 [hep-th].

[116] D. V. Singh and S. Sachan, "How are the degree of freedom responsible for entropy in BTZ spacetime?," arXiv:1612.09387 [hep-th].

[117] G. 't Hooft, "On the Quantum Structure of a Black Hole," *Nucl. Phys.* **B256** (1985) 727–745.

[118] R. B. Mann and S. N. Solodukhin, "Quantum scalar field on three-dimensional (BTZ) black hole instanton: Heat kernel, effective action and thermodynamics," *Phys. Rev.* **D55** (1997) 3622–3632, arXiv:hep-th/9609085 [hep-th].

[119] V. Balasubramanian, B. D. Chowdhury, B. Czech, and J. de Boer, "Entwinement and the emergence of spacetime," *JHEP* **01** (2015) 048, arXiv:1406.5859 [hep-th].

[120] V. Balasubramanian, A. Bernamonti, B. Craps, V. Keränen, E. Keski-Vakkuri, B. Müller, L. Thorlacius, and J. Vanhoof, "Thermalization of the spectral function in strongly coupled two dimensional conformal field theories," *JHEP* **04** (2013) 069, arXiv:1212.6066 [hep-th].

[121] D. V. Singh and S. Siwach, "Scalar Fields in BTZ Black Hole Spacetime and Entanglement Entropy," *Class. Quant. Grav.* **30** (2013) 235034, arXiv:1106.1005 [hep-th].

[122] D. V. Singh and S. Sachan, "Logarithmic corrections to the entropy of scalar field in BTZ black hole spacetime," *Int. J. Mod. Phys.* **D26** no. 04, (2016) 1750038, arXiv:1412.7170 [hep-th].

[123] N. Shiba and T. Takayanagi, "Volume Law for the Entanglement Entropy in Non-local QFTs," *JHEP* **02** (2014) 033, arXiv:1311.1643 [hep-th].

[124] S. J. Olson and T. C. Ralph, "Entanglement between the future and past in the quantum vacuum," *Phys. Rev. Lett.* **106** (2011) 110404, arXiv:1003.0720 [quant-ph].

[125] S. J. Olson and T. C. Ralph, "Extraction of timelike entanglement from the quantum vacuum," *Phys. Rev.* **A85** (2012) 012306, arXiv:1101.2565 [quant-ph].

[126] V. E. Hubeny and M. Rangamani, "Causal Holographic Information," *JHEP* **06** (2012) 114, arXiv:1204.1698 [hep-th].

[127] V. Balasubramanian, B. D. Chowdhury, B. Czech, J. de Boer, and M. P. Heller, "Bulk curves from boundary data in holography," *Phys. Rev.* **D89** no. 8, (2014) 086004, arXiv:1310.4204 [hep-th].

[128] I. Ya. Aref'eva, M. A. Khramtsov, and M. D. Tikhanovskaya, "Improved image method for a holographic description of conical defects," *Theor. Math. Phys.* **189** no. 2, (2016) 1660–1672, arXiv:1604.08905 [hep-th]. [Teor. Mat. Fiz.189,no.2,296(2016)].

[129] T. Hartman and J. Maldacena, "Time Evolution of Entanglement Entropy from Black Hole Interiors," *JHEP* **05** (2013) 014, arXiv:1303.1080 [hep-th].

[130] P. Jain, V. Malvimat, S. Mondal, and G. Sengupta, "Holographic entanglement negativity conjecture for adjacent intervals in AdS_3/CFT_2," arXiv:1707.08293 [hep-th].

[131] P. Calabrese, J. Cardy, and E. Tonni, "Entanglement entropy of two disjoint intervals in conformal field theory," *J. Stat. Mech.* **0911** (2009) P11001, arXiv:0905.2069 [hep-th].

[132] P. Calabrese, J. Cardy, and E. Tonni, "Entanglement entropy of two disjoint intervals in conformal field theory II," *J. Stat. Mech.* **1101** (2011) P01021, arXiv:1011.5482 [hep-th].

[133] M. Kulaxizi, A. Parnachev, and G. Policastro, "Conformal Blocks and Negativity at Large Central Charge," *JHEP* **09** (2014) 010, arXiv:1407.0324 [hep-th].

[134] A. Coser, E. Tonni, and P. Calabrese, "Entanglement negativity after a global quantum quench," *J. Stat. Mech.* **1412** no. 12, (2014) P12017, arXiv:1410.0900 [cond-mat.stat-mech].

[135] X. Wen, P.-Y. Chang, and S. Ryu, "Entanglement negativity after a local quantum quench in conformal field theories," *Phys. Rev.* **B92** no. 7, (2015) 075109, arXiv:1501.00568 [cond-mat.stat-mech].

[136] P. Jain, V. Malvimat, S. Mondal, and G. Sengupta, "Holographic Entanglement Negativity for Conformal Field Theories with a Conserved Charge," arXiv:1804.09078 [hep-th].

[137] S. Kundu and J. F. Pedraza, "Aspects of Holographic Entanglement at Finite Temperature and Chemical Potential," *JHEP* **08** (2016) 177, arXiv:1602.07353 [hep-th].